Università degli Studi della Basilicata

Unione Europea
Fondo Sociale Europeo

Regione Basilicata

Realizzato con il contributo FONDO SOCIALE EUROPEO - FSE
PROGRAMMA OPERATIVO REGIONALE 2000/2006

UNIVERSITÀ DEGLI STUDI DELLA BASILICATA

DIPARTIMENTO DI INGEGNERIA E FISICA DELL'AMBIENTE

DOTTORATO DI RICERCA IN INGEGNERIA DELL'AMBIENTE XIX CICLO

SETTORE SCIENTIFICO-DISCIPLINARE: AUTOMATICA ING/INF 04

Modeling, Control and Fault Diagnosis for Chemical Batch Reactors

Francesco Pierri

ADVISOR:

Prof. Ing. Fabrizio Caccavale

PH. D. COURSE COORDINATOR:

Prof. Ing. Gian Lorenzo Valenti

Acknowledgments

This thesis is the conclusion of the work carried out in the period from November 2003 to November 2006 at the Department of Ingegneria e Fisica dell'Ambiente of the University of Basilicata, under the supervision of Professor Fabrizio Caccavale.

I would like to thank several people for their contribution to this work. First of all, Professor Fabrizio Caccavale, my supervisor, for his many teachings and suggestions and for his constant support during these years. I am very grateful for all the time he has given to me.

I am also thankful to Ing. Mario Iamarino and to Professor Vincenzo Tufano for their support to this research.

Finally, I wish to thank Professor Rolf Johansson, Dr. Anders Robertsson and all the Department of Automatic Control of the Lund Institute of Technology for their friendly welcome and for the joyful time spent in Lund.

Abstract

The objectives of this thesis are modeling, control and fault diagnosis for chemical batch reactors. Due to their strong nonlinearities, intrinsically unsteady operating conditions and lack of complete state and parameters measurements, control, optimization and diagnosis of chemical plants and processes are major technical challenges for industrial engineers and control experts. The benefits of advanced control for chemical reactors include increased productivity and improvements in safety, product quality and batch to batch uniformity. Although the control and diagnosis techniques presented here are applicable to a broad range of nonlinear systems, the application of these methods to a nonlinear process control problems has been emphasized. To this aim, a complex reaction scheme has been chosen as application to test the effectiveness of the proposed techniques on a simulation model built in the Matlab/Simulink© environment.

First, a complete model, involving a large number of reaction and intermediate chemical species, has been developed. Then a number of simplified reaction schemes, involving only a limited number of reaction and chemical species, has been considered in order to reproduce the behavior of the complete model. The parameters of these simplified models have been identified via a nonlinear estimation method. Therefore, the high-order complete model has been adopted to build a reliable and accurate simulation model, while the design of the control and diagnosis schemes has been achieved by resorting to the reduced-order simplified model, thanks to its limited complexity and computational burden.

An original Feedback Linearizing Controller has been designed for the reactor temperature control and a stability analysis has been rigourously developed. First, an adaptive nonlinear observer has been designed to estimate the heat released by the reaction, then, a temperature control scheme has been designed, based on the closure of two control loops. Two different observers have been designed, the first one compute the heat on the basis of the concentration estimate and of the knowledge of the reaction kinetics, the latter one estimates the heat as unknown parameter.

Finally, assuming the presence of redundant temperature sensors both in the reactor and in the jacket, a fault detection and isolation scheme, based on a bank of two diagnostic observers, has been developed. As diagnostic observer the observers designed for control purpose have been adopted.

All the proposed approaches have been tested via a realistic simulation model, built in the Matlab/Simulink© environment, and have been compared with other well-established techniques.

Contents

Contents i

List of Figures iii

List of Tables v

Introduction vi

I.1 Overview of previous and related work . . . vii

I.1.1 Modeling . . . vii

I.1.2 Control . . . ix

I.1.3 Fault diagnosis . . . x

I.2 Objectives and results of the thesis . . . xii

I.3 Outline of the thesis . . . xiv

1 Modeling 1

1.1 Introduction to chemical kinetics . . . 1

1.2 Reactor types . . . 2

1.3 The mathematical model of an ideal jacketed batch reactor . . . 4

1.3.1 The heat released by the reaction . . . 6

1.4 Compartment reactor model . . . 7

1.5 Phenol-formaldehyde reaction . . . 10

1.5.1 Reaction scheme . . . 11

1.5.2 Mathematical model . . . 13

1.5.3 Mass balances . . . 21

1.5.4 Heat released by the reaction . . . 22

2 Identification of reaction dynamics 24

2.1 Introduction . . . 24

2.2 Model identification . . . 24

2.3 Parameter estimation . . . 26

2.4 Optimization algorithms for parameters estimation . . . 27

2.4.1 Linear models . . . 27

2.4.2 Nonlinear models . . . 29

2.4.3 Implicit nonlinear models . . . 32

2.5 Model identification for the phenol-formaldehyde polymerization . . . 34

2.5.1 Generation of input-output data . . . 34
2.5.2 Selection of candidate models . . . 35
2.5.3 Parameters estimation . . . 38
2.5.4 Model validation . . . 40

3 Control **42**
3.1 Introduction . . . 42
3.2 Modeling . . . 43
3.3 Estimation of the heat released by the reaction . . . 47
3.3.1 Model-based nonlinear observer . . . 48
3.3.2 Model-free approaches . . . 51
3.4 Model-based controller . . . 55
3.5 Stability analysis of the controller-observer scheme . . . 57
3.6 Addition of an integral action . . . 59
3.7 Concluding remarks . . . 60
3.8 Application to the phenol-formaldehyde reaction . . . 61

4 Fault diagnosis **64**
4.1 Introduction . . . 64
4.2 Basic Principles of model-based fault diagnosis . . . 66
4.2.1 Fault isolation . . . 68
4.2.2 Performance evaluation of a fault diagnosis system . . . 69
4.3 Fault classification . . . 69
4.4 Proposed FDI scheme . . . 71
4.4.1 Residuals generation . . . 72
4.4.2 Sensor faults . . . 72
4.4.3 Actuators faults . . . 73
4.4.4 Decision Making System . . . 73

5 Case studies **76**
5.1 Introduction . . . 76
5.2 Simulation model . . . 76
5.3 Identification of the reaction kinetics . . . 78
5.3.1 Estimation of kinetic parameters . . . 78
5.3.2 Estimation of the molar enthalpy changes . . . 79
5.3.3 Model validation . . . 85
5.4 Control . . . 95
5.5 Fault diagnosis . . . 102

Conclusions and future work **112**

Bibliography **114**

List of Figures

1.1 a) Batch Stirred Tank Reactor (BSTR); (b) Continuous Stirred Tank Reactor (CSTR); (c) Tubular Reactor, or Plug Flow Reactor (PFR). 3
1.2 Structure of compartments around the impeller. 8
1.3 (a) Phenol; (b) Formaldehyde. 10
1.4 Formation of the reactive compounds from phenol (a) and formaldehyde (b). . . . 11
1.5 Reactive positions on the phenol ring. 11
1.6 Addition reactions 12
1.7 Examples of possible condensation reactions: (a) condensation of two methylols; (b) condensation of a methylol with a free position of phenol. 13
1.8 Dimers regarded as compound D_1. 14

3.1 Block scheme of the control. 56

4.1 Physical versus Analytical redundancy. 66
4.2 Model-based fault diagnosis. 67
4.3 Fault diagnosis and control loop. 68
4.4 Open-loop system. 70
4.5 Sensor fault. 70
4.6 Actuator fault. 71
4.7 DMS Voter Logic. 75

5.1 *Model* α first-order kinetics: temperature profile no.1. 87
5.2 *Model* α second-order kinetics: temperature profile no.1. 87
5.3 *Model* β first-order kinetics: temperature profile no.1. 88
5.4 *Model* β second-order kinetics: temperature profile no.1. 88
5.5 *Model* α first-order kinetics: temperature profile no.2. 89
5.6 *Model* α second-order kinetics: temperature profile no.2. 89
5.7 *Model* β first-order kinetics: temperature profile no.2. 90
5.8 *Model* β second-order kinetics: temperature profile no.2. 90
5.9 *Model* α first-order kinetics: temperature profile no.3. 91
5.10 *Model* α second-order kinetics: temperature profile no.3. 91
5.11 *Model* β first-order kinetics: temperature profile no.3. 92

5.12 *Model* β second-order kinetics: temperature profile no.3. 92
5.13 *Model* α first-order kinetics: temperature profile no.4. 93
5.14 *Model* α second-order kinetics: temperature profile no.4. 93
5.15 *Model* β first-order kinetics: temperature profile no.4. 94
5.16 *Model* β second-order kinetics: temperature profile no.4. 94
5.17 Desired reactor temperature profile. 96
5.18 Case study 1: reactor temperature tracking errors. 98
5.19 Case study 1: commanded temperature of the fluid entering the jacket. 98
5.20 Case study 1: estimates of the heat released by the reaction. 99
5.21 Case study 1: estimates of θ. 99
5.22 Case study 2: reactor temperature tracking errors. 100
5.23 Case study 2: commanded temperature of the fluid entering the jacket. 100
5.24 Case study 2: estimates of the heat released by the reaction. 101
5.25 Case study 2: estimates of θ. 101
5.26 Output errors of the observers in healthy conditions. 103
5.27 Voting measure of T_j (abrupt bias at sensor $S_{j,1}$). 105
5.28 Detection and isolation residuals (abrupt bias at sensor $S_{j,1}$). 105
5.29 Voting measure of T_r (abrupt switch to zero at sensor $S_{r,2}$). 106
5.30 Detection and isolation residuals (abrupt switch to zero at sensor $S_{r,2}$). 106
5.31 Voting measure of T_j (slow drift at sensor $S_{j,1}$). 107
5.32 Detection and isolation residuals (slow drift at sensor $S_{j,1}$). 107
5.33 Voting measure of T_r (increasing noise at sensor $S_{r,1}$). 108
5.34 Detection and isolation residuals (increasing noise at sensor $S_{r,1}$). 108
5.35 Voting measure of T_j (abrupt freezing of the measured signal on sensor $S_{j,1}$). . . . 109
5.36 Detection and isolation residuals (abrupt freezing of the measured signal on sensor $S_{j,1}$). 109
5.37 Actuator fault: faulted input (abrupt constant bias). 110
5.38 Actuator fault: residuals (abrupt constant bias). 110
5.39 Actuator fault: faulted input (abrupt freezing). 111
5.40 Actuator fault: residuals (abrupt freezing). 111

List of Tables

1.1 Methylolphenols. . . . 12
1.2 Dimers. . . . 14
1.3 Parameters of addition reactions. . . . 16
1.4 Pre-exponential factors of reactions of addition of dimers. . . . 20
1.5 Pre-exponential factors, in $[m^3 \cdot mol^{-1} \cdot s^{-1}]$, of condensation reactions. . . . 23

4.1 Decisions of DMS on the basis of the residuals. . . . 74

5.1 Simulation parameters. . . . 77
5.2 Best fit kinetic parameters for *Model* α. . . . 79
5.3 Best fit kinetic parameters for *Model* β. . . . 80
5.4 Kinetic parameters for *Model* α: pre-exponential factors and activation energies. . . . 81
5.5 Kinetic parameters for *Model* β: pre-exponential factors and activation energies. . . . 81
5.6 Molar enthalpy changes for *Model* α. . . . 82
5.7 Molar enthalpy changes for *Model* β. . . . 82
5.8 Molar enthalpy changes variable with the temperature for *Model* α with first-order kinetics. . . . 82
5.9 Molar enthalpy changes variable with the temperature for *Model* α with second-order kinetics. . . . 83
5.10 Molar enthalpy changes variable with the temperature for *Model* β with first-order kinetics. . . . 83
5.11 Molar enthalpy changes variable with the temperature for *Model* β with second-order kinetics. . . . 84
5.12 $RMSE$ on the test temperature profiles. . . . 86
5.13 Controller-observer parameters. . . . 97

Introduction

Discontinuous reactors (batch and semi-batch) are used extensively for the production of specialty chemicals, polymers or bioproducts, because of their flexibility in operation mode. Usually these processes are characterized by small volume production and by reaction systems quite complex and not entirely known. The control of batch reactors can have widely differing immediate objectives, from simple rejection of small disturbances to development of a complete on-line operational strategy in response to the observed system behavior, [13]. From the practical point of view, safety and product quality are the mostly interesting aspects. Process control engineers have developed considerable expertise in continuous processes, characterized by steady-state operation condition, but the application of this expertise to discontinuous processes rarely achieves comparable success. Control and optimization of batch processes are real challenges for process control engineers, [13], because of some technical and operational considerations as:

- *Time-varying characteristic*. In a batch reactor, chemical transformation proceed from an initial state to a very different final state. Even if the temperature is kept constant, the concentration, the heat produced and the reaction rates change significantly during a batch run. Therefore there exists no single operation point around which the control system can be designed.

- *Nonlinear behavior*. The batch processes are characterized by strong nonlinearities, which are originated, for instance, from the nonlinear dependency of the reaction rates on concentrations (often) and on temperature (always), or from the nonlinear relationship between the heat exchanged from the reactor to the cooling jacket. Since the reactor operates over a wide range of conditions, it is not possible to use, for the purpose of control design, approximate models linearized around a single operating point.

- *Model inaccuracies*. The development of reliable models for batch processes is very time consuming. Hence, in many cases, even the number of significant reactions

is unknown, not to mention their stoichiometry or kinetics. As consequence only approximated models are available.

- *Few specific measurements*. Chemical composition is usually determined by drawing a sample and analyzing it off-line, i.e., by using invasive and destructive methods. On-line specific chemical sensor, e.g., spectroscopic sensors, are still rare. Furthermore, the available measurements of physical quantities such as temperature, pressure, torque of the impeller, might present low accuracy due to the wide range of operation that the measuring instrument has to cover.

- *Presence of disturbances*. Some disturbances cannot be totally ruled out. These disturbances can be due to operator mistakes (e.g., wrong solvent choice or incorrect material balances), processing problems (e.g., fouling of sensors and reactor walls, insufficient mixing), presence of impurity in the raw material. Also the evolution of the heat produced can be seen as an important nonstationary disturbance. Although it is typically unmeasured, in some cases it can be estimated and used in the control scheme.

- *Irreversible behavior*. In batch processes with history-dependent product properties (e.g. polymerization), it is impossible to introduce remedial correction. Instead in continuous processes, an appropriate control action can bring the process back to the desired steady state.

- *Limited corrective action*. Due to the finite duration of a batch run, the possibility to influence the reaction typically decreases with the time. Often, if a batch run shows a deviation in product quality, the charge has to be discarded.

I.1 Overview of previous and related work

In the following, a brief overview of the state of the art and of previous work on the topics related to the thesis is presented.

I.1.1 Modeling

A reactor comprises a chemical reaction system and a processing equipment (reactor vessel). The reaction systems are often poorly known; even when the desired product and the main side reactions are well known, since there might exist additional poorly known

or totally unknown side reactions or partial product. Moreover, sometimes the reaction involves a great number of chemical species and a detailed model of all of them may be useless. Hence, often the kinetic model involves few real and pseudo (lumped) reaction in order to follow the behavior of the concentration of interest. To this aim, many techniques aimed at reducing the complexity of models and to identify the model parameters have been introduced in the last two decades, (see, e.g., [11,12,51,94,96]). These problems are not trivial, because the model structure is unknown and one is faced with choosing many various candidate models. Moreover, the equations describing the system are often nonlinear differential and/or algebraic equations and the parameters may vary over a wide range of values. Three different kind of model have been used in the literature for batch processes:

1. *Data-driven black box models*. These are empirical input-output models, often able to represent the relationship between manipulated and observed variables. To this aim, ARMAX-type models [81], models based on neural network [10], and, more recently, multivariate statistical PLS models [89] have been proposed. These models are relatively easy to obtain, but present two main drawbacks: (i) they are, usually, inadequate for predicting the reactor behavior outside the experimental domain in which the data were collected for model building; (ii) they are able to represent only relationships between variables that are manipulated or measured; hence, key variables, such as the heat or the concentrations, are difficult to represent.

2. *Knowledge-driven white box models*. This is the preferred approach for modeling batch reactors. It is a mechanistic, state-space representation based on stoichiometric and kinetic knowledge, as well as on energy and mass balances for the reactor. The kinetic model describes the effect that temperature and concentrations have on the rate of each reaction. The energy and mass balances relate the states (concentrations, temperature and volume) to the inlet streams and possible disturbances. The drawbacks of these models are the following: (i) no realistic model is purely mechanistic, so a few physical parameters typically need to be estimated on the basis of experimental data; (ii) their derivation is very time-consuming and they are difficult to build for industrially-relevant reaction systems (e.g. polymerization); (iii) they cannot be derived in presence of unknown side-reactions or unknown partial products.

3. *Hybrid grey-box models*. They are a combination of the previous ones. Typically

they are characterized by a simple (simplified) structure based on some qualitative knowledge of the process [49]. Pseudo or lumped reaction are often exercised within hybrid models, so it is necessary to identify some model parameters and, sometimes, adjust them on-line. To this purpose, tendency models have been proposed in literature [35]. Parameters identification is based on nonlinear optimization techniques, as the steepest descent method (gradient method), the Newton-Raphson method and the Levenberg-Marquardt method. The drawback of this approach is that, often, is not possible to follow, using a simplified model, all the species involved in the reaction, but only the species of major interest.

I.1.2 Control

Usually, the main task of the control system of a batch reactor is that of imposing a given temperature profile inside the vessel. Control of the temperature allows to determine the behavior of the chemical reaction, and thus the final product of the batch. In particular, for each product, a suitable temperature profile is defined, including heating and cooling phases: the capability of tracking the desired profile determines directly the quality of the final product. Usually the temperature is controlled via the heat exchange between the reactor and a heating/coolant fluid, circulating in a jacket surrounding the vessel or in a coil inside the vessel.

Frequently, a cascade controller is adopted. The most common cascade configuration is characterized by two temperature controllers: the output of the reactor temperature controller (master) becomes the set-point of the cooling jacket temperature controller (slave).

The most commonly used control strategies are based on conventional linear PID controllers. If the process is only mildly nonlinear or it operates near a nominal steady-state condition these controllers can provide good performance. But, often, industrial processes, including polymerization process, can exhibit highly nonlinear behavior and operate within a wide range of conditions. In these cases, the conventional PID controllers must be tuned very conservatively, in order to provide stable behavior over the entire range of operation; of course this may cause a degradation of control system performance.

In the last two decades, nonlinear model-based control strategies began to be preferred for complex processes, [45]. The development of these strategies has been motivated by the development of efficient identification methods for experimental nonlinear

models and significant improvements in the capability of computer-control hardware and software, that permit a high level of online computation.

Nonlinear control design methods mostly investigated are the input/output linearization, also known as feedback linearization, and the nonlinear model predictive control (MPC).

The input/output linearization provides an exact linearization of the model, independent of the operating point. The control laws include the inverse of the dynamical model of the process, provided that such an inverse exists. Several process control design methods, such as generic model control [59], globally linearizing control [54], internal decoupling control [5], reference system synthesis [8] and a nonlinear version of internal model control [43], are based on this approach.

The model predictive control theory is a well-established design framework for linear systems. It is an optimal-control based method to select control inputs by minimizing an objective function. This function is defined in terms of both present and predicted system variables, and is evaluated by using an explicit model to predict future process outputs. The success of this techniques for linear systems has motivated the extension to nonlinear systems (nonlinear MPC). The control problem formulation is analogous to linear MPC except that a nonlinear dynamic model is used to predict future process behavior. It needs the solution, at each sampling instant, of a nonlinear programming problem [9]; the computational effort is compensated by the benefits of the nonlinear approach.

Both the previous approaches need an accurate model of the process and the measures of the state variables. As aforementioned, the measures of the whole state is, often, not available, but a possible solution to this problem is the state estimation via nonlinear observers [34, 41].

An alternative approach is to design the controller on the basis of empirical model, developed from experimental data. To this aim the most interesting and investigated tool are the artificial neural networks [10, 30, 33].

I.1.3 Fault diagnosis

Safety problems in chemical reactors are due to many causes, e.g. equipment failures, human errors, loss of utility and instrument failures. The occurrence of a fault may cause a process performance degradation (e.g., lower product quality) or, in the worst cases, fatal accidents, such as run-away. Depending on the nature of the problem, the proper response can be to *hold* the reaction sequence until the failure has been removed, or to

initiate an orderly emergency shutdown. The adoption of automatic fault detection techniques, achieving fast and reliable detection of faults, is necessary in order to develop an automatic correction system. Faults can be divided in actuator faults (e.g., electric-power failure, pomp failure, valve failure), process faults (e.g., abrupt variation of the heat transfer coefficient, side reaction due to impurity in the raw material) and sensor faults. Often, sensor redundancy is adopted and a suitable voting scheme is developed in order to recognize the faulty sensor and output a healthy measure.

Several fault diagnosis approaches have been proposed for steady-state processes (e.g., continuous reactors), but the application of these techniques to batch chemical processes are usually difficult because of the reasons previously introduced. Existing fault diagnosis approach for chemical batch reactors can be roughly classified in model free approaches (i.e., approaches based on statistical analysis, neural networks or expert systems) and model-based approaches (e.g., observer-based techniques). Statistical techniques can be classified in univariate statistical techniques (e.g., simple thresholding [67]) and multivariate statistical techniques (e.g., principal component analysis (PCA) [31,56,99] and projection to latent structures (PLS) [66,105]). The univariate statistical approaches use upper and lower bounds for individual variables to detect and identify faults. They are easy to implement but lead to a significant number of false alarms; furthermore, not all faults can be detected by the violation of the normal variation range of individual variables. Multivariate techniques achieve best performance both in term of accuracy and of robustness. Multivariate techniques in conjunction with methods based on PCA/PLS project most of the information on the measured process variables onto low dimensional spaces, where a region of normal operative conditions can be easily defined. Namely, measurements are projected onto a low dimensional space and compared with the normal or common-cause variation predicted by the model. Then, statistical tests are used to detect any abnormal behavior. The major benefit of the multivariate statistical techniques is that a model of the system is not needed, and only a database of historical data regarding normal operation conditions is required.

Knowledge-based expert system approaches to fault diagnosis have been proposed in the literature. The main drawbacks of these approaches are in the knowledge acquisition and the unpredictability of the expert system response outside its domain of expertise. These problems can be overcame by using artificial neural networks (ANNs). The ANNs do not require explicit encoding of knowledge or a deep knowledge of the mathematical model of the process. The first applications of ANNs in fault diagnosis for chemical

process are based on back-propagation networks [47, 101]. More recently, different neural networks architectures have been preferred because their best generalization performance; for instance Radial Basis Functions (RBFs) networks, [106], or Dynamic Neural Networks, [75], have been adopted. In [87, 88] a combination of ANNs and knowledge-based expert systems (i.e., fuzzy systems) is presented. Recently, Bayesian Belief Network (BBNs) have been adopted for detecting faults in processes both in steady-state operation conditions, [71, 86], and in unsteady operation conditions, [70].

Model-based analytical redundancy methods [20,37,76,100] are based on the comparison between the measurements of a set of variables characterizing the behavior of the monitored system and the corresponding estimates predicted via a mathematical model of the system. The deviations between measured and estimated variables provide a set of residuals sensitive to the occurrence of faults; then, by processing the information carried by the residuals, the faults can be detected (i.e., the presence of one or more faults can be recognized) and isolated (i.e., the faulty components are determined). Among the model-based analytical redundancy methods, the observer-based methods require a model of the system to be operated in parallel to the process, i.e., the so called diagnostic observer. To the purpose, Luenberger observers [39, 50, 95], Unknown Input Observers [93] and Extended Kalmann Filters [48] have been mostly used in fault detection and identification for chemical processes and plants. Since perfect knowledge of the model is rarely a reasonable assumption, soft computing methods, integrating quantitative and qualitative modeling information, have been developed to improve the performance of FD observer-based schemes for uncertain systems (see, e.g., the survey in [77]). Remarkably, a major contribution to the observer-based approach has been given by [84, 108], where the failures are identified by the so-called on-line interpolator (e.g., ANNs whose weights are updated on line).

I.2 Objectives and results of the thesis

This thesis deals with the problems of modeling, control and fault diagnosis for batch reactors. The objectives of the thesis are:

- The development of an accurate model of a batch reactor in which a complex reaction takes place. Then, the development of a simplified model suitable for control purposes; in order to be used in the control laws, this model could be sufficiently accurate, but, at same time, not too much complex.

- The development of a novel control scheme more efficient and robust then the conventional linear schemes.
- The development of a fault diagnosis method for batch chemical processes, that could detect and isolate sensors and actuators faults.

In order to pursue the above objectives, first of all, a complex exothermic reaction scheme, modeling the production of a pre-polymer of the phenolic resin and involving phenol and formaldehyde, has been considered.

First, a complete model, involving a large number of reaction and intermediate chemical species, has been derived. Then, a number of simplified reaction schemes, involving only a limited number of reaction and chemical species, has been considered in order to reproduce the behavior of the complete model. The parameters of these simplified models have been identified via a nonlinear estimation method. The obtained models are able to effectively predict the heat produced by the reaction and the concentration of the desired product. Therefore, the high-order complete model has been adopted to build a reliable and accurate simulation model, while the design of the control and diagnosis schemes has been achieved by resorting to the reduced-order simplified model, thanks to its limited complexity and computational burden.

Then, a nonlinear controller-observer scheme, based on input/output linearization, has been designed, [17, 83]. First, an adaptive nonlinear observer has been designed to estimate the heat released by the reaction, then, a temperature control scheme has been designed, based on the closure of two control loops. Namely, an outer control loop, closed on the reactor temperature, computes the reference signal for the inner control loop, closed on the jacket temperature. The convergence of the overall scheme, in terms of observer estimation errors and controller tracking errors, is rigourously proven, via a Lyapunov-like argument, for a large class of reaction schemes.

Finally, assuming the presence of redundant temperature sensors both in the reactor and in the jacket, a fault detection and isolation scheme, based on a bank of two diagnostic observers, is developed, [80]. Two different observer designs have been proposed: the adaptive observer previously introduced for control purposes, and a model-free observer, based on an online general purpose interpolator for estimating the heat released by the reaction.

All the proposed approaches have been tested via a realistic simulation model, built in the Matlab/Simulink© environment, and have been compared with other well-established

techniques.

I.3 Outline of the thesis

The thesis is organized as follows:

Chapter 1 concerns the modeling of batch reactors, with a brief description of the reactor types and of the basic principles of the chemical kinetics. Furthermore, the phenol-formaldehyde reaction, chosen as application during all the thesis, is described and modeled.

Chapter 2 presents an overview on identification techniques and their application to the phenol-formaldehyde reaction.

Chapter 3 illustrates the controller-observer proposed scheme for temperature control of batch reactors. Two novel nonlinear observers are presented for the estimation of the heat released by the reaction, and a two-loop control scheme, based on feedback linearization, is designed. Stability analysis both for the observers and for the overall scheme, are rigourously developed via Lyapunov arguments.

Chapter 4, after a brief introduction to fault diagnosis, presents the proposed fault detection and isolation technique, based on temperature sensors redundancy and on the generation of residuals via the nonlinear observers presented in Chapter 3.

Chapter 5 gives some simulation results about the application of identification, control and diagnosis techniques for a batch reactor in which the phenol-formaldehyde reaction takes place. In particular a comparison between the proposed control scheme and a well-established technique is presented.

Chapter 1

Modeling

1.1 Introduction to chemical kinetics

Chemical kinetics deals with the study of the rates of chemical reactions. The reaction rate can be defined as the change of concentration of reactants, ΔX, that occurs during a given period of time, Δt

$$R_{\Delta} = \frac{\Delta X}{\Delta t}.$$

When infinitesimally small change in concentration dX, occurring over an infinitesimally short period of time, dt, is considered, the instantaneous rate of reaction is defined as

$$R_r = \frac{dX}{dt}.$$

Several factors influence the reaction rate: the physical state of reactants and products, the concentration of reactants, the temperature, the presence or absence of catalysts. To the aim of this thesis only reactions in liquid phase are considered. In general, according to the collision theory, increasing the reactants concentrations increases the reaction rate, because molecules must collide in order to react. The dependence of the reaction rate from the concentrations can be expressed via the following exponential law

$$R_r = k(T_r) \prod_j C_j^{n_j} \tag{1.1}$$

where C_j is the concentration ([mol·m^{-3}]) of the j_{th} reactant, $k(T_r)$ is the rate constant, depending on the reaction temperature ([K]), T_r, and n_j is the order of the reaction with respect to j_{th} reactant . The overall order n of the reaction is given by the sum of all the individual orders

$$n = \sum_j n_j.$$

For elementary reactions the exponents n_j should be the same as the stoichiometric coefficients in the balanced equation, but for more complex reactions this is usually not true and they must be determined experimentally.

The rate constant $k(T_r)$, usually, contains the temperature dependence of the reaction rate. The simplest, but remarkably accurate, formula for the rate constant is the Arrhenius law. It was first proposed by the Dutch chemist H. van't Hoff in 1884; five years later the Swedish chemist Swante Arrhenius provided a physical justification and interpretation for it.

The basic idea is that the reactants, in order to react, first need to acquire enough energy to form an *activated complex*. This minimum energy is called *activation energy* ([J·mol^{-1}]), E_a, for the reaction. In thermal equilibrium at the temperature T_r, the fraction of molecules, that have a kinetic energy greater than E_a, can be calculated from the Maxwell-Boltzmann distribution and turn out to be proportional to $exp\left(-\frac{E_a}{RT_r}\right)$, where R is the universal gas constant ([J·mol^{-1}·K^{-1}]). This leads to following law for the rate constant

$$k(T_r) = k_0\, exp\left(-\frac{E_a}{RT_r}\right). \tag{1.2}$$

The constant k_0 is a frequency factor, usually called *pre-exponential factor*, and it is a specific constant of each particular reaction. The physical dimensions of the pre-exponential factor depend on the order of the reaction. It can be seen that either increasing temperature or decreasing the activation energy, will result in an increase in rate of reaction.

In the XX^{th} century, several improvement to the Arrhenius law were proposed; for instance, in 1916-18, Trautz and Lewis proposed a pre-exponential factor proportional to the square root of the temperature. This reflects the fact that the overall rate of all collisions, reactive or not, is proportional to the average molecular speed, which, in turn, on the basis of collision theory, is proportional to $\sqrt{T_r}$. In practice, the dependance of the pre-exponential factor from $\sqrt{T_r}$ is, usually, very slow compared to the exponential dependance associated with E_a, so it can be easily disregarded.

1.2 Reactor types

In a chemical process, at least two compounds are brought together in order to react or aid the reaction (catalysts). Hence, multiple material flows must be considered. These flows can either occur as:

- batch, where process occurs repeatedly, interrupted when the reactants are loaded and the product are unloaded;
- semi-batch, where some material flows are discontinuous while others are continuous;
- continuous, in this case is possible to distinguish between counter current, co-current and cross current flow.

The chemical reactors can be roughly classified into three categories, based on three ideal models:

a) Continuous Stirred Tank Reactor (CSTR);

b) Tubular Reactor, or Plug Flow Reactor (PFR);

c) Batch Stirred Tank Reactor (BSTR).

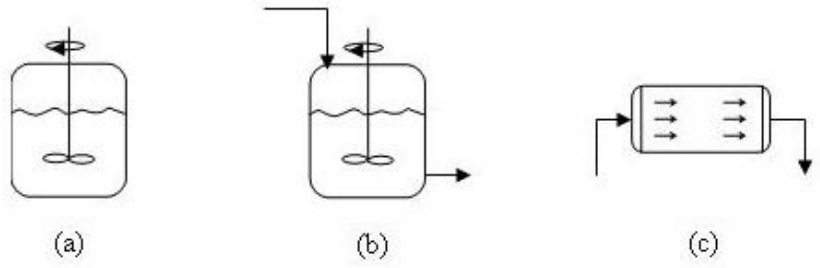

Figure 1.1: a) Batch Stirred Tank Reactor (BSTR); (b) Continuous Stirred Tank Reactor (CSTR); (c) Tubular Reactor, or Plug Flow Reactor (PFR).

The CSTR and BSTR models are based on the assumption of perfect (instantaneous) mixing. Therefore, the entire content of the reactor is assumed to be homogeneous with respect to the temperature and the concentration. The PFR model is based on the assumption of no mixing in axial direction and perfect mixing in radial direction.

The continuous reactors are characterized by a continuous inlet stream of reactant and by a continuous outlet stream of products. Except an initial transient they operate in steady-state conditions.

The CSTRs consist of a well-stirred tank, where, under the hypothesis of perfect mixing, the product composition is identical to the one inside the reactor, and invariant with respect to time. They are used for large productions, so they tend to be rather large and

need to be efficiently mixed. Deviations from ideal behavior occur when there is a less effective mixing regime and may generally be overcome by increasing the stirrer speed or by more effective reactor baffling.

The PFRs consist of a pipe, or tube, where a stream of reactants is pumped through. The reaction proceeds as the reactants travel through the tube. At the inlet the reaction rate is very high, because of the high concentrations of reactants, but, as the concentrations of reactants decrease, the reaction rate slows down. These reactors are characterized by perfect radial mixing and no axial mixing. Therefore, the system parameters vary along the axes of the tube, but are constant with respect to time.

The BSTRs are used for small scale production. They consist of a well-stirred tank, where all the reactants are loaded at once and then left for a long time, in order to obtain high conversion degree. The concentrations vary with respect to time, but, under the hypothesis of perfect mixing, are uniform in all the volume. Other important features are that the total mass of each batch is fixed, each batch is a closed system and the reaction time for all the reagents is the same. Batch reactors are diffused, in practice, because of their flexibility with respect to reaction time and to the kind and quantities of reaction that can be performed.

The reactors are often characterized by a heating/cooling system, where a flow of heating/cooling fluid is injected in order to heat the reacting mixture or to remove the excess heat. Different heating/cooling systems are available in the industrial practice:

1. A jacket in which the inlet temperature of heating/cooling fluid is adjusted.
2. Both a jacket and an inside coil are present. Cooling water circulates in the coil, while heating fluid is injected in the jacket.
3. A jacket in which heating and cooling can be performed alternatively by choosing a hot or cold fluid.

1.3 The mathematical model of an ideal jacketed batch reactor

The mathematical model of a jacketed batch reactor is given by the mass balances for each species involved in the reaction and by the energy balances in the reactor and in the jacket.

On the basis of mass and energy conservation principles, the mass and energy that enter a system must either leave the system or accumulate within the system, i.e, a generic

balance must be written as

$$IN = OUT + ACC$$

where IN denotes what enters the system, OUT denotes what leaves the system and ACC denotes accumulation within the system. IN and OUT must be positive terms, instead ACC may be positive or negative. In the particular case of chemical systems, a production term (PR), due to the reaction, is introduced such as

$$IN + PR = OUT + ACC. \tag{1.3}$$

The production term can be positive or negative.

The batch reactor is a closed system in which there are no input and output terms. Therefore, the mass balance simply becomes

$$ACC = PR.$$

For the generic i_{th} chemical species in the reactor, the mass balance can be written as

$$\frac{d}{dt}\int_V C_i dV = \int_V R_i dV, \tag{1.4}$$

where C_i is the concentration ([mol·m^{-3}]) of the i_{th} species, V is the reaction volume ([m^3]), R_i is the rate ([mol s^{-1} m^{-3}]) at which the i_{th} species is produced ($R_i > 0$) or consumed ($R_i < 0$).

In the following, it is assumed that the reaction occurs in liquid phase; therefore, the reaction volume can be considered constant and equation (1.4) becomes

$$\frac{dC_i}{dt}V = R_i V \qquad \Rightarrow \qquad \frac{dC_i}{dt} = R_i. \tag{1.5}$$

The term R_i can be written as

$$R_i = \pm \nu_i R_r,$$

where ν_i is the stoichiometric coefficient of the i_{th} species and R_r is the reaction rate computed via (1.1). The sign is plus if the species is a product and minus if it is a reagent. Hence, the mass balance for the i_{th} species becomes

$$\frac{dC_i}{dt} = \pm \nu_i k(T_r) \prod_j C_j^{n_j}. \tag{1.6}$$

The energy balance in the reactor is given by

$$\frac{d}{dt}\left(\rho_r c_{pr} V_r T_r\right) = Q - US\ \left(T_r - T_j\right), \tag{1.7}$$

where $\frac{d}{dt}(\rho_r c_{pr} V_r T_r)$ is the accumulation term, V_r is the reactor volume, ρ_r is the density of the reacting mixture ([kg·m^{-3}]), c_{pr} is the mass heat capacity of the reactor contents ([J·kg^{-1}·K^{-1}]), Q is the heat produced ($Q > 0$) or consumed ($Q < 0$) by the reaction and represents the production term, $US\ (T_r - T_j)$ is the heat exchanged with the jacket, U ([J·m^{-2}·K^{-1}·s^{-1}]) is the heat transfer coefficient, S ([m^2]) is the heat transfer area and T_j is the temperature of the fluid in the jacket.

Under the assumption of liquid phase, the density and the mass heat capacity can be considered constants

$$\frac{dT_r}{dt} = \frac{Q}{\rho_r c_{pr} V_r} - \frac{US}{\rho_r c_{pr} V_r}(T_r - T_j). \tag{1.8}$$

In the cooling jacket, there are a cool (or hot) fluid, entering the jacket with temperature T_{in} and flow rate F ([m^3·s^{-1}]), and a stream leaving the jacket with temperature T_{out} and flow rate F. The temperature T_{out}, because of the assumption of perfect mixing in the jacket, is equal to the temperature of the fluid in the jacket, T_j. In the jacket there is no reaction and, therefore, no production term, so the energy balance is the following

$$\frac{d}{dt}(\rho_j c_{pj} V_j T_j) = US\ (T_r - T_j) + \rho_j c_{pj} F (T_{\text{in}} - T_j), \tag{1.9}$$

where V_j is the jacket volume, ρ_j is the density of the fluid in the jacket, c_{pj} is the mass heat capacity of the fluid in the jacket.

Under the usual assumption of liquid phase, equation (1.9) becomes

$$\frac{dT_j}{dt} = \frac{US}{\rho_j c_{pj} V_j}(T_r - T_j) + \frac{F}{V_j}(T_{\text{in}} - T_j). \tag{1.10}$$

In conclusion, the mathematical model of an ideal jacketed batch reactor, in which a reaction, involving p species, takes place, is given by p mass balances (1.6) and two energy balances, the first written for the reactor (1.8) and the latter written for the jacket (1.10).

1.3.1 The heat released by the reaction

During a chemical reaction, some molecular links are broken an new ones are created. In order to broke or create a link, the system needs to absorb or release some energy, usually in form of heat. The energy released (or absorbed) by the reaction can be computed analyzing the molar enthalpy change, ΔH ([J·mol^{-1}]), between reactants and products

$$\Delta H = H_{\text{pr}} - H_{\text{re}}, \tag{1.11}$$

where H_{pr} is the sum of the enthalpy of all the products and H_{re} is the sum of the enthalpy of all the reactant species.

ΔH can be positive, i.e. $H_{\mathrm{pr}} > H_{\mathrm{re}}$, or negative, i.e. $H_{\mathrm{re}} > H_{\mathrm{pr}}$. In the first case the reaction absorbs energy as it moves towards completion and it is called endothermic; instead, if $\Delta H < 0$, the energy is released during the reaction, which is called exothermic.

The molar enthalpy change gives the heat released or consumed for each mole, in order to obtain the effective heat for time unit, involved in a reaction, it is possible to use the following expression

$$Q = -\Delta H V_r R_r = -\Delta H V_r k(T_r) \prod_j C_j^{n_j}. \tag{1.12}$$

The sign minus is used in order to have a positive heat for exothermic reactions and a negative heat for endothermic reactions.

1.4 Compartment reactor model

In the presence of a non-perfect fluid mixing, the ideal models are not adequate to describe real chemical reactors. To this aim, many complex models have been introduced. In this section, the compartment reactor model is described.

Industrial stirred tank reactors are often characterized by non-uniformities of concentrations and temperature as a result of non-perfect fluid mixing. These effects become more and more critical when the reaction heat and/or the reactor volume increase. Networks composed of fictitious interacting compartments have been applied to describe a large numbers of industrial processes in which partial mixing phenomena take place [23]. A compartment model approach has been also proposed for modeling of non-ideal stirred tank reactors [16, 25, 107], since, when compared to the alternative approach of Computational Fluid Dynamics, it has important computational advantages. In the following, a compartment model for a single-phase jacketed batch reactor is developed as described in [16].

A vessel agitated by means of a Rushton turbine located halfway with respect to the liquid depth is considered. If the vorticity is eliminated by suitable baffles, the main liquid circulation flow rate, F_c, generated by the impeller is radially directed and then split in two equal returning flows, $F_c/2$, which are recirculated to the turbine. Additionally, secondary flow rates F_e must be considered to account for the axial mixing occurring at the ideal planes of separation between the main circulation streams (Figure 1.2).

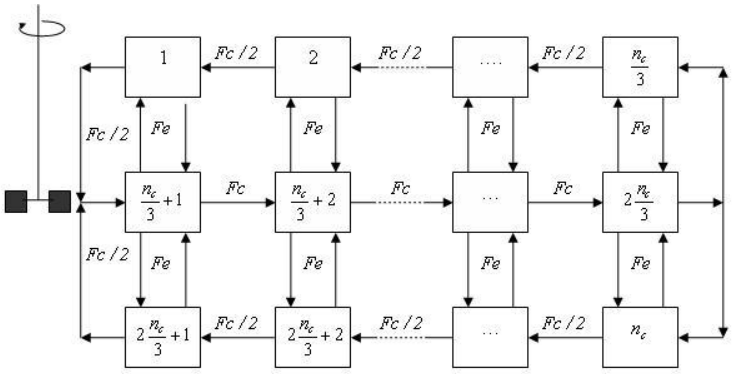

Figure 1.2: Structure of compartments around the impeller.

The circulation and exchange flow rates are related to both the impeller speed N and the blade diameter D via the following relationships, [73, 98]

$$F_c = K_c N D^3,$$

$$F_e = K_e N D^3,$$

where the factors K_c and K_e mainly depend on system geometry [25]. Hence, for any given system, a linear relationship between F_c and F_e holds

$$F_e = \delta F_c,$$

where δ is a positive constant.

On the basis of the considered macroscopic flow pattern, the dominant circulation flows, F_c and $F_c/2$, subdivide the reactor into three parallel levels; each level, in turn, is divided into $n_c/3$ equally sized compartments of volume $V_c = V_r/n_c$, where V_r is the volume of the whole reactor. Every compartment is modeled as a non-stationary ideal continuous stirred tank reactor, with a main inlet and outlet flow which connects the given compartment with adjacent compartments on the same level, and secondary exchange flows accounting for the turbulent mixing with adjacent compartments laying on the upper and/or lower level (Figure 1.2).

The mass balance written for a generic compartment contains the terms given by the mass exchange between the adjacent compartments. For instance, for the i_{th} species and a generic h_{th} compartment on the central level the following relationship holds

$$\dot{C}_{i,h} = R_{i,h} + \frac{F_c(C_{i,s} - C_{i,h})}{V_c} + \frac{F_e(C_{i,l} + C_{i,u} - 2C_{i,h})}{V_c}, \tag{1.13}$$

where $C_{i,h}$, $R_{i,h}$ and T_h are the concentration of the i_{th} species, the rate of production of the i_{th} species and the temperature in the h_{th} compartment, respectively. The subscripts u and l denote the adjacent compartment lying on the upper and lower level, respectively, while subscript s denotes the compartment located on the same level but upstream with respect to the dominant circulation flow. When the balance is written for the first compartment of the central level, (i.e., $h = \frac{n_c}{3} + 1$), the term accounting for the inlet circulation flow is modified, since it is composed by two different contributes originating from the corresponding compartment located on the upper and lower level, respectively.

$$\dot{C}_{i,h} = R_{i,h} + \frac{F_c}{2}\frac{(C_{i,u} + C_{i,l} - C_{i,h})}{V_c} + \frac{F_e(C_{i,l} + C_{i,u} - 2C_{i,h})}{V_c}. \tag{1.14}$$

Moreover, equations (1.13) and (1.14) must be suitably modified when the balance is referred to compartments laying on levels 1 and 3, where C_u and C_l are, respectively, equal to zero and F_c has to be replaced by $F_c/2$. Therefore for the h_{th} compartment of level 1 the following relationship holds

$$\dot{C}_{i,h} = R_{i,h} + \frac{F_c}{2}\frac{(C_{i,s} - C_{i,h})}{V_c} + \frac{F_e(C_{i,l} - 2C_{i,h})}{V_c}, \tag{1.15}$$

and for the h_{th} compartment of level 3

$$\dot{C}_{i,h} = R_{i,h} + \frac{F_c}{2}\frac{(C_{i,s} - C_{i,h})}{V_c} + \frac{F_e(C_{i,u} - 2C_{i,h})}{V_c}. \tag{1.16}$$

Analogously, the energy balance in the generic compartment on the central level yields

$$\dot{T}_h = \frac{(-\Delta H)R_h}{\rho_r c_{pr}} - \beta_h \frac{US\,(T_h - T_j)}{V_c \rho_r c_{pr}} + \frac{F_c(T_s - T_h)}{V_c} + \frac{F_e(T_l + T_u - 2T_h)}{V_c}, \tag{1.17}$$

where R_h is the reaction rate in the h_{th} compartment, β_h is the geometric ratio between the effective heat exchange surface of the considered compartment and the whole heat transfer area, S, ($\beta = 0$ for compartments not bordering the jacket). Moreover, the same corrections as for mass balances must be introduced in the energy balance written for the first compartment on the central level and for the compartments on levels 1 and 3.

Finally, the energy balance in the jacket reads

$$\dot{T}_j = \sum_{h=1}^{n_c} \beta_h \frac{US\,(T_h - T_j)}{V_j \rho_j c_{pj}} + \frac{(T_{\text{in}} - T_j)}{V_j} F. \tag{1.18}$$

1.5 Phenol-formaldehyde reaction

In this section a detailed mathematical model of a complex reaction scheme is developed. This model forms the basis for a detailed simulation scheme, which will be used for testing and validation of the control and diagnosis scheme developed in this thesis.

The phenol-formaldehyde reaction for the production of a pre-polymer of a resol-type phenolic resin is considered. Phenolic resins are the oldest thermosetting polymers, therefore several authors have studied this reaction. The polymerization process of phenol-formaldehyde was carried out in the early XX^{th} century, but the studies of the reaction were carried out later [32,36]. A few works have been tackled the problem of the mathematical modeling of resol-type phenolic resins, because of the complexity of the kinetic scheme. In [74] a theoretical model for the branching reactions has been developed, but the kinetic parameters were taken from the novolak chemistry, which differs widely in the nature of reactions, reactivity ratios and substitution effects. More recently, in [68, 85], a model of the synthesis of resol-type phenolic resins, including the effect of various parameters as pH, formaldehyde-to-phenol molar ratio and catalyst, has been proposed.

Phenol (C_6H_5OH) and formaldehyde (CH_2O) can react in the presence of a catalyst and with different formaldehyde-to-phenol molar ratios. On the basis of formaldehyde-to-phenol molar ratio, r_α, it is possible to obtain resol-type resins ($r_\alpha > 1$), or novolak-type resins ($r_\alpha < 1$). For the resol-type resins an alkaline catalyst is used, while novolak-type resins need an acid catalyst. Phenol and alkaline catalysts are commercial products, used without further purification; formaldehyde is available as a 37% aqueous solution. In an alkaline aqueous solution, phenol and formaldehyde react in the form of phenolate and methylene glycol, respectively. In Figure 1.4 the formation of these compounds from phenol and formaldehyde is shown.

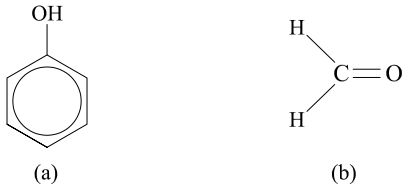

Figure 1.3: (a) Phenol; (b) Formaldehyde.

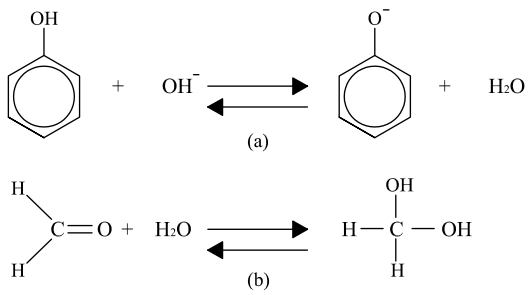

Figure 1.4: Formation of the reactive compounds from phenol (a) and formaldehyde (b).

Phenol presents three reactive sites, two located in *-ortho* and one in *-para* positions (see Figure 1.5), that are characterized by different reactivity; the formaldehyde as methylene glycol presents two reactive positions.

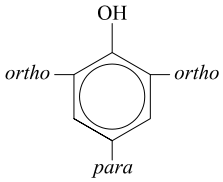

Figure 1.5: Reactive positions on the phenol ring.

1.5.1 Reaction scheme

The reaction for the production of phenolic resin occurs in two phases:

(i) Addition; the formaldehyde reacts with the reactive positions of the phenol ring and produces methylolphenols, in which the hydrogen of the phenol is substituted by a methylol group (CH_2OH). During this phase, mono-, di- and tri- substituted phenols are formed.

(ii) Condensation; the methylolphenols condense either with other methylol groups to form ether linkages or, more generally, with available reactive unsubstituted position in the phenol ring to form methylene bridges.

The initial addition reactions of formaldehyde with phenol are faster than the subsequent condensation reactions; therefore, the methylolphenols are initially the predom-

inant intermediate compounds. The addition reactions are shown in Figure 1.6, [85]. During this phase, a mixture of phenol, formaldehyde and five different methylolphenols (monomers) is present. In the following, the notation E_1 and E_2 will be used for phenol and formaldehyde, respectively, and the notation E_i ($i = 3 \dots 7$), will be used for the methylolphenols. In Table 1.1 all methylolphenols produced in the addition phase are reported.

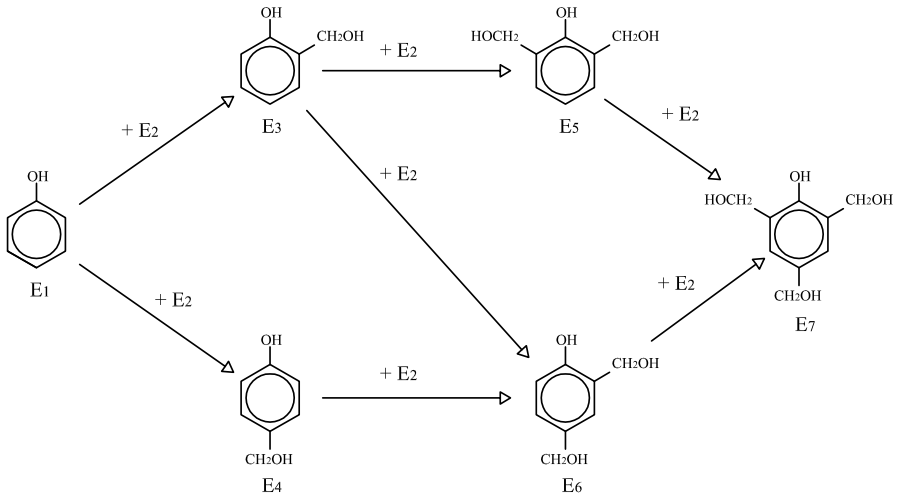

Figure 1.6: Addition reactions

Symbol	Chemical Formula
E_3	$C_6H_4OH(CH_2OH)$
E_4	$C_6H_4OH(CH_2OH)$
E_5	$C_6H_3OH(CH_2OH)_2$
E_6	$C_6H_3OH(CH_2OH)_2$
E_7	$C_6H_3OH(CH_2OH)_3$

Table 1.1: Methylolphenols.

During the condensation phase, the methylolphenols react either with other methylolphenols or with phenol, and the products are characterized by the presence of two phenol rings (dimers). Examples of possible condensation reactions are shown in Figure 1.7, [85].

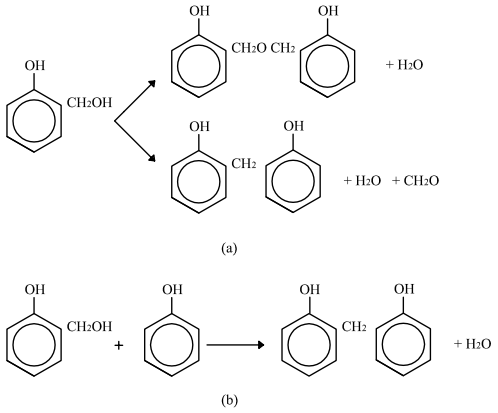

Figure 1.7: Examples of possible condensation reactions: (a) condensation of two methylols; (b) condensation of a methylol with a free position of phenol.

The obtained dimers can be different both for the number of methylol groups and for the position of these groups. These compounds can react either with formaldehyde to produce dimers with a different structure (addition reaction), or with other dimers or methylolphenols in order to obtain compounds characterized by three phenol rings (trimers). In this way, it is possible to obtain even long chains (polymers).

1.5.2 Mathematical model

The pre-polymer with the highest concentration of the tri-substituted phenols, E_7, has been considered as desired product. Therefore, to our purposes, the reaction must be stopped after the addition phase, hence, dimers and trimers can be considered as waste products. For this reason, in the model all the monomers, some aggregate dimers and an aggregate trimer are considered. Elements characterized by more than three phenol rings have not been taken into account, because the reaction must be stopped before their production. All the dimers with the same number of methylol groups are regarded as unique species; in this way only five different aggregate dimers are considered, reported on Table 1.2. In the following, the notation D_j, ($j = 0 \dots 4$), where j is the number of methylol groups, is used. As an example, in Figure 1.8, all the species, regarded as aggregate dimer D_1 are represented.

In this reaction, the trimers are produced in very low quantities; therefore, all the trimers are considered as unique species, denoted as E_{13}.

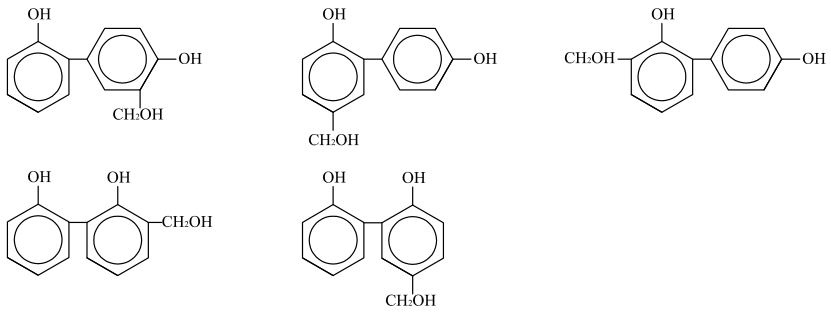

Figure 1.8: Dimers regarded as compound D_1.

Symbol	Chemical Formula
D_0	$(C_6H_4)_2(OH)_2CH_2$
D_1	$C_6H_4C_6H_3(OH)_2(CH_2OH)CH_2$
D_2	$C_6H_4C_6H_2(OH)_2(CH_2OH)_2CH_2$
D_3	$C_6H_3C_6H_2(OH)_2(CH_2OH)_3CH_2$
D_4	$C_6H_2C_6H_2(OH)_2(CH_2OH)_4CH_2$

Table 1.2: Dimers.

In conclusion, a reaction scheme involving thirteen chemical species is modeled. The elements E_1 and E_2 are the initial reactants (phenol and formaldehyde, respectively), E_i, ($i = 3 \dots 7$), are the methylolphenols produced during the addition phase, D_j, ($j = 0 \dots 4$), are the aggregate dimers and E_{13} is the aggregate trimer.

1.5.2.1 Selected reactions

Among all the possible reactions, 89 reactions have been selected. In particular, the 7 addition reactions of Figure 1.6 and the 77 condensation reactions characterized by the highest values of the reaction rate, have been considered. The remaining reactions are fictitious reactions: 4 are the addition reactions of formaldehyde with the aggregate dimers, which represent sets of real reactions, and the last one is representative of the condensation of dimers with monomers.

1.5.2.2 Reaction rates

According to [32, 85], both addition and condensation reactions are characterized by second order kinetics. In order to obtain the constant rates of the reactions, the procedure developed by [68, 85] has been used. In [85] the synthesis of a number of different resol-type resins is studied and the obtained model is experimentally validated. The constant rates at temperature of $80°C$ are computed by referring to the constant rate of a reference reaction, experimentally obtained. For the remaining reactions, the constant rate is adjusted using some coefficients, which take into account the different reactivity of the position *-ortho* and *-para* of the phenol ring, the reactivity due to the presence or absence of methylol groups and a frequency factor. The whole procedure and the values of all these coefficients for a number of resins can be found in [85].

Once the constant rates at $80°C$ and the activation energies are obtained, it is possible to compute the pre-exponential factors of each reaction using the Arrhenius law (1.2).

In this thesis, the numerical values obtained for the resin $RT84$ have been adopted. This resin is obtained via the reaction of phenol and formaldehyde in the presence of an alkaline catalyst ($(CH_3CH_2)_3N$) and with excess of formaldehyde. Values of the activation energies for the addition reactions are present in literature, for instance in [32] and [85]. Here, the values proposed by [85] are used. For the condensation reactions and the following addition reactions of the dimers, an average value has been adopted.

1.5.2.3 Reactions

In the following, all the considered reactions are reported, with the expression of their reaction rates and the values of their pre-exponential factors and activation energies. The notation C_i, ($i = 1, \dots, 7$ and $i = 13$), is adopted to denote the concentration of the element E_i and the notation C_j, ($j = 8, \dots, 12$), is used for the concentration of dimer D_{j-8}.

Addition

1) $E_1 + E_2 \rightarrow E_3$; $\qquad R_1 = k_1 C_1 C_2.$

2) $E_1 + E_2 \rightarrow E_4$; $\qquad R_2 = k_2 C_1 C_2.$

3) $E_3 + E_2 \rightarrow E_5$; $\qquad R_3 = k_3 C_3 C_2.$

4) $E_3 + E_2 \rightarrow E_6$; $\qquad R_4 = k_4 C_3 C_2.$

5) $E_4 + E_2 \rightarrow E_6$; $R_5 = k_5 C_4 C_2$.

6) $E_5 + E_2 \rightarrow E_7$; $R_6 = k_6 C_5 C_2$.

7) $E_6 + E_2 \rightarrow E_7$; $R_7 = k_7 C_6 C_2$.

The values of the pre-exponential factors, $k_{0,i}$, and of the activation energies, $E_{a,i}$ are reported in Table 1.3.

Parameter	Value	Parameter	Value
$k_{0,1}$	$1.13 \cdot 10^5$ [$m^3 \cdot mol^{-1} \cdot s^{-1}$]	$E_{a,1}$	89.1 [kJ$\cdot$ mol^{-1}]
$k_{0,2}$	$2.26 \cdot 10^5$ [$m^3 \cdot mol^{-1} \cdot s^{-1}$]	$E_{a,2}$	91.7 [kJ$\cdot$ mol^{-1}]
$k_{0,3}$	$4.34 \cdot 10^5$ [$m^3 \cdot mol^{-1} \cdot s^{-1}$]	$E_{a,3}$	98.5 [kJ$\cdot$ mol^{-1}]
$k_{0,4}$	$2.09 \cdot 10^5$ [$m^3 \cdot mol^{-1} \cdot s^{-1}$]	$E_{a,4}$	88.2 [kJ$\cdot$ mol^{-1}]
$k_{0,5}$	$1.11 \cdot 10^7$ [$m^3 \cdot mol^{-1} \cdot s^{-1}$]	$E_{a,5}$	99.0 [kJ$\cdot$ mol^{-1}]
$k_{0,6}$	$1.68 \cdot 10^2$ [$m^3 \cdot mol^{-1} \cdot s^{-1}$]	$E_{a,6}$	91.5 [kJ$\cdot$ mol^{-1}]
$k_{0,7}$	$6.99 \cdot 10^5$ [$m^3 \cdot mol^{-1} \cdot s^{-1}$]	$E_{a,7}$	92.2 [kJ$\cdot$ mol^{-1}]

Table 1.3: Parameters of addition reactions.

Condensation

The selected reactions are the following:

8) $E_1 + E_3 \rightarrow D_0$; $R_8 = k_8 C_1 C_3$

9) $E_1 + E_3 \rightarrow D_0$; $R_9 = k_9 C_1 C_3$

10) $E_1 + E_4 \rightarrow D_0$; $R_{10} = k_{10} C_1 C_4$

11) $E_1 + E_4 \rightarrow D_0$; $R_{11} = k_{11} C_1 C_4$

12) $E_1 + E_5 \rightarrow D_1$; $R_{12} = k_{12} C_1 C_5$

13) $E_1 + E_5 \rightarrow D_1$; $R_{13} = k_{13} C_1 C_5$

14) $E_1 + E_6 \rightarrow D_1$; $R_{14} = k_{14} C_1 C_6$

15) $E_1 + E_6 \rightarrow D_1$; $R_{15} = k_{15} C_1 C_6$

16) $E_1 + E_6 \rightarrow D_1$; $R_{16} = k_{16} C_1 C_6$

17) $E_1 + E_6 \rightarrow D_1$; $R_{17} = k_{17}C_1C_6$

18) $E_1 + E_7 \rightarrow D_2$; $R_{18} = k_{18}C_1C_7$

19) $E_1 + E_7 \rightarrow D_2$; $R_{19} = k_{19}C_1C_7$

20) $E_1 + E_7 \rightarrow D_2$; $R_{20} = k_{20}C_1C_7$

21) $E_1 + E_7 \rightarrow D_2$; $R_{21} = k_{21}C_1C_7$

22) $E_3 + E_3 \rightarrow D_0 + E_2$; $R_{22} = k_{22}C_3^2$

23) $E_3 + E_3 \rightarrow D_1$; $R_{23} = k_{23}C_3^2$

24) $E_3 + E_3 \rightarrow D_1$; $R_{24} = k_{24}C_3^2$

25) $E_3 + E_4 \rightarrow D_0 + E_2$; $R_{25} = k_{25}C_3C_4$

26) $E_3 + E_4 \rightarrow D_1$; $R_{26} = k_{26}C_3C_4$

27) $E_3 + E_4 \rightarrow D_1$; $R_{27} = k_{27}C_3C_4$

28) $E_3 + E_4 \rightarrow D_1$; $R_{28} = k_{28}C_3C_4$

29) $E_3 + E_5 \rightarrow D_1 + E_2$; $R_{29} = k_{29}C_3C_5$

30) $E_3 + E_5 \rightarrow D_2$; $R_{30} = k_{30}C_3C_5$

31) $E_3 + E_5 \rightarrow D_2$; $R_{31} = k_{31}C_3C_5$

32) $E_3 + E_5 \rightarrow D_2$; $R_{32} = k_{32}C_3C_5$

33) $E_3 + E_6 \rightarrow D_1 + E_2$; $R_{33} = k_{33}C_3C_6$

34) $E_3 + E_6 \rightarrow D_1 + E_2$; $R_{34} = k_{34}C_3C_6$

35) $E_3 + E_6 \rightarrow D_2$; $R_{35} = k_{35}C_3C_6$

36) $E_3 + E_6 \rightarrow D_2$; $R_{36} = k_{36}C_3C_6$

37) $E_3 + E_6 \rightarrow D_2$; $R_{37} = k_{37}C_3C_6$

38) $E_3 + E_6 \rightarrow D_2$; $R_{38} = k_{38}C_3C_6$

39) $E_3 + E_6 \rightarrow D_2$; $R_{39} = k_{39}C_3C_6$

40) $E_3 + E_7 \rightarrow D_2 + E_2$; $R_{40} = k_{40}C_3C_7$

41) $E_3 + E_7 \rightarrow D_2 + E_2$; $R_{41} = k_{41}C_3C_7$

42) $E_3 + E_7 \rightarrow D_2 + E_2$; $R_{42} = k_{42}C_3C_7$

43) $E_3 + E_7 \rightarrow D_3$; $R_{43} = k_{43}C_3C_7$

44) $E_3 + E_7 \rightarrow D_3$; $R_{44} = k_{44}C_3C_7$

45) $E_3 + E_7 \rightarrow D_3$; $R_{45} = k_{45}C_3C_7$

46) $E_4 + E_4 \rightarrow D_0 + E_2$; $R_{46} = k_{46}C_4^2$

47) $E_4 + E_4 \rightarrow D_1$; $R_{47} = k_{47}C_4^2$

48) $E_4 + E_5 \rightarrow D_1 + E_2$; $R_{48} = k_{48}C_4C_5$

49) $E_4 + E_5 \rightarrow D_2$; $R_{49} = k_{49}C_4C_5$

50) $E_4 + E_5 \rightarrow D_2$; $R_{50} = k_{50}C_4C_5$

51) $E_4 + E_6 \rightarrow D_1 + E_2$; $R_{51} = k_{51}C_4C_6$

52) $E_4 + E_6 \rightarrow D_1 + E_2$; $R_{52} = k_{52}C_4C_6$

53) $E_4 + E_6 \rightarrow D_2$; $R_{53} = k_{53}C_4C_6$

54) $E_4 + E_6 \rightarrow D_2$; $R_{54} = k_{54}C_4C_6$

55) $E_4 + E_6 \rightarrow D_2$; $R_{55} = k_{55}C_4C_6$

56) $E_4 + E_7 \rightarrow D_2 + E_2$; $R_{56} = k_{56}C_4C_7$

57) $E_4 + E_7 \rightarrow D_2 + E_2$; $R_{57} = k_{57}C_4C_7$

58) $E_4 + E_7 \rightarrow D_3$; $R_{58} = k_{58}C_4C_7$

59) $E_4 + E_7 \rightarrow D_3$; $R_{59} = k_{59}C_4C_7$

60) $E_5 + E_5 \rightarrow D_2 + E_2$; $R_{60} = k_{60}C_5^2$

61) $E_5 + E_5 \rightarrow D_3$; $R_{61} = k_{61}C_5^2$

62) $E_5 + E_6 \rightarrow D_2 + E_2$; $R_{62} = k_{62}C_5C_6$

63) $E_5 + E_6 \rightarrow D_2 + E_2$; $R_{63} = k_{63}C_5C_6$

64) $E_5 + E_6 \rightarrow D_3$; $R_{64} = k_{64}C_5C_6$

65) $E_5 + E_6 \rightarrow D_3$; $R_{65} = k_{65} C_5 C_6$

66) $E_5 + E_6 \rightarrow D_3$; $R_{66} = k_{66} C_5 C_6$

67) $E_5 + E_7 \rightarrow D_3 + E_2$; $R_{67} = k_{67} C_5 C_7$

68) $E_5 + E_7 \rightarrow D_3 + E_2$; $R_{68} = k_{68} C_5 C_7$

69) $E_5 + E_7 \rightarrow D_4$; $R_{69} = k_{69} C_5 C_7$

70) $E_5 + E_7 \rightarrow D_4$; $R_{70} = k_{70} C_5 C_7$

71) $E_6 + E_6 \rightarrow D_2 + E_2$; $R_{71} = k_{71} C_6^2$

72) $E_6 + E_6 \rightarrow D_2 + E_2$; $R_{72} = k_{72} C_6^2$

73) $E_6 + E_6 \rightarrow D_2 + E_2$; $R_{73} = k_{73} C_6^2$

74) $E_6 + E_6 \rightarrow D_3$; $R_{74} = k_{74} C_6^2$

75) $E_6 + E_6 \rightarrow D_3$; $R_{75} = k_{75} C_6^2$

76) $E_6 + E_7 \rightarrow D_3 + E_2$; $R_{76} = k_{76} C_6 C_7$

77) $E_6 + E_7 \rightarrow D_3 + E_2$; $R_{77} = k_{77} C_6 C_7$

78) $E_6 + E_7 \rightarrow D_3 + E_2$; $R_{78} = k_{78} C_6 C_7$

79) $E_6 + E_7 \rightarrow D_3 + E_2$; $R_{79} = k_{79} C_6 C_7$

80) $E_6 + E_7 \rightarrow D_4$; $R_{80} = k_{80} C_6 C_7$

81) $E_6 + E_7 \rightarrow D_4$; $R_{81} = k_{81} C_6 C_7$

82) $E_7 + E_7 \rightarrow D_4 + E_2$; $R_{82} = k_{82} C_7^2$

83) $E_7 + E_7 \rightarrow D_4 + E_2$; $R_{83} = k_{83} C_7^2$

84) $E_7 + E_7 \rightarrow D_4 + E_2$; $R_{84} = k_{84} C_7^2$

As aforementioned, the activation energies of these reactions have been considered equal to an average value of 90 [kJ$\cdot$ mol^{-1}]; the values of the pre-exponential factors, $k_{0,i}$ are reported in Table 1.5.

Addition of dimers

In this phase the dimers react with the formaldehyde to produce dimers characterized by a different structure. Because of the use of aggregate dimers, these reactions are fictitious and each of them represents a set of real reactions.

A85) $D_0 + E_2 \rightarrow D_1$; $\qquad R_{85} = k_{85} C_8 C_2$

A86) $D_1 + E_2 \rightarrow D_2$; $\qquad R_{86} = k_{86} C_9 C_2$

A87) $D_2 + E_2 \rightarrow D_3$; $\qquad R_{87} = k_{87} C_{10} C_2$

A88) $D_3 + E_2 \rightarrow D_4$; $\qquad R_{88} = k_{88} C_{11} C_2$

As for the condensation reactions, an average activation energy of 90 [kJ$\cdot$ mol^{-1}] has been considered as well. The pre-exponential factors are computed as average values of the pre-exponential factors of addition reactions. Their values are reported in Table 1.4.

Parameter	Value	Parameter	Value
$k_{0,85}$	$1.40 \cdot 10^5$ [m$^3 \cdot$ mol$^{-1} \cdot$ s^{-1}]	$k_{0,86}$	$2.41 \cdot 10^5$ [m$^3 \cdot$ mol$^{-1} \cdot$ s^{-1}]
$k_{0,87}$	$2.20 \cdot 10^5$ [m$^3 \cdot$ mol$^{-1} \cdot$ s^{-1}]	$k_{0,88}$	$2.52 \cdot 10^5$ [m$^3 \cdot$ mol$^{-1} \cdot$ s^{-1}]

Table 1.4: Pre-exponential factors of reactions of addition of dimers.

Condensation of dimers

In this phase the dimers react with the monomers. There are hundreds of possible reaction, but, here, only this fictitious one is considered

$$\sum_{i=1, i\neq 2}^{7} E_i + \sum_{j=0}^{4} D_j \rightarrow E_{13},$$

with reaction rate

$$R_{89} = k_{89} \left(\sum_{i=1, i\neq 2}^{7} C_i \right) \left(\sum_{j=8}^{12} C_j \right).$$

The pre-exponential factor is an average values of the pre-exponential factors of the selected condensation reactions and it has the value of $k_{0,89} = 9.69 \cdot 10^3$ [m$^3 \cdot$ mol$^{-1} \cdot$ s^{-1}]. As usual, the activation energy, $E_{a,89}$, is adopted equal to 90.0 [kJ$\cdot$ mol^{-1}].

1.5.3 Mass balances

Let us consider an ideal jacketed batch reactor, in which the phenol-formaldehyde reaction takes place. The mathematical model for this system is given by the mass balances of the thirteen chemical species and by the energy balances in the reactor and in the jacket.

The mass balances, according to equation (1.5), are the following:

$$
\begin{aligned}
\dot{C}_1 &= -R_1 - R_2 - R_8 - R_9 - R_{10} - R_{11} - R_{12} - R_{13} - R_{14} - R_{15} - R_{16} \\
&\quad -R_{17} - R_{18} - R_{19} - R_{20} - R_{21} - \frac{1}{6}R_{89}; \\
\dot{C}_2 &= -R_1 - R_2 - R_3 - R_4 - R_5 - R_6 - R_7 - R_{85} - R_{86} - R_{87} - R_{88} \\
&\quad +R_{22} + R_{26} + R_{29} + R_{33} + R_{34} + R_{40} + R_{41} + R_{42} + R_{47} + R_{50} + R_{51} \\
&\quad +R_{54} + R_{58} + R_{59} + R_{60} + R_{62} + R_{63} + R_{67} + R_{68} + R_{71} + R_{72} + R_{74} \\
&\quad +R_{76} + R_{77} + R_{78} + R_{79} + R_{82} + R_{83} + R_{84}; \\
\dot{C}_3 &= -R_3 - R_4 - R_8 - R_9 - 2R_{22} - 2R_{23} - 2R_{24} - R_{25} - R_{26} - R_{27} \\
&\quad -R_{28} - R_{29} - R_{30} - R_{31} - R_{32} - R_{33} - R_{34} - R_{35} - R_{36} - R_{37} \\
&\quad -R_{38} - R_{39} - R_{40} - R_{41} - R_{42} - R_{43} - R_{44} - R_{45} - \frac{1}{6}R_{89} + R_1; \\
\dot{C}_4 &= -R_5 - R_{10} - R_{11} - R_{25} - R_{26} - R_{27} - R_{28} - 2R_{46} - 2R_{47} - R_{48} \\
&\quad -R_{49} - R_{50} - R_{51} - R_{52} - R_{53} - R_{54} - R_{55} - R_{56} - R_{57} - R_{58} \\
&\quad -R_{59} - \frac{1}{6}R_{89} + R_2; \\
\dot{C}_5 &= -R_6 - R_{12} - R_{13} - R_{29} - R_{30} - R_{31} - R_{32} - R_{53} - R_{54} - R_{55} \\
&\quad -2R_{60} - 2R_{61} - R_{62} - R_{63} - R_{64} - R_{65} - R_{66} - R_{67} - R_{68} \\
&\quad -R_{69} - R_{70} - \frac{1}{6}R_{89} + R_3; \\
\dot{C}_6 &= -R_7 - R_{14} - R_{15} - R_{16} - R_{17} - R_{33} - R_{34} - R_{35} - R_{36} - R_{37} - R_{38} \\
&\quad -R_{39} - R_{48} - R_{49} - R_{50} - R_{51} - R_{52} - R_{62} - R_{63} - R_{64} - R_{65} - R_{66} \\
&\quad -2R_{71} - 2R_{72} - 2R_{73} - 2R_{74} - 2R_{75} - R_{76} - R_{77} - R_{78} - R_{79} \\
&\quad -R_{80} - R_{81} - \frac{1}{6}R_{89} + R_4 + R_5; \\
\dot{C}_7 &= -R_{18} - R_{19} - R_{20} - R_{21} - R_{40} - R_{41} - R_{42} - R_{43} - R_{44} - R_{45} - R_{56} \\
&\quad -R_{57} - R_{58} - R_{59} - R_{67} - R_{68} - R_{69} - R_{70} - R_{76} - R_{77} - R_{78} - R_{79} \\
&\quad -R_{80} - R_{81} - 2R_{82} - 2R_{83} - 2R_{84} - \frac{1}{6}R_{89} + R_6 + R_7; \\
\dot{C}_8 &= -R_{85} - \frac{1}{5}R_{89} + R_8 + R_9 + R_{10} + R_{11} + R_{22} + R_{26} + R_{47};
\end{aligned}
$$

$$
\begin{aligned}
\dot{C}_9 &= -R_{86} - \frac{1}{5}R_{89} + R_{12} + R_{13} + R_{14} + R_{15} + R_{16} + R_{17} + R_{23} + R_{24} \\
&\quad + R_{25} + R_{27} + R_{28} + R_{29} + R_{33} + R_{34} + R_{46} + R_{50} + R_{51} + R_{54} + R_{85}; \\
\dot{C}_{10} &= -R_{87} - \frac{1}{5}R_{89} + R_5 + R_{18} + R_{19} + R_{20} + R_{21} + R_{30} + R_{31} + R_{32} \\
&\quad + R_{35} + R_{36} + R_{37} + R_{38} + R_{39} + R_{40} + R_{41} + R_{42} + R_{48} + R_{49} + R_{52} \\
&\quad + R_{53} + R_{55} + R_{58} + R_{59} + R_{60} + R_{62} + R_{63} + R_{71} + R_{72} + R_{74} + R_{86}; \\
\dot{C}_{11} &= -R_{88} - \frac{1}{5}R_{89} + R_{43} + R_{44} + R_{45} + R_{56} + R_{57} + R_{61} + R_{64} + R_{65} \\
&\quad + R_{66} + R_{67} + R_{68} + R_{73} + R_{75} + R_{76} + R_{77} + R_{78} + R_{79} + R_{87}; \\
\dot{C}_{12} &= -\frac{1}{5}R_{89} + R_{69} + R_{70} + R_{80} + R_{81} + R_{82} + R_{83} + R_{84} + R_{88}; \\
\dot{C}_{13} &= R_{89}.
\end{aligned}
$$

1.5.4 Heat released by the reaction

In order to write the energy balance in the reactor (equation (1.8)), the following expression for the heat released by the reaction can be adopted

$$
Q = -V_r \Delta H_{ad} \left(\sum_{i=1}^{7} R_i + \sum_{i=85}^{88} R_i \right) - V_r \Delta H_{con} \left(\sum_{i=8}^{84} R_i + R_{89} \right), \tag{1.19}
$$

where V_r is the volume of the reactor; ΔH_{ad} and ΔH_{con} are the average molar enthalpy changes for the addition and condensation phases, respectively. The values of these parameter are $\Delta H_{ad} = -20.3$ [kJ mol^{-1}] and $\Delta H_{con} = -98.7$ [kJ mol^{-1}], [46]. According to equation (1.11), both the addition and the condensation reactions are exothermic.

Parameter	Value	Parameter	Value	Parameter	Value
$k_{0,8}$	$3.65 \cdot 10^3$	$k_{0,9}$	$3.01 \cdot 10^3$	$k_{0,10}$	$1.91 \cdot 10^3$
$k_{0,11}$	$2.31 \cdot 10^3$	$k_{0,12}$	$2.75 \cdot 10^4$	$k_{0,13}$	$2.28 \cdot 10^4$
$k_{0,14}$	$1.59 \cdot 10^3$	$k_{0,15}$	$1.32 \cdot 10^3$	$k_{0,16}$	$2.04 \cdot 10^3$
$k_{0,17}$	$1.68 \cdot 10^3$	$k_{0,18}$	$7.38 \cdot 10^3$	$k_{0,19}$	$6.10 \cdot 10^3$
$k_{0,20}$	$8.57 \cdot 10^3$	$k_{0,21}$	$7.08 \cdot 10^3$	$k_{0,22}$	$1.45 \cdot 10^3$
$k_{0,23}$	$1.83 \cdot 10^4$	$k_{0,24}$	$2.89 \cdot 10^3$	$k_{0,25}$	$9.17 \cdot 10^2$
$k_{0,26}$	$1.23 \cdot 10^4$	$k_{0,27}$	$5.81 \cdot 10^3$	$k_{0,28}$	$3.62 \cdot 10^2$
$k_{0,29}$	$1.09 \cdot 10^4$	$k_{0,30}$	$2.39 \cdot 10^0$	$k_{0,31}$	$6.92 \cdot 10^4$
$k_{0,32}$	$4.32 \cdot 10^3$	$k_{0,33}$	$6.32 \cdot 10^2$	$k_{0,34}$	$8.08 \cdot 10^2$
$k_{0,35}$	$7.86 \cdot 10^3$	$k_{0,36}$	$5.12 \cdot 10^3$	$k_{0,37}$	$4.00 \cdot 10^3$
$k_{0,38}$	$2.50 \cdot 10^2$	$k_{0,39}$	$3.19 \cdot 10^2$	$k_{0,40}$	$2.93 \cdot 10^3$
$k_{0,41}$	$3.40 \cdot 10^3$	$k_{0,42}$	$1.85 \cdot 10^4$	$k_{0,43}$	$2.15 \cdot 10^4$
$k_{0,44}$	$1.16 \cdot 10^3$	$k_{0,45}$	$1.34 \cdot 10^3$	$k_{0,46}$	$5.82 \cdot 10^2$
$k_{0,47}$	$1.56 \cdot 10^4$	$k_{0,48}$	$6.93 \cdot 10^3$	$k_{0,49}$	$9.29 \cdot 10^4$
$k_{0,50}$	$1.52 \cdot 10^0$	$k_{0,51}$	$5.12 \cdot 10^2$	$k_{0,52}$	$4.01 \cdot 10^2$
$k_{0,53}$	$5.37 \cdot 10^3$	$k_{0,54}$	$6.87 \cdot 10^3$	$k_{0,55}$	$4.98 \cdot 10^3$
$k_{0,56}$	$1.86 \cdot 10^3$	$k_{0,57}$	$2.15 \cdot 10^3$	$k_{0,58}$	$2.49 \cdot 10^4$
$k_{0,59}$	$2.89 \cdot 10^4$	$k_{0,60}$	$8.26 \cdot 10^4$	$k_{0,61}$	$3.61 \cdot 10$
$k_{0,62}$	$4.78 \cdot 10^3$	$k_{0,63}$	$6.10 \cdot 10^3$	$k_{0,64}$	$5.93 \cdot 10^4$
$k_{0,65}$	$1.05 \cdot 10^0$	$k_{0,66}$	$1.34 \cdot 10^0$	$k_{0,67}$	$2.21 \cdot 10^4$
$k_{0,68}$	$2.68 \cdot 10^4$	$k_{0,69}$	$4.48 \cdot 10^0$	$k_{0,70}$	$5.62 \cdot 10^0$
$k_{0,71}$	$2.76 \cdot 10^2$	$k_{0,72}$	$7.06 \cdot 10^2$	$k_{0,73}$	$4.51 \cdot 10^2$
$k_{0,74}$	$6.87 \cdot 10^3$	$k_{0,75}$	$8.78 \cdot 10^3$	$k_{0,76}$	$1.28 \cdot 10^3$
$k_{0,77}$	$1.49 \cdot 10^3$	$k_{0,78}$	$1.64 \cdot 10^3$	$k_{0,79}$	$1.90 \cdot 10^3$
$k_{0,80}$	$1.59 \cdot 10^4$	$k_{0,81}$	$1.85 \cdot 10^4$	$k_{0,82}$	$5.93 \cdot 10^3$
$k_{0,83}$	$1.38 \cdot 10^4$	$k_{0,84}$	$7.98 \cdot 10^3$		

Table 1.5: Pre-exponential factors, in $[m^3 \cdot mol^{-1} \cdot s^{-1}]$, of condensation reactions.

Chapter 2

Identification of reaction dynamics

2.1 Introduction

Most nonlinear process control and diagnosis strategies require an explicit mathematical model of process dynamics. Thus, control or diagnosis of the phenol-formaldehyde reaction may require a reliable model of the reaction dynamics. Since the model of phenol-formaldehyde reaction devised in Chapter 1 is characterized by 15 differential equations, it could be unsuitable for on-line computations. Also, such a complex and high dimensional model could be not useful to design control and diagnosis schemes. In fact, the computational complexity of a control scheme grows rapidly as the model complexity increases. For this reason, to control purposes, a model that satisfies two important criteria is needed. First, it must be compatible, in structure and complexity with the requirements of the control system design methodology. The second criterion is that the model must approximate the process dynamics well enough so as the resulting control system will perform adequately in practice. In this thesis, an identification technique has been adopted to estimate the parameters of a number of reduced-order models, able to effectively predict the heat released by the reaction as well as the concentration of the desired product.

2.2 Model identification

In general, a systematic approach to model identification consists of the following steps [45, 63]:

1. generation of a set of input-output data;

2. selection of a general class of models to be considered;

3. selection of a number of models to be fit;

4. estimation of model parameters;

5. validation of identified models.

The problem of model identification is not strictly a mathematical problem. In particular, the model structure selection, the choice of the parameter number and the model validation involve considerable subjective judgement.

The input-output data can be obtained via an experimental procedure or via a simulation study. In the first case the problem is to find the model that better fit the experimental data; if the data are produced in simulation, the problem consists in finding a simplified model which has a behavior as similar as possible to the complete one.

As regards the model structure, the following options should be considered [13, 45]:

- black-box model;
- parameter white-box model;
- hybrid grey-box model.

In the first case, the system is represented as an empirical input-output model, e.g., an ARMAX-type model or a model based on Artificial Neural Networks. The parameter white-box models are based on the knowledge of the system dynamics and are characterized by some poorly known parameters to be estimated. The hybrid grey-box models are a combination of the previous ones; they are characterized by a simplified structure based on some qualitative knowledge of the system and by unknown parameters to be identified. All of these class of models have some advantages and some drawbacks: white box models have the best performance, but they can be adopted only in the presence of a deep knowledge of the system; empirical input-output models (black-box models) are the simplest to obtain, but they, usually, are able to represent the system only in the expertise domain in which the data are collected; grey box models allow to preserve the physical sense of the system, but, due to the simplified structure, they lose some information with respect to the white-box models.

Once a model structure is chosen, the parameters appearing in it must be estimated. To this aim, an objective function, that determines the goodness of data fitting must be selected. From maximum likelihood analysis, several alternative objective functions can

be chosen. These can range from simple least-squares functions to fairly complex non-linear functions, that incorporate general unknown covariance of the measurements (see e.g., [6]). The final step is to optimize the model parameters in the objective function. Since the optimization problem formed by the model and the objective function, may require repeated and expensive solutions of differential equations, an efficient algorithm should minimize the number of evaluations and, at the same time, converge easily to solution. Usually, these algorithms require gradient information and some approximation to the second derivatives matrix. For least-squares type objective functions, the Newton-Raphson and the Levenberg-Marquardt algorithms provide the second derivative information quite easily [11,63].

In this Chapter, a general overview of the optimization methods for parameter identification and an application of these methods to the phenol-formaldehyde reaction are presented.

2.3 Parameter estimation

Consider a system, whose input-output relationship is described by the function $\zeta : \mathbb{R}^q \rightarrow \mathbb{R}^m$, and a set of input-output data $\mathcal{D} = \{(\boldsymbol{x}_i, \boldsymbol{y}_i), \boldsymbol{x}_i \in \mathbb{R}^q, \boldsymbol{y}_i \in \mathbb{R}^m, i = 1, \cdots, n\}$. The output data $\boldsymbol{y}_i$ and the input data $\boldsymbol{x}_i$ are related by the following relationship

$$\boldsymbol{y}_i = \zeta(\boldsymbol{x}_i) + \boldsymbol{\varepsilon}_i$$

where $\boldsymbol{\varepsilon}_i$ models the effect of disturbances and measurement errors.

Let suppose that a certain model structure $\mathcal{M}(\boldsymbol{\theta})$ has been selected, which is parametrized via the parameters vector $\boldsymbol{\theta} \in \mathbb{R}^p$. The set of candidate models $\mathcal{M}^*$ is defined as

$$\mathcal{M}^* = \{\mathcal{M}(\boldsymbol{\theta}) : \boldsymbol{\theta} \in \mathbb{R}^p\}.$$

The search of the best model within the set $\mathcal{M}^*$ becomes a problem of determining or estimating the parameters vector $\boldsymbol{\theta}$. Hence, it is necessary looking for testing procedure aimed at evaluating the different models ability to reproduce the experimental data.

Define n vectors of residual errors as ($i = 1, \cdots, n$)

$$\boldsymbol{r}_i(\boldsymbol{\theta}) = \boldsymbol{y}_i - \widehat{\boldsymbol{y}}_i(\boldsymbol{\theta}), \tag{2.1}$$

where $\widehat{\boldsymbol{y}}_i(\boldsymbol{\theta})$ is the output computed by the model $\mathcal{M}(\boldsymbol{\theta})$ corresponding to the input $\boldsymbol{x}_i$.

The simplest way to describe the goodness of each model is the least-squares criterion. This criterion leads to the following objective function

$$U(\boldsymbol{\theta}) = \sum_{i=1}^{n} \|\boldsymbol{r}_i(\boldsymbol{\theta})\|^2 = \sum_{i=1}^{n}\sum_{j=1}^{m} r_{i,j}^2(\boldsymbol{\theta}), \tag{2.2}$$

where $r_{i,j}(\boldsymbol{\theta})$ is the j_{th} component of the vector $\boldsymbol{r}_i(\boldsymbol{\theta})$.

An alternative is represented by the weighted least-squares criterion, in which different weights, $w_{i,j}$, are assigned at the different residuals, $r_{i,j}(\boldsymbol{\theta})$. The resulting objective function is the following

$$U(\boldsymbol{\theta}) = \sum_{i=1}^{n}\sum_{j=1}^{m} w_{i,j}\, r_{i,j}^2(\boldsymbol{\theta}). \tag{2.3}$$

The weighted least-squares criterion is useful when different measurement data are characterized by different precision: in this case a suitable choice for the weights can be the following

$$w_{i,j} = \frac{1}{\sigma_{i,j}^2},$$

where $\sigma_{i,j}^2$ is the variance of the component j_{th} of the measured value $\boldsymbol{y}_i$.

The value of the objective function (2.2) or (2.3) depends on the value of the parameters vector. Hence, the parameters estimation problem becomes an optimization problem, i.e., the target is to find the vector $\boldsymbol{\theta}^*$ that optimize the objective function.

2.4 Optimization algorithms for parameters estimation

Several algorithms have been developed to optimize the least-squares objective function, [11,61,69]. The problem is relatively straightforward to solve for linear in the parameters models, but it becomes more and more complex in the presence of models nonlinear in the parameters. In this section the most used methods to solve the optimization problem are presented.

2.4.1 Linear models

The linear regression model structure is very used in practice, in which the model $\mathcal{M}(\boldsymbol{\theta})$ is characterized by the following structure

$$\widehat{\boldsymbol{y}}(\boldsymbol{\theta}) = \boldsymbol{\Phi}(\boldsymbol{x})\,\boldsymbol{\theta}, \tag{2.4}$$

where

$$\widehat{\boldsymbol{y}}(\boldsymbol{\theta}) = \begin{bmatrix} \widehat{y}_1(\boldsymbol{\theta}) \\ \widehat{y}_2(\boldsymbol{\theta}) \\ \vdots \\ \widehat{y}_m(\boldsymbol{\theta}) \end{bmatrix}, \quad \boldsymbol{\Phi}(\boldsymbol{x}) = \begin{bmatrix} \phi_{1\,1}(\boldsymbol{x}) & \phi_{1\,2}(\boldsymbol{x}) & \cdots & \phi_{1\,p}(\boldsymbol{x}) \\ \phi_{2\,1}(\boldsymbol{x}) & \phi_{2\,2}(\boldsymbol{x}) & \cdots & \phi_{2\,p}(\boldsymbol{x}) \\ \vdots & \vdots & \vdots & \vdots \\ \phi_{m\,1}(\boldsymbol{x}) & \phi_{m\,2}(\boldsymbol{x}) & \cdots & \phi_{m\,p}(\boldsymbol{x}) \end{bmatrix}, \quad \boldsymbol{\theta} = \begin{bmatrix} \theta_1 \\ \theta_2 \\ \vdots \\ \theta_p \end{bmatrix}.$$

The optimal value of the parameters vector is given by the solution of the following system of equations ($k = 1, \cdots, p$)

$$\frac{\partial U(\boldsymbol{\theta})}{\partial \theta_k} = 0. \tag{2.5}$$

From equation (2.3) the following chain of equalities can be derived

$$\begin{aligned} \frac{\partial U(\boldsymbol{\theta})}{\partial \theta_k} &= -2 \sum_{i=1}^{n} \sum_{j=1}^{m} w_{i,j} \left[\left(y_{i,j} - \widehat{y}_{i,j}(\boldsymbol{\theta}) \right) \frac{\partial \widehat{y}_{i,j}(\boldsymbol{\theta})}{\partial \theta_k} \right] = \\ &= -2 \sum_{i=1}^{n} \sum_{j=1}^{m} w_{i,j} \left[r_{i,j} \frac{\partial \widehat{y}_{i,j}(\boldsymbol{\theta})}{\partial \theta_k} \right], \end{aligned} \tag{2.6}$$

where $\widehat{y}_{i,j}(\boldsymbol{\theta})$ is the j_{th} component of the vector $\widehat{\boldsymbol{y}}_i(\boldsymbol{\theta})$ obtained via (2.4) for $\boldsymbol{x} = \boldsymbol{x}_i$.

For the linear regression model (2.4) the following is obtained

$$\frac{\partial \widehat{y}_{i,j}(\boldsymbol{\theta})}{\partial \theta_k} = \frac{\partial}{\partial \theta_k} \left(\sum_{h=1}^{p} \theta_h \phi_{j\,h}(\boldsymbol{x}_i) \right) = \phi_{j\,k}(\boldsymbol{x}_i). \tag{2.7}$$

Therefore, equation (2.6) becomes

$$\frac{\partial U(\boldsymbol{\theta})}{\partial \theta_k} = -2 \sum_{i=1}^{n} \sum_{j=1}^{m} w_{i,j} \left[r_{i,j} \phi_{j\,k}(\boldsymbol{x}_i) \right], \qquad (k = 1, \cdots, p). \tag{2.8}$$

Substituting the equation (2.8) in the equation (2.5) a system of linear equation in the parameters is obtained. In matrix form it becomes

$$\frac{\partial U(\boldsymbol{\theta})}{\partial \boldsymbol{\theta}} = -2 \left(\boldsymbol{y}^T \boldsymbol{W} \boldsymbol{\Psi} - \boldsymbol{\theta}^T \boldsymbol{\Psi}^T \boldsymbol{W} \boldsymbol{\Psi} \right) = \boldsymbol{0}, \tag{2.9}$$

where

$$\boldsymbol{\Psi} = \begin{bmatrix} \boldsymbol{\Phi}(\boldsymbol{x}_1) \\ \boldsymbol{\Phi}(\boldsymbol{x}_2) \\ \vdots \\ \boldsymbol{\Phi}(\boldsymbol{x}_n) \end{bmatrix}, \quad \boldsymbol{y} = \begin{bmatrix} \boldsymbol{y}_1 \\ \boldsymbol{y}_2 \\ \vdots \\ \boldsymbol{y}_n \end{bmatrix},$$

$$\boldsymbol{W} = diag\{\boldsymbol{W}_1, \cdots, \boldsymbol{W}_n\}, \quad \boldsymbol{W}_j = diag\{w_{j,1}, \cdots, w_{j,m}\}, \quad j = (1, \cdots, n).$$

The solution of equation (2.9) can be obtained via the well-known left (weighted) pseudoinverse of $\boldsymbol{\Psi}$

$$\boldsymbol{\theta}^* = (\boldsymbol{\Psi}^T \boldsymbol{W} \boldsymbol{\Psi})^{-1} \boldsymbol{\Psi}^T \boldsymbol{W} \boldsymbol{y}. \tag{2.10}$$

If the least-squares objective function (2.2) is adopted, the weight matrix $\boldsymbol{W}$ is the identity matrix, and equations (2.9) and (2.10) become

$$\frac{\partial U(\boldsymbol{\theta})}{\partial \boldsymbol{\theta}} = -2 \left(\boldsymbol{y}^T \boldsymbol{\Psi} - \boldsymbol{\theta}^T \boldsymbol{\Psi}^T \boldsymbol{\Psi} \right) = \mathbf{0}, \tag{2.11}$$

$$\boldsymbol{\theta}^* = (\boldsymbol{\Psi}^T \boldsymbol{\Psi})^{-1} \boldsymbol{\Psi}^T \boldsymbol{y}. \tag{2.12}$$

It is worth noticing that the solution (2.10), or (2.12), is the optimal solution, i.e., it corresponds to the global minimum of the objective function.

2.4.2 Nonlinear models

For nonlinear in the parameters models the optimization problem is much more complex. The optimization of the objective function, i.e., the best estimate of the parameters, is obtained via iterative methods. These methods can be classified in [6]:

1. *zero-order methods*, based only on the values taken by the objective function at each step;

2. *first-order methods*, based on the values taken by the objective function and of its gradient at each step;

3. *second-order methods*, based on the values taken by the objective function, its gradient and its Hessian matrix (or an approximation of Hessian) at each step.

The zero-order methods are, generally, very inefficient to converge to the solution. A number of gradient-based algorithms have been developed; they are characterized by the computation of a search direction and by the determination of the step length to take along this direction. The first and second-order algorithms may ensure efficient and fast convergence of the algorithm, but they usually converge to a local minimum of the objective function, i.e., they provide a sub-optimal solution. For this reason, they can give different solution varying the initial estimate of the parameters vector, $\boldsymbol{\theta}_0$. To overcome this problem, it is advisable to compare the results obtained using different initial guesses of the parameters vector.

In the following, the most used optimization algorithm are briefly described.

2.4.2.1 Steepest descent algorithm

The steepest descent algorithm, proposed by Cauchy in 1845, is the simplest first-order algorithm. The gradient vector of the objective function, $\nabla U(\boldsymbol{\theta})$, represents the direction of faster increasing of the function. Hence, if

$$\overline{\boldsymbol{\theta}} = \boldsymbol{\theta} - \kappa \nabla U(\boldsymbol{\theta}), \tag{2.13}$$

for a step size, $\kappa > 0$, small enough, then $U(\overline{\boldsymbol{\theta}}) \leq U(\boldsymbol{\theta})$. In this way a recursive law can be adopted in order to compute a sequence of parameter vectors such as

$$\boldsymbol{\theta}_{i+1} = \boldsymbol{\theta}_i - \kappa \nabla U(\boldsymbol{\theta}_i). \tag{2.14}$$

The gradient computed in $\boldsymbol{\theta}_i$ is the best direction only in the neighborhood of $\boldsymbol{\theta}_i$; therefore this algorithm may require a large number of iterations to converge towards a local minimum. In particular, it converges very slowly in the neighborhood of the minimum. If the curvature of the objective function is very different along distinct directions, a possible solution can be to adopt a different value for the step size, κ, at every iteration; however finding the optimal value of κ for each step can be very time-consuming.

To overcome these drawbacks of the steepest descent, the second-order algorithms, based on the inversion of the Hessian matrix, can be adopted.

2.4.2.2 Newton-Raphson algorithm

It is the simplest second-order algorithm. The function $U(\boldsymbol{\theta})$ may be approximated by the linear portion of the Taylor's series expansion, i.e.,

$$U(\boldsymbol{\theta}) \simeq U(\boldsymbol{\theta}_0) + \nabla U(\boldsymbol{\theta}_0)(\boldsymbol{\theta} - \boldsymbol{\theta}_0) + \frac{1}{2}(\boldsymbol{\theta} - \boldsymbol{\theta}_0)^T \boldsymbol{H}(\boldsymbol{\theta}_0)(\boldsymbol{\theta} - \boldsymbol{\theta}_0), \tag{2.15}$$

where $\boldsymbol{H}(\boldsymbol{\theta})$ is the Hessian matrix, whose elements, h_{ij}, are given by

$$h_{ij} = \frac{\partial^2 U(\boldsymbol{\theta})}{\partial \theta_i \partial \theta_j}. \tag{2.16}$$

The derivative of the function (2.15) yields

$$\frac{\partial U(\boldsymbol{\theta})}{\partial \boldsymbol{\theta}} = \nabla U(\boldsymbol{\theta}_0) + \boldsymbol{H}(\boldsymbol{\theta}_0)(\boldsymbol{\theta} - \boldsymbol{\theta}_0) = 0. \tag{2.17}$$

From equation (2.17) the value of the parameters vector can be obtained

$$\boldsymbol{\theta} = \boldsymbol{\theta}_0 - \boldsymbol{H}^{-1}(\boldsymbol{\theta}_0) \nabla U(\boldsymbol{\theta}_0). \tag{2.18}$$

In order to obtain an iterative estimation law, equation (2.18) is corrected by introducing a step size, κ

$$\boldsymbol{\theta}_{i+1} = \boldsymbol{\theta}_i - \kappa \boldsymbol{H}^{-1}(\boldsymbol{\theta}_i) \nabla U(\boldsymbol{\theta}_i). \tag{2.19}$$

The direction given by $-\boldsymbol{H}^{-1}(\boldsymbol{\theta}_i)\nabla U(\boldsymbol{\theta}_i)$ is a descent direction only when the Hessian matrix is positive definite. For this reason the Newton-Raphson algorithm is less robust than the steepest descent, and thus does not guarantee the convergence towards a local minimum. On the other hand, when the Hessian matrix is positive definite, and in particular in a neighborhood of the minimum, the algorithm converges much faster than the first-order methods.

2.4.2.3 Levenberg-Marquardt algorithm

This method interpolates between the Newton-Raphson algorithm and the steepest descent. It is more robust than the Newton-Raphson algorithm, i.e., in many cases it is able to find a solution even if starts very far off the minimum. On the other hand, for well behaved functions and for reasonable starting points, it tends to be a bit slower than the Newton-Raphson algorithm.

If the Hessian matrix is bad conditioned, the computation of $\boldsymbol{H}^{-1}(\boldsymbol{\theta})$ becomes numerically unstable and the solution may be brought to divergence. To overcome this problem, several algorithms in which the Hessian matrix is replaced by a suitable positive definite matrix $\boldsymbol{G}(\boldsymbol{\theta})$ have been proposed. The most important of these algorithms was firstly proposed by Kenneth Levenberg in 1944 [61], and then rediscovered and improved by Donald Marquardt in 1963 [69].

In detail, the iterative law is given by

$$\boldsymbol{\theta}_{i+1} = \boldsymbol{\theta}_i - \kappa \boldsymbol{G}^{-1}(\boldsymbol{\theta}_i) \nabla U(\boldsymbol{\theta}_i), \tag{2.20}$$

with

$$\boldsymbol{G}(\boldsymbol{\theta}_i) = \boldsymbol{H}(\boldsymbol{\theta}_i) + \lambda_i \boldsymbol{I}, \tag{2.21}$$

where $\boldsymbol{I}$ is the identity matrix having the same dimensions of $\boldsymbol{H}(\boldsymbol{\theta})$ and λ_i is a nonnegative damping factor. The damping factor is of the utmost importance for the Levenberg-Marquardt algorithm: if $\lambda_i = 0$, it coincides with the Newton-Raphson algorithm; if $\lambda_i >> 0$ the matrix $\boldsymbol{G}(\boldsymbol{\theta}_i)$ is diagonal dominant and it means that $\boldsymbol{G}(\boldsymbol{\theta}_i)\nabla U(\boldsymbol{\theta}_i) \approx \lambda_i \nabla U(\boldsymbol{\theta}_i)$, in other words the Levenberg-Marquardt algorithm coincides with the steepest descent method.

Various more or less heuristic arguments have been put forward for the best choice of the damping factor. Marquardt recommended to start with a reasonable high value λ_0 and a factor $\nu > 1$ [69]. Initially, setting $\lambda = \lambda_0$ the Levenberg-Marquardt algorithm proceeds as the steepest descent method, then the damping factor can be reduced, step by step, of a factor ν in such a way that in the neighborhood of the minimum the algorithm proceeds as the Newton-Raphson one.

The Levenberg-Marquardt algorithm can be summarized in the following steps:

1. Choose a reasonable value of initial point $\boldsymbol{\theta}_0$, an initial value of the damping factor λ_0 and a factor ν.
2. Set $\boldsymbol{\theta} = \boldsymbol{\theta}_0$, $\lambda = \lambda_0$.
3. Compute $U(\boldsymbol{\theta})$.
4. Using (2.20), compute $\boldsymbol{\theta}_{new}$
5. Compute $U(\boldsymbol{\theta}_{new})$ and compare with $U(\boldsymbol{\theta})$:
   - **(i)** if $U(\boldsymbol{\theta}_{new}) \leq U(\boldsymbol{\theta})$ the algorithm proceeds in the right direction, therefore set $\boldsymbol{\theta} = \boldsymbol{\theta}_{new}$ and $\lambda = \lambda/\nu$;
   - **(ii)** if $U(\boldsymbol{\theta}_{new}) \geq U(\boldsymbol{\theta})$ the algorithm proceeds in the wrong direction, therefore set $\lambda = \nu\lambda$ and return to step 4.
6. Repeat step $3 - 4$ until a minimum of the objective function is not found.

2.4.3 Implicit nonlinear models

Several systems can be represented only via implicit functions, for which it is very difficult, or sometimes impossible at all, obtain the explicit function $\widehat{\boldsymbol{y}}(\boldsymbol{x}, \boldsymbol{\theta})$.

This is the typical case of chemical reactors, which are described via balance equations of the following type

$$\frac{d\widehat{\boldsymbol{y}}}{dt} = \Omega(t, \widehat{\boldsymbol{y}}, \boldsymbol{x}, \boldsymbol{\theta}). \tag{2.22}$$

Since for these models the explicit function $\widehat{\boldsymbol{y}}(\boldsymbol{x}, \boldsymbol{\theta})$ to compare with the experimental data is not available, it is also impossible to directly compute both the gradient and the Hessian matrix of the least squares objective function.

Therefore, in order to apply the algorithms previously introduced for parameters estimation of implicit models, a procedure to obtain the gradient and the Hessian matrix, based on the sensitivity coefficients, is reported [6, 11, 96].

The k_{th} component of the gradient vector of the objective function (2.3), has the form

$$\frac{\partial U(\boldsymbol{\theta})}{\partial \theta_k} = -2 \sum_{i=1}^{n} \sum_{j=1}^{m} w_{i,j} \left[r_{i,j} \frac{\partial \widehat{y}_{i,j}(\boldsymbol{\theta})}{\partial \theta_k} \right]. \tag{2.23}$$

By differentiating equation (2.23), the generic term, $h_{k\,h}$ of the Hessian matrix can be obtained

$$\frac{\partial^2 U(\boldsymbol{\theta})}{\partial \theta_k \partial \theta_h} = 2 \sum_{i=1}^{n} \sum_{j=1}^{m} w_{i,j} \frac{\partial \widehat{y}_{i,j}(\boldsymbol{\theta})}{\partial \theta_k} \frac{\partial \widehat{y}_{i,j}(\boldsymbol{\theta})}{\partial \theta_h} - 2 \sum_{i=1}^{n} \sum_{j=1}^{m} w_{i,j} r_{i,j} \frac{\partial^2 \widehat{y}_{i,j}(\boldsymbol{\theta})}{\partial \theta_k \partial \theta_h}. \tag{2.24}$$

The second term contains the residuals $r_{i,j}$; assuming that the residuals are small, the Hessian can be approximated only by the first term. This assumption can be always done in a neighborhood of the minimum. Therefore, the following simplified form of the Hessian can be considered

$$\frac{\partial^2 U(\boldsymbol{\theta})}{\partial \theta_k \partial \theta_h} = 2 \sum_{i=1}^{n} \sum_{j=1}^{m} w_{i,j} \frac{\partial \widehat{y}_{i,j}(\boldsymbol{\theta})}{\partial \theta_k} \frac{\partial \widehat{y}_{i,j}(\boldsymbol{\theta})}{\partial \theta_h}. \tag{2.25}$$

The term $S^i_{jk} = \partial \widehat{y}_{i,j}(\boldsymbol{\theta}) / \partial \theta_k$ is called sensitivity coefficient [6], and it is a measure of the influence of the parameter θ_k on the j_{th} component of the vector $\widehat{\boldsymbol{y}}(\boldsymbol{x}_i, \boldsymbol{\theta})$.

In order to obtain the gradient and the Hessian it is necessary obtain the sensitivity coefficients. Differentiating both sides of equation (2.22) with respect to the parameter θ_k the following equality is obtained

$$\frac{\partial}{\partial \theta_k} \left(\frac{d \widehat{y}_{i,j}}{dt} \right) = \frac{\partial \Omega_{i,j}}{\partial \theta_k} + \sum_{l=1}^{m} \left(\frac{\partial \Omega_{i,j}}{\partial \widehat{y}_{i,l}} \frac{\partial \widehat{y}_{i,l}}{\partial \theta_k} \right). \tag{2.26}$$

Interchanging the order of differentiation yields

$$\dot{S}^i_{jk} = \frac{\partial \Omega_{i,j}}{\partial \theta_k} + \sum_{l=1}^{m} \left(\frac{\partial \Omega_{i,j}}{\partial \widehat{y}_{i,l}} S^i_{lk} \right). \tag{2.27}$$

In order to obtain the sensitivity coefficients, one must solve the model (2.22) together with the set of differential equations given by (2.27), with the quantities $\partial \Omega_{i,j} / \partial \theta_k$ and $\partial \Omega_{i,j} / \partial \widehat{y}_{i,l}$ determined by simple differentiation. Equations (2.27) are called sensitivity equations [6].

Once the values of the sensitivity coefficients are determined, the gradient and the Hessian matrix, at each step of the optimization algorithm, can be easily computed via equations (2.23) and (2.25), respectively.

$$\frac{\partial U(\boldsymbol{\theta})}{\partial \theta_k} = -2 \sum_{i=1}^{n} \sum_{j=1}^{m} w_{i,j} r_{i,j} S^i_{jk}\ , \tag{2.28}$$

$$\frac{\partial^2 U(\boldsymbol{\theta})}{\partial \theta_k \partial \theta_h} = 2 \sum_{i=1}^{n} \sum_{j=1}^{m} w_{i,j} S^i_{jk} S^i_{jh}\ . \tag{2.29}$$

2.5 Model identification for the phenol-formaldehyde polymerization

In this section the application of an identification technique for the parameters estimation of a number of reduced order models, describing the phenol-formaldehyde reaction, is presented.

2.5.1 Generation of input-output data

In order to simulate an experimental campaign and generate the experimental data set, $\mathcal{D}$, a simulation model of a jacketed batch reactor, in which the phenol-formaldehyde reaction takes place, has been developed.

This model is a nonlinear implicit model, in the form (2.22), characterized by the thirteen differential equations of the mass balances introduced in Section $1.5.3$ and by the energy balances written for the reactor and the jacket

$$\dot{T}_r = \frac{Q}{\rho_r c_{pr} V_r} - \frac{US}{\rho_r c_{pr} V_r} (T_r - T_j) \ , \tag{2.30}$$

$$\dot{T}_j = \frac{US}{\rho_j c_{pj} V_j} (T_r - T_j) + \frac{F}{V_j} (T_{\text{in}} - T_j) \ , \tag{2.31}$$

where the heat released by the reaction Q is computed via equation (1.19).

The reaction, at μ different constant temperatures, has been simulated in the Matlab/ Simulink© environment, and, for each temperature, the values of the concentration of the 13 compounds and the heat released by the reaction, at ν different time instants, t_i, have been stored. More details regarding the values of μ and ν, the batch time of each simulation and the sampling time will be presented in the Chapter 5.

The concentrations can be measured by drawing a sample of reacting mixture and analyzing it off-line.

The heat released by the reaction can be obtained via calorimetric measures. The most diffused industrial calorimeters are the so-called reaction calorimeters: basically they are jacketed vessels in which the reaction takes place and the heat released is measured by monitoring the temperature of the fluid in the jacket [27]. An alternative instrument is the differential scanning calorimeter (DSC), in which the heat flow into a sample, usually contained in a capsule, is measured differentially, i.e., by comparing it to the flow into an empty reference capsule. The amount of heat required to increase the temperature of the sample and the reference are measured as a function of temperature. Both the

sample and reference are maintained at very nearly the same temperature throughout the experiment. Generally, the temperature program for a DSC analysis is designed such that the sample holder temperature increases linearly as a function of time [27].

In order to simulate a realistic industrial context, the following assumptions on the set-up have been done:

- the initial temperature of the reactor is set to $20°C$;
- a PID controller, based on the feedback of the reactor temperature, has been used to heat the reactor until the desired temperature and to keep it constant during the reaction;
- gaussian white noise, with zero mean and variance equal to $5 \cdot 10^{-3}$, is added to the temperature measurements.

Finally, gaussian white noise is added both to the concentration measurements and to the heat measurements.

In this way, two set of data $\mathcal{D}_C$ and $\mathcal{D}_Q$ have been generated, such as

$$\mathcal{D}_C = \bigcup_{h=1}^{\mu} \mathcal{D}_C^h = \bigcup_{h=1}^{\mu} \{(\boldsymbol{C}_h^{ex}(t_i) + \varepsilon_C, T_h), \quad \boldsymbol{C}_h^{ex}(t_i) \in \mathbb{R}^{13}, \quad i = 1, \cdots, \nu\},$$

$$\mathcal{D}_Q = \bigcup_{h=1}^{\mu} \mathcal{D}_Q^h = \bigcup_{h=1}^{\mu} \{(Q_h^{ex}(t_i) + \varepsilon_Q, T_h), \quad Q_h^{ex}(t_i) \in \mathbb{R}, \quad i = 1, \cdots, \nu\},$$

where $\boldsymbol{C}_h(t_i)$ and $Q_h(t_i)$ are the vector of concentrations and heat released, respectively, obtained at the time t_i, when the reaction takes place at temperature T_h, while ε_C and ε_Q are the measurement noises. The total number of experimental data is given by $n = \mu \times \nu$.

2.5.2 Selection of candidate models

The objective of the identification procedure is to obtain a simplified model able to represent the phenol-formaldehyde reaction as accurately as possible. To this aim a choice on the compounds to be monitored has been done. Two different reaction schemes, involving four different chemical species and three and four reactions, respectively, have been considered.

As regards the species, the simplified models involve the phenol, E_1, the desired product, E_7, and two aggregate compounds M and D, given by the sum of the remaining

monomers and by the sum of dimers and trimers, respectively,

$$M = \sum_{i=3}^{6} E_i, \qquad D = \sum_{j=0}^{4} D_j + E_{13}. \tag{2.32}$$

The first kinetic scheme is a simple series reaction, the second one includes also a parallel reaction. For each scheme both first order kinetics and second order kinetics have been considered.

For the sake of simplicity, in the following, the candidate models will be denoted as *Model* α and *Model* β.

Model α

The following reactions have been considered

$$E_1 \longrightarrow M \longrightarrow E_7 \longrightarrow D. \tag{2.33}$$

The addition phase has been represented as a reaction from phenol, E_1, to the trisubstituted phenol, E_7, in which the other methylolphenols, M, are considered as intermediate products. The formaldehyde is not considered.

In order to take into account the consumption of the desired product, E_7, the condensation of monomers has been considered via the reaction $E_7 \longrightarrow D$.

The mass balances for the considered species are the following

$$\begin{aligned} \dot{C}_{E_1} &= -R_1 \\ \dot{C}_M &= R_1 - R_2 \\ \dot{C}_{E_7} &= R_2 - R_3 \end{aligned} \tag{2.34}$$

where C_{E_1}, C_M and C_{E_7} are the concentrations of E_1, M and E_7, respectively, and R_i, $(i = 1, 2, 3)$ are the reaction rates. Denoting with k_i the constant rates, given by the Arrhenius law (1.2), the reaction rates are:

- First order kinetics

$$R_1 = k_1(T_r)C_{E_1}, \qquad R_2 = k_2(T_r)C_M, \qquad R_3 = k_3(T_r)C_{E_7}. \tag{2.35}$$

- Second order kinetics

$$R_1 = k_1(T_r)C_{E_1}^2, \qquad R_2 = k_2(T_r)C_M^2, \qquad R_3 = k_3(T_r)C_{E_7}^2. \tag{2.36}$$

The heat released by the reaction for a unit volume is given by

$$Q = (-\Delta H_1)R_1 + (-\Delta H_2)R_2 + (-\Delta H_3)R_3, \tag{2.37}$$

where ΔH_i are the molar enthalpy changes of the reactions in (2.33).

Model β

This model presents an additional reaction, in parallel to the series of reactions in the previous model. Hence, the reaction scheme is the following:

$$\begin{aligned} &E_1 \longrightarrow M \longrightarrow E_7 \longrightarrow D \\ &E_1 + M \longrightarrow D \end{aligned} \tag{2.38}$$

The reaction $E_1 + M \longrightarrow D$ has been added so as to model the condensation phase, more accurately. In fact, the production of dimers do not depend only by the tri-substituted phenol, but also by the other monomers, M.

The mass balances are

$$\begin{aligned} \dot{C}_{E_1} &= -R_1 - R_2 \\ \dot{C}_M &= R_1 - R_2 - R_3 \\ \dot{C}_{E_7} &= R_3 - R_4 \end{aligned} \tag{2.39}$$

where the reaction rates are:

- First order kinetics

$$\begin{aligned} R_1 &= k_1(T_r)C_{E_1}, & R_2 &= k_2(T_r)C_M, \\ R_3 &= k_3(T_r)C_M, & R_4 &= k_4(T_r)C_{E_7}. \end{aligned} \tag{2.40}$$

- Second order kinetics

$$\begin{aligned} R_1 &= k_1(T_r)C_{E_1}^2, & R_2 &= k_2(T_r)C_{E_1}C_M, \\ R_3 &= k_3(T_r)C_M^2, & R_4 &= k_4(T_r)C_{E_7}^2. \end{aligned} \tag{2.41}$$

The heat released by the reaction for a unit volume is given by

$$Q = (-\Delta H_1)R_1 + (-\Delta H_2)R_2 + (-\Delta H_3)R_3 + (-\Delta H_4)R_4. \tag{2.42}$$

2.5.3 Parameters estimation

On the basis of equations (2.34), (3.40), (2.37) and (2.42), the unknown parameters to be identified are:

- the pre-exponential factors, $k_{0,i}$;
- the activation energies, $E_{a,i}$;
- the molar enthalpy changes, ΔH_i,

with $i = 1, \cdots, p$, $p = 3$ for *Model* α and $p = 4$ for *Model* β.

The parameters identification problem has been divided into two sub-problems: first the best kinetic parameters have been found, then the molar enthalpy changes have been estimated.

2.4.3.1 Estimation of the kinetic parameters

The system of differential equations (2.34) or (3.40), containing the kinetic parameters, is an implicit nonlinear model.

The following objective function has been adopted

$$U_k = \sum_{i=1}^{n} \sum_{j=1}^{3} r_{i,j}^2, \tag{2.43}$$

where n is the number of experimental data and $r_{i,j}$ is the j_{th} component of the vector $\boldsymbol{r}_i$

$$\boldsymbol{r}_i = \begin{bmatrix} r_{i,1} \\ r_{i,2} \\ r_{i,3} \end{bmatrix} = \begin{bmatrix} C_{E_1}^{ex} - C_{E_1} \\ C_M^{ex} - C_{M_1} \\ C_{E_7}^{ex} - C_{E_7} \end{bmatrix}, \tag{2.44}$$

$C_{E_1}^{ex}$, C_M^{ex} and $C_{E_7}^{ex}$ are the experimental data and C_{E_1}, C_M and C_{E_7} are the values computed by the model.

The Levenberg-Marquardt algorithm has been adopted to perform the optimization; the gradient and the Hessian matrix of the objective function have been computed via equations (2.28) and (2.29).

Usually, pre-exponential factors and activation energies are characterized by different orders of magnitude; this may generate numerical problems when they are identified

simultaneously. To avoid these problems and improve convergence, a suitable transformation of the kinetic parameters can be used. In this thesis, the following reparameterization, proposed by [12], has been adopted

$$\varphi = \ln(k_0) - \frac{E_a}{RT^*}, \tag{2.45}$$

$$\psi = \ln\left(\frac{E_a}{R}\right), \tag{2.46}$$

where T^* is a reference temperature. The constant rate k with the new parameters becomes

$$k = \exp\left[\varphi + \exp(\psi)\left(\frac{1}{T^*} - \frac{1}{T}\right)\right]. \tag{2.47}$$

The parameters φ and ψ, instead of k_0 and E_a have been identified.

The best fit values of the parameters, the values of the algorithm parameters and the initial parameters estimate are reported in the Chapter 5.

2.4.3.2 Estimation of the molar enthalpy changes

Once the kinetic parameters have been estimated, equations (2.37) and (2.42) become linear in the unknown parameters ΔH_i. Therefore, it is possible to use the equation (2.12) to compute the values of the molar enthalpy changes that minimize the following objective function

$$U_Q = \sum_{i=1}^{n} \rho_i^2, \tag{2.48}$$

where $\rho_i = Q_i^{ex} - Q_i$, Q_i^{ex} is the measured value of the heat released by the reaction for unity of volume and Q_i is the value computed by the model.

The parameters have been estimated, first, by considering them as constant with respect to the temperature. Then, in order to improve the heat estimation, they have been estimated by assuming a dependence upon the temperature. In the following both the procedures have been described.

Parameters constant with respect to the temperature

Referring to equation (2.12), the parameters vector is the following

$$\boldsymbol{\theta} = [\Delta H_1, \cdots, \Delta H_p]^T, \tag{2.49}$$

The best parameters estimate is given by the least-squares solution:

$$\boldsymbol{\theta}^* = (\boldsymbol{\Psi}^T\boldsymbol{\Psi})^{-1}\boldsymbol{\Psi}^T\boldsymbol{y}, \tag{2.50}$$

where $\boldsymbol{\Psi}$ is the $(n \times p)$ matrix

$$\boldsymbol{\Psi} = \begin{bmatrix} \boldsymbol{\Psi}_1 \\ \boldsymbol{\Psi}_2 \\ \vdots \\ \boldsymbol{\Psi}_\mu \end{bmatrix}, \qquad \boldsymbol{\Psi}_h = \begin{bmatrix} -R_1^h(t_1) & \cdots & -R_p^h(t_1) \\ \vdots & \vdots & \vdots \\ -R_1^h(t_\nu) & \cdots & -R_p^h(t_\nu) \end{bmatrix},$$

and $R_i^h(t_j)$ is the reaction rate evaluated at time t_j when the reaction takes place at the constant temperature T_h.

The $(n \times 1)$ vector $\boldsymbol{y}$ collects the experimental data

$$\boldsymbol{y} = \begin{bmatrix} \boldsymbol{y}_1 \\ \boldsymbol{y}_2 \\ \vdots \\ \boldsymbol{y}_\mu \end{bmatrix}, \qquad \boldsymbol{y}_h = \begin{bmatrix} Q_h^{ex}(t_1) \\ Q_h^{ex}(t_2) \\ \vdots \\ Q_h^{ex}(t_\nu) \end{bmatrix}.$$

Parameters variable with respect to the temperature

If ΔH_i are assumed to be variable with the temperature, μ different vectors of parameters, $\boldsymbol{\theta}^h = \left[\Delta H_1^h, \cdots, \Delta H_p^h\right]^T$, one for each considered temperature, are to be estimated.

For each vector, the estimate (2.50) becomes

$$\boldsymbol{\theta}^{h*} = (\boldsymbol{\Psi}_h^T \boldsymbol{\Psi}_h)^{-1} \boldsymbol{\Psi}_h^T \boldsymbol{y}_h, \tag{2.51}$$

where $\boldsymbol{y}_h$ is the above defined $(\nu \times 1)$ vector of experimental data obtained when the reaction takes place at temperature T_h.

Once the value of ΔH_i for each temperature has been estimated, an interpolating polynomial function is considered such as

$$\Delta H_i(T) = p_0 + p_1 T + p_2 T^2 + \cdots + p_m T^m, \tag{2.52}$$

$$\Delta H_i^h = p_0 + p_1 T_h + p_2 T_h^2 + \cdots + p_m T_h^m,$$

More details, such as the order of polynomial functions for each parameter, can be found in the Chapter 5.

2.5.4 Model validation

The accuracy of the obtained models has been tested comparing their behavior with the behavior of the complete model (see Section 1.5.3), when they are forced to track an assigned temperature profile.

The comparison between the different models has been done on the basis of the root mean squared error. For the concentration it is given by

$$RMSE_C = \sqrt{\frac{\sum_{i=1}^{m} \left[\left(C^c_{E_1} - C^s_{E_1}\right)^2 + \left(C^c_M - C^s_M\right)^2 + \left(C^c_{E_7} - C^s_{E_7}\right)^2 \right]}{m}}, \tag{2.53}$$

where the superscripts c and s denote the value computed by the complete model and by the simplified model, respectively, and m is the number of samples.

For the heat released by the reaction the root mean squared error is given by

$$RMSE_Q = \sqrt{\frac{\sum_{i=1}^{m} \left(Q^c_i - Q^s_i\right)}{m}} \tag{2.54}$$

The results will be presented in the Chapter 5.

Chapter 3

Control

3.1 Introduction

Research on temperature control of batch reactors has been focused mainly on nonlinear model-based control strategies, since approaches based on linearized models do not guarantee satisfactory performance. Early approaches to nonlinear control include differential geometric approaches [55], nonlinear robust control [65,90], predictive control [57,72,78] and Generic Model Control (GMC) [4,15,24,58–60,109].

In the presence of parametric model uncertainties, a few adaptive control strategies have been proposed: in [44] a nonlinear controller, designed via a differential geometric approach, is augmented with an indirect parameters estimation algorithm, while in [22] an extended Kalmann filter is adopted. In [92], [104] and [41] three different approaches to adaptive GMC have been proposed: in [92] an adaptive scheme is designed, based on the minimization of the mismatch between process measurements and the predicted reference trajectory; in [104] a Strong Tracking Filter is adopted to estimate the unknown parameters, and the concept of input equivalent disturbance is used to further improve the robustness of the control scheme; in [41] the estimation of some unknown quantities –namely, the heat released by the reaction and the heat transfer coefficient– are estimated by adopting the nonlinear adaptive observer proposed in [34]. Also, an adaptive cascade temperature controller has been proposed in [97] for multiproduct jacketed stirred reactors; the controller is based on a master/slave scheme, while the poorly known model parameters are updated via a suitable model-based estimator. Further developments have been achieved in [102] and [103] by extending some of the previous adaptive approaches to systems affected by input time delays.

In this thesis, a novel controller-observer control strategy is proposed for a jacketed batch reactor. First, an observer is designed to estimate the heat released by the reaction; in order to improve the estimation accuracy, the heat transfer coefficient is adaptively estimated. Then, a temperature control scheme is designed, based on the closure of two control loops. Namely, an outer control loop, closed on the reactor temperature, computes the reference signal for the inner control loop closed on the jacket temperature. The two-loop arrangement improves the robustness of the scheme, while preserving a simple structure for both the controllers. Also, tracking performance of the controller are further improved by adopting an adaptive algorithm based on the on-line estimation of the heat transfer coefficient. It must be remarked that the observer and the controller can be designed and tuned separately. The scheme has been proposed in [17, 83] for a simple series reaction, and it is generalized here for a class of irreversible consecutive reaction schemes.

The convergence of the overall scheme, in terms of observer estimation errors and controller tracking errors, is proven via a Lyapunov-like argument.

Furthermore, an alternative approach, in which the observer does not need the knowledge of the reaction kinetics, is presented and its stability rigourously proven. In this observer the heat released is approximated via a linear-in-the-parameters on-line approximator, based on an universal interpolator (e.g., a Radial Basis Functions Network).

Finally, the application of the proposed methods to the phenol-formaldehyde reaction, reviewed in Chapter 1, will be presented.

3.2 Modeling

In this section the model of a jacketed batch reaction, in which takes place an irreversible exothermic reaction, is presented and rewritten in the form of state equations.

Let us consider the following kinetic scheme, in which each reaction has been assumed to be irreversible and exothermic

$$\begin{array}{llll} A_1 \longrightarrow \nu_{1,2} A_2 & & & \\ A_1 \longrightarrow \nu_{1,3} A_3 & A_2 \longrightarrow \nu_{2,3} A_3 & & \\ \vdots & \vdots & & \\ A_1 \longrightarrow \nu_{1,p+1} A_{p+1} & A_2 \longrightarrow \nu_{2,p+1} A_{p+1} & \dots & A_p \longrightarrow \nu_{p,p+1} A_{p+1} \end{array}$$

where A_i denotes the i_{th} chemical species, $\nu_{i,h} \geq 0$ is the stoichiometric coefficient of the reaction $A_i \rightarrow A_h$ and A_{p+1} is the final product. The above scheme represents a

general irreversible non-chain reactions network, and can be reduced to simpler series and/or parallel reaction schemes by assuming $\nu_{i,h} = 0$ for the reactions to be eliminated. Remarkably, the inclusion of all the significant reaction intermediates allows a correct description of the system evolution to the final product, especially for the rate of heat release as a function of system composition.

Assuming first-order kinetics and perfect mixing, the mass balances give

$$\begin{aligned}
\dot{C}_1 &= -k_1(T_r)C_1 \\
\dot{C}_2 &= \nu_{1,2}\, k_{1,2}(T_r)C_1 - k_2(T_r)C_2 \\
\dot{C}_3 &= \nu_{1,3}\, k_{1,3}(T_r)C_1 + \nu_{2,3}\, k_{2,3}(T_r)C_2 - k_3(T_r)C_3 \\
&\vdots \\
\dot{C}_p &= \nu_{1,p}\, k_{1,p}(T_r)\, C_1 + \ldots + \nu_{p-1,p}\, k_{p-1,p}(T_r)C_{p-1} - k_p(T_r)C_p
\end{aligned} \tag{3.1}$$

where C_i ($i = 1 \ldots p$) is the concentration of the chemical species A_i, T_r is, as usual, the reactor temperature and $k_{i,h}(T_r)$ ($h = 2 \ldots p$), is the rate constant of the reaction $A_i \rightarrow A_h$, given by the Arrhenius law (1.2). Moreover, the lumped overall rate constants of the reactions of disappearance, $k_i(T_r)$, are defined, for each reactant, as

$$k_i(T_r) = \sum_{h=i+1}^{p+1} k_{i,h}(T_r)\,, \tag{3.2}$$

which are strictly positive if A_i is involved at least in one reaction.

Under the assumption of perfect mixing, the energy balances in the reactor and in the jacket (see equations (1.8) and (1.10)) take the form

$$\dot{T}_r = q(\boldsymbol{x}_M, T_r) - \frac{US\,(T_r - T_j)}{V_r \rho_r c_{pr}}, \tag{3.3}$$

$$\dot{T}_j = \frac{US\,(T_r - T_j)}{V_j \rho_j c_{pj}} + \frac{(T_{\text{in}} - T_j)}{V_j}\, F, \tag{3.4}$$

where $\boldsymbol{x}_M = [C_1 \ldots C_p]^T$ is the vector of reactants concentrations and the other variables have been defined in Chapter 1. The heat released by the reaction, Q, is taken into account via the term q, given by

$$q(\boldsymbol{x}_M, T_r) = \frac{Q(\boldsymbol{x}_M, T_r)}{V_r \rho_r c_{pr}} = \frac{\displaystyle\sum_{i=1}^{p} \sum_{h=i+1}^{p+1} (-\Delta H_{i,h}) k_{i,h}(T_r) C_i}{\rho_r c_{pr}}\,, \tag{3.5}$$

where, as usual, $\Delta H_{i,h}$ is the molar enthalpy change of each reaction.

It can be easily recognized that the rate constants are nonnegative and strictly increasing functions of the reactor temperature T_r. Since the reaction is assumed to be exothermic and T_{in} is bounded, i.e., $T_{\text{in},m} \leq T_{\text{in}} \leq T_{\text{in},M}$, the temperature in the reactor is lower bounded by the value

$$T_{r,m} = \min\left\{T_{r,0}, T_{j,m}\right\},$$

where $T_{r,0}$ is the initial reactor temperature and $T_{j,m}$ is the minimum attainable jacket temperature, which coincides with the minimum attainable value, $T_{\text{in},m}$, of T_{in}. Moreover, an upper bound for T_r can be computed by considering the ideal heating/reaction scheme composed by the following two steps:

- the reacting mixture is first heated up to the maximum temperature value, $T_{\text{in},M}$, of the fluid entering the jacket,
- then, the complete reactants conversion takes place adiabatically.

The numerical value of the upper bound is then given by

$$T_{r,M} = T_{\text{in},M} + C_{1,0}\,\frac{(-\Delta H_{1,p+1})}{\rho_r c_{pr}},$$

where $C_{1,0}$ is the initial concentration of A_1. Hence, the rate constants are bounded as follows

$$0 < \underline{k}_{i,h} \leq k_{i,h}(T_r) \leq \overline{k}_{i,h}\,, \quad \forall T_r\,, \quad i = 1\ldots p\,, \quad h = i+1\ldots p+1\,, \tag{3.6}$$

where $\underline{k}_{i,h} = k_{i,h}(T_{r,m})$ and $\overline{k}_{i,h} = k_{i,h}(T_{r,M})$. Also, the above defined inequalities lead to the following bounds for the rate constants k_i

$$0 < \underline{k}_i \leq k_i(T_r) \leq \overline{k}_i\,, \quad \forall T_r\,, \quad i = 1\ldots p\,, \tag{3.7}$$

where $\underline{k}_i = \sum_{h=i+1}^{p+1} \underline{k}_{i,h}$ and $\overline{k}_i = \sum_{h=i+1}^{p+1} \overline{k}_{i,h}$.

In order to rewrite the whole model in the form of state equations, let define the $(p+2)\times 1$ state vector

$$\boldsymbol{x} = \begin{bmatrix} C_1 \\ \vdots \\ C_p \\ T_r \\ T_j \end{bmatrix} = \begin{bmatrix} x_1 \\ \vdots \\ x_p \\ x_{p+1} \\ x_{p+2} \end{bmatrix} = \begin{bmatrix} \boldsymbol{x}_M \\ \boldsymbol{x}_E \end{bmatrix},$$

the control input

$$u = T_{\text{in}},$$

the output vector of measurable variables

$$\boldsymbol{y} = \begin{bmatrix} T_r \\ T_j \end{bmatrix} = \begin{bmatrix} y_1 \\ y_2 \end{bmatrix} = \boldsymbol{x}_E$$

and the parameter

$$\theta = US\,.$$

Then, equations (3.1), (3.3) and (3.4) can be rewritten in the following state-space form

$$\begin{cases} \dot{\boldsymbol{x}} &= \boldsymbol{A}(\boldsymbol{y})\,\boldsymbol{x} + \boldsymbol{b}(\boldsymbol{y}, u) + \boldsymbol{C}^T \boldsymbol{\psi}(\boldsymbol{y})\,\theta \\ \boldsymbol{y} &= \boldsymbol{C}\boldsymbol{x}\,, \end{cases} \tag{3.8}$$

where the matrix $\boldsymbol{A}(\boldsymbol{y})$ is

$$\boldsymbol{A}(\boldsymbol{y}) = \begin{bmatrix} \boldsymbol{A}_M(\boldsymbol{y}) & \boldsymbol{O}_{p\times 2} \\ \boldsymbol{A}_{M,E}(\boldsymbol{y}) & \boldsymbol{O}_{2\times 2} \end{bmatrix},$$

$\boldsymbol{O}_{m\times n}$ denotes the $m \times n$ null matrix, and

$$\boldsymbol{A}_M = \begin{bmatrix} -k_1 & 0 & \dots & 0 \\ \nu_{1,2}\,k_{1,2} & -k_2 & \dots & 0 \\ \vdots & \vdots & \vdots & \vdots \\ \nu_{1,p}\,k_{1,p} & \nu_{2,p}\,k_{2,p} & \dots & -k_p \end{bmatrix},$$

$$\boldsymbol{A}_{M,E}(\boldsymbol{y}) = \begin{bmatrix} a_1(y_1) & \dots & a_p(y_1) \\ 0 & \dots & 0 \end{bmatrix} = \begin{bmatrix} \boldsymbol{a}^T(\boldsymbol{y}) \\ \boldsymbol{0}_{p\times 1}^T \end{bmatrix},$$

$$a_i(\boldsymbol{y}) = \sum_{h=i+1}^{p+1} \alpha_{i,h} k_{i,h}(y_1)\,, \quad \alpha_{i,h} = \frac{(-\Delta H_{i,h})}{\rho_r c_{pr}}\,.$$

It is worth noticing that the off-diagonal terms in $\boldsymbol{A}_M$ are nonnegative (for all T_r) and may be null if the corresponding reactions $A_i \to A_h$ does not take place ($\nu_{i,h} = 0$), whereas all the terms on the main diagonal are strictly negative (for all T_r).

The vector $\boldsymbol{b}$ in (3.8) is defined as follows

$$\boldsymbol{b}(\boldsymbol{y}, u) = \begin{bmatrix} \boldsymbol{0}_{p\times 1} \\ \boldsymbol{b}_E(\boldsymbol{y}, u) \end{bmatrix}, \quad \boldsymbol{b}_E = \begin{bmatrix} 0 \\ \beta_j(u - y_2) \end{bmatrix}, \quad \beta_j = \frac{F}{V_j}\,,$$

the vector $\boldsymbol{\psi}$ is given by ($* = r, j$)

$$\boldsymbol{\psi}(\boldsymbol{y}) = \begin{bmatrix} -\alpha_r \left(y_1 - y_2\right) \\ \alpha_j (y_1 - y_2) \end{bmatrix}, \quad \alpha_* = \frac{1}{V_* \rho_* c_{p*}},$$

and the output matrix is given by

$$\boldsymbol{C} = \begin{bmatrix} \boldsymbol{O}_{2\times p} & \boldsymbol{I}_{2\times 2} \end{bmatrix},$$

where $\boldsymbol{I}_{m\times n}$ denotes the $m \times n$ identity matrix.

3.3 Estimation of the heat released by the reaction

From equation (3.8), it can be recognized that the heat released by the reaction affects the dynamics of the reactor temperature via the term $q(\boldsymbol{x}_M, T_r)$. In turn, this term depends on the reactants concentrations, which are usually measurable at very low sampling rates, not suitable for real-time control. Hence, the design of a model-based control law for the reactor temperature should use an estimate of this term.

The heat released by the reaction can be estimated by adopting the approach known as *calorimetric method* [14,91], in which the energy balance is used together with measured values of temperature and its time derivative. In order to avoid numerical differentiation of the temperature measurements, an observer can be used to estimate both the heat released by the reaction and the heat-transfer coefficient (see, e.g., [22, 41]). In [22], a nonlinear adaptive control strategy is adopted, based on an extended Kalmann filter to achieve on-line estimation of the time varying parameters involved in the control law; however, convergence and robustness of the overall scheme are not theoretically proven. In [41] the estimation law suffers from singularities; moreover, the dynamics of the mass balance in the reactor is not taken into account, since the heat released by the reaction is estimated as an unknown parameter.

In the following three different approaches, based on adaptive observers, to estimate the heat released by the reaction are presented, the first two are original contributions of this thesis, the third is one of the most interesting approaches in the recent literature on control of batch reactors. They are:

- A nonlinear adaptive observer is adopted to estimate the reactant concentrations (i.e., the state variables $x_1, \ldots, x_p$), while the heat transfer coefficient, usually assumed unknown, is estimated via an adaptive update law. Then, the heat is reconstructed from the estimated concentrations.

- A model-free approach, based on the adoption of an universal interpolators, i.e., a Radial Basis Function Network, for the estimation of the heat released by the reaction. Differently from the previous approach, knowledge of the reaction kinetics is not required.
- The model-free approach proposed in [41], in which both the heat transfer coefficient and the heat released by the reaction are estimated as unknown parameters. As the previous, also this approach does not need the estimation of the concentrations.

3.3.1 Model-based nonlinear observer

The observer has the form

$$\begin{cases} \dot{\widehat{\boldsymbol{x}}} &= \boldsymbol{A}(\boldsymbol{y})\,\widehat{\boldsymbol{x}} + \boldsymbol{b}(\boldsymbol{y},u) + \boldsymbol{L}\widetilde{\boldsymbol{y}} + \boldsymbol{C}^T\,\boldsymbol{\psi}(\boldsymbol{y})\,\widehat{\theta}_o \\ \widehat{\boldsymbol{y}} &= \boldsymbol{C}\widehat{\boldsymbol{x}} \end{cases} \tag{3.9}$$

where $\widehat{\boldsymbol{x}}$ denotes the vector of the state estimates; $\widehat{\boldsymbol{y}}$ and $\widetilde{\boldsymbol{y}} = \boldsymbol{y} - \widehat{\boldsymbol{y}}$ denote the vectors of output estimates and output estimation errors, respectively; $\boldsymbol{L}$ is a $(p+2) \times 2$ matrix of positive gains

$$\boldsymbol{L} = \begin{bmatrix} \boldsymbol{L}_M \\ \boldsymbol{L}_E \end{bmatrix}, \quad \boldsymbol{L}_M = \begin{bmatrix} l_1 & 0 \\ l_2 & 0 \\ \vdots & \vdots \\ l_p & 0 \end{bmatrix}, \quad \boldsymbol{L}_E = \begin{bmatrix} l_r & 0 \\ 0 & l_j \end{bmatrix},$$

and the estimate $\widehat{\theta}_o$ of θ is given by the update law

$$\dot{\widehat{\theta}}_o = \lambda^{-1}\,\boldsymbol{\psi}^T(\boldsymbol{y})\,\widetilde{\boldsymbol{y}}, \tag{3.10}$$

where λ is a positive gain setting the parameter estimate update rate.

Therefore, an estimate of q can be easily computed via (3.5) from the estimates of the reactants concentrations

$$\widehat{q}(\boldsymbol{y},\widehat{\boldsymbol{x}}) = \sum_{i=1}^{p} \sum_{h=i+1}^{p+1} \alpha_{i,h}\,k_{i,h}(y_1)\,\widehat{x}_i = \sum_{i=1}^{p} a_i(\boldsymbol{y})\,\widehat{x}_i = \boldsymbol{a}^T(\boldsymbol{y})\widehat{\boldsymbol{x}}_M\,. \tag{3.11}$$

The convergence properties of both the state estimation error $\widetilde{\boldsymbol{x}} = \boldsymbol{x} - \widehat{\boldsymbol{x}}$ and the parameter estimation error $\widetilde{\theta}_o = \theta - \widehat{\theta}_o$ are stated by the following theorem.

Theorem 1. *If the rate constants are bounded as in (3.6),(3.7), then, there exists a set of observer gains such that the state estimation error $\widetilde{\boldsymbol{x}}$ is globally uniformly convergent to $\mathbf{0}$ as $t \to \infty$ and the parameter estimation error $\widetilde{\theta}_o$ is bounded for every t.*

Proof. The dynamics of the estimation errors can be readily derived from equations (3.8) and (3.9)

$$\begin{cases} \dot{\widetilde{\boldsymbol{x}}} &= \boldsymbol{A}_o(\boldsymbol{y})\,\widetilde{\boldsymbol{x}} + \boldsymbol{C}^T\,\boldsymbol{\psi}(\boldsymbol{y})\,\widetilde{\theta}_o \\ \dot{\widetilde{\theta}}_o &= -\lambda^{-1}\,\boldsymbol{\psi}^T(\boldsymbol{y})\,\boldsymbol{C}\,\widetilde{\boldsymbol{x}} \\ \widetilde{\boldsymbol{y}} &= \boldsymbol{C}\widetilde{\boldsymbol{x}}\,, \end{cases} \tag{3.12}$$

where $\boldsymbol{A}_o(\boldsymbol{y}) = \boldsymbol{A}(\boldsymbol{y}) - \boldsymbol{L}\boldsymbol{C}$. Let us consider the following positive definite function

$$V_o(\widetilde{\boldsymbol{x}}, \widetilde{\theta}_o) = \frac{1}{2}\,\widetilde{\boldsymbol{x}}^T\boldsymbol{P}_o\,\widetilde{\boldsymbol{x}} + \frac{1}{2}\,\lambda\,\widetilde{\theta}_o^2\,, \tag{3.13}$$

where $\boldsymbol{P}_o$ is the following positive definite diagonal matrix

$$\boldsymbol{P}_o = \mathrm{diag}\,\{\sigma_1, \ldots, \sigma_p, 1, 1\}\,,$$

and the σ_i are constant positive values to be determined.

The derivative of V_o along the trajectories of the error dynamics is given by

$$\begin{aligned} \dot{V}_o = &-\sum_{i=1}^{p} \sigma_i\,k_i\widetilde{x}_i^2 - l_r\,\widetilde{x}_{p+1}^2 - l_j\,\widetilde{x}_{p+2}^2 + \\ &\sum_{i=1}^{p-1}\sum_{h=i+1}^{p} \sigma_h\,\nu_{i,h}\,k_{i,h}\,\widetilde{x}_i\,\widetilde{x}_h + \sum_{i=1}^{p}(a_i - \sigma_i\,l_i)\,\widetilde{x}_i\,\widetilde{x}_{p+1} + \\ &\boldsymbol{\psi}^T(\boldsymbol{y})\,\boldsymbol{C}\,\widetilde{\boldsymbol{x}}\widetilde{\theta}_o - \lambda\,\dot{\widetilde{\theta}}_o\,\widetilde{\theta}_o\,, \end{aligned}$$

where the dependence of the rate constants upon the temperature has been dropped for notation compactness. By considering the update law (3.10) and the inequalities in (3.6),(3.7), $\dot{V}_o$ can be bounded as follows:

$$\begin{aligned} \dot{V}_o \;\leq\; &-\sum_{i=1}^{p} \sigma_i\,\underline{k}_i\widetilde{x}_i^2 - l_r\,\widetilde{x}_{p+1}^2 - l_j\,\widetilde{x}_{p+2}^2 + \\ &\sum_{i=1}^{p-1}\sum_{h=i+1}^{p} \sigma_h\,\nu_{i,h}\,\overline{k}_{i,h}\,|\widetilde{x}_i|\,|\widetilde{x}_h| + \sum_{i=1}^{p}(\overline{a}_i + \sigma_i\,l_i)\,|\widetilde{x}_i|\,|\widetilde{x}_{p+1}| \\ = \;&-\sum_{i=1}^{p-1}\sum_{h=i+1}^{p} \begin{bmatrix} |\widetilde{x}_i| \\ |\widetilde{x}_h| \end{bmatrix}^T \boldsymbol{\Omega}_{i,h} \begin{bmatrix} |\widetilde{x}_i| \\ |\widetilde{x}_h| \end{bmatrix} - \sum_{i=1}^{p} \begin{bmatrix} |\widetilde{x}_i| \\ |\widetilde{x}_{p+1}| \end{bmatrix}^T \boldsymbol{\Phi}_i \begin{bmatrix} |\widetilde{x}_i| \\ |\widetilde{x}_{p+1}| \end{bmatrix} - l_j\,\widetilde{x}_{p+2}^2\,, \end{aligned}$$

where

$$\overline{a}_i = \sum_{h=i+1}^{p+1} \alpha_{i,h} \overline{k}_{i,h}.$$

The matrices on the right-hand-side of the above inequality

$$\mathbf{\Omega}_{i,h} = \begin{bmatrix} \dfrac{\sigma_i \, \underline{k}_i}{p} & -\dfrac{\sigma_h \, \nu_{i,h} \, \overline{k}_{i,h}}{2} \\ -\dfrac{\sigma_h \, \nu_{i,h} \, \overline{k}_{i,h}}{2} & \dfrac{\sigma_h \, \underline{k}_h}{p} \end{bmatrix},$$

$$\mathbf{\Phi}_i = \begin{bmatrix} \dfrac{\sigma_i \, \underline{k}_i}{p} & -\dfrac{\overline{a}_i + \sigma_i \, l_i}{2} \\ -\dfrac{\overline{a}_i + \sigma_i \, l_i}{2} & \dfrac{l_r}{p} \end{bmatrix},$$

are all positive definite if the gains satisfy the following inequality

$$l_r > \max_{i=1,\dots,p} \left\{ \frac{p^2 \, (\overline{a}_i + \sigma_i l_i)^2}{4 \, \sigma_i \, \underline{k}_i} \right\} \tag{3.14}$$

and the positive constants σ_i satisfy the inequalities

$$\sigma_i > \max_{h=i+1,\dots,p} \left\{ \frac{p^2 \, \nu_{i,h}^2 \, \overline{k}_{i,h}^2}{4 \, \underline{k}_i \, \underline{k}_h} \sigma_h \right\}, \quad i = p-1, \dots, 1 \,. \tag{3.15}$$

Therefore, $\dot{V}_o$ can be upper bounded as follows

$$\dot{V}_o \leq -\sum_{i=1}^{p-1} \sum_{h=i+1}^{p} \underline{\omega}_{i,h} (\widetilde{x}_i^2 + \widetilde{x}_h^2) - \sum_{i=1}^{p} \underline{\phi}_i (\widetilde{x}_i^2 + \widetilde{x}_{p+1}^2) - l_j \, \widetilde{x}_{p+2}^2 \,, \tag{3.16}$$

where $\underline{\omega}_{i,h}$ ($\underline{\phi}_i$) is the smallest eigenvalue of $\mathbf{\Omega}_{i,h}$ ($\mathbf{\Phi}_i$). Thus,

$$\dot{V}_o \leq -\zeta_o \, \|\widetilde{\boldsymbol{x}}\|^2, \tag{3.17}$$

where

$$\zeta_o = \min \left\{ (p-1) \, \underline{\omega} + \underline{\phi} \, , p \, \underline{\phi} \, , l_j \right\},$$

$$\underline{\omega} = \min_{\substack{i \, = \, 1, \, \dots \, , \, p \, - \, 1 \\ h \, = \, i \, + \, 1, \, \dots \, , \, p}} \left\{ \underline{\omega}_{i,h} \right\}, \quad \underline{\phi} = \min_{i=1,\dots,p} \left\{ \underline{\phi}_i \right\}.$$

Hence, $\dot{V}_o$ is negative semi-definite: this guarantees boundedness of $\widetilde{\boldsymbol{x}}$ and $\widetilde{\theta}_o$. By invoking the Barbalat's Lemma [53], it can be recognized that $\dot{V}_o \to 0$, which implies global uniform convergence to $\mathbf{0}$ of $\widetilde{\boldsymbol{x}}$ as $t \to \infty$, while $\widetilde{\theta}_o$ is only guaranteed to be bounded (see Remark 1 hereafter).

□

Remark 1. As usual in direct adaptive estimation and/or control schemes, the convergence to 0 of the parameter estimation error $\widetilde{\theta}_o$ is not guaranteed, unless the *persistency of excitation* condition is fulfilled [3, 53]. In detail, if there exist three scalars $\lambda_1 > 0$, $\lambda_2 > 0$ and $T > 0$ such that:

$$\lambda_1 \leq \int_t^{t+T} \boldsymbol{\psi}^T(\boldsymbol{y}(\tau))\, \boldsymbol{\psi}(\boldsymbol{y}(\tau))\, d\tau \leq \lambda_2\,, \quad \forall t \geq 0\,, \tag{3.18}$$

then, both the state estimation error $\widetilde{\boldsymbol{x}}$ and the parameter estimation error $\widetilde{\theta}_o$ are globally exponentially convergent to zero.

Remark 2. In the case of perfect knowledge of θ, the observer takes the form (3.9), where the estimate $\widehat{\theta}_o$ is replaced by the true value of the coefficient.

The above two remarks are of the utmost importance for evaluating the potential of the proposed observer in a real set-up. In fact, exponential stability would ensure robustness of the state estimation against bounded and/or vanishing model uncertainties and disturbances [53], due to inaccurate and/or incomplete knowledge of reaction kinetics, as well as to usual simplifying assumptions adopted for the model derivation (e.g., perfect mixing).

3.3.2 Model-free approaches

When an accurate model of the reaction kinetics cannot be adopted (e.g., due to the lack of reliable data for identification), the approach previously developed may be ineffective and different strategies (i.e., model-free) for the estimation of the heat released must be adopted. Under this regard, the approach in [41] can be considered, where the heat released by the reaction (seen as a further unknown parameter to be estimated) is estimated, together with the heat transfer coefficient, via a suitably designed nonlinear observer [34]. Other model-free approaches can be adopted, e.g., based on the adoption of universal interpolators (neural networks, polynomials) for the direct on-line estimation of the heat (see, e.g., the work in [18] and references therein), as well as purely neural approaches [10]. Also, the approaches based on the combination of neural and model-based paradigms [1] or on tendency models [35] can be considered.

In the following two model-free approaches, based on adaptive observer will be presented: the first one is an original contribute of this thesis, the second one is the well-established observer proposed by [34] and adopted for batch reactors by [41].

3.3.2.1 Approach based on universal interpolators

In order to present this observer, the state space equation referred to the vector $\boldsymbol{x}_E$ is rewritten as

$$\begin{cases} \dot{\boldsymbol{x}}_E &= \boldsymbol{A}_E(\theta)\boldsymbol{x}_E + \boldsymbol{\xi}(\boldsymbol{x}_M, \boldsymbol{x}_E) + \boldsymbol{b}_E(\boldsymbol{y}, u) \\ \boldsymbol{y} &= \boldsymbol{x}_E \end{cases} \tag{3.19}$$

where $\boldsymbol{b}_E(\boldsymbol{y}, u)$ is the vector defined in section 3.2 and

$$\boldsymbol{A}_E(\theta) = \begin{bmatrix} -\alpha_r\theta & \alpha_r\theta \\ \alpha_j\theta & -\alpha_j\theta \end{bmatrix}, \qquad \boldsymbol{\xi}(\boldsymbol{x}_M, \boldsymbol{x}_E) = \begin{bmatrix} q(\boldsymbol{x}_M, \boldsymbol{x}_E) \\ 0 \end{bmatrix}.$$

The following observer can be adopted

$$\begin{cases} \dot{\widehat{\boldsymbol{x}}}_E &= \boldsymbol{A}_E(\widehat{\theta}_o)\widehat{\boldsymbol{x}}_E + \widehat{\boldsymbol{\xi}}(\boldsymbol{y}, \boldsymbol{\eta}) + \boldsymbol{b}_E(\boldsymbol{y}, u) + \boldsymbol{L}_E\widetilde{\boldsymbol{y}} \\ \widehat{\boldsymbol{y}} &= \widehat{\boldsymbol{x}}_E \end{cases} \tag{3.20}$$

where

$$\boldsymbol{A}_E(\widehat{\theta}_o) = \begin{bmatrix} -\alpha_r\widehat{\theta}_o & \alpha_r\widehat{\theta}_o \\ \alpha_j\widehat{\theta}_o & -\alpha_j\widehat{\theta}_o \end{bmatrix}, \qquad \boldsymbol{L}_E = \begin{bmatrix} l_r & 0 \\ 0 & l_j \end{bmatrix}, \qquad \widehat{\boldsymbol{\xi}}(\boldsymbol{y}, \boldsymbol{\eta}) = \begin{bmatrix} \widehat{q}(\boldsymbol{y}, \boldsymbol{\eta}) \\ 0 \end{bmatrix},$$

and the estimate $\widehat{\theta}_o$ of θ is given by the update law

$$\dot{\widehat{\theta}}_o = \lambda^{-1}\,\boldsymbol{\psi}^T(\widehat{\boldsymbol{y}})\,\widetilde{\boldsymbol{y}} = \lambda^{-1}\,\begin{bmatrix} -\alpha_r(\widehat{y}_1 - \widehat{y}_2) \\ \alpha_j(\widehat{y}_1 - \widehat{y}_2) \end{bmatrix}^T \begin{bmatrix} \widetilde{y}_1 \\ \widetilde{y}_2 \end{bmatrix}. \tag{3.21}$$

An approximation of the term q can be obtained via a linear-in-the-parameters on-line approximator (see, e.g., [84], [108], [64])

$$q(\boldsymbol{y}, \boldsymbol{\eta}) = \sum_{i=1}^{w} \eta_i\,\varphi_i(y_1) + \varsigma = \boldsymbol{\eta}^T\boldsymbol{\varphi}(y_1) + \varsigma, \tag{3.22}$$

where ς represents the interpolation error, $\varphi_i(y_1)$ are w known basis functions and η_i are the parameters assumed to be unknown and constant (or slowly varying). The vectors $\boldsymbol{\eta}$ and $\boldsymbol{\varphi}(y_1)$ are defined as

$$\boldsymbol{\eta} = \begin{pmatrix} \eta_1 \\ \eta_2 \\ \vdots \\ \eta_w \end{pmatrix}, \qquad \boldsymbol{\varphi}(y_1) = \begin{pmatrix} \varphi_1(y_1) \\ \varphi_2(y_1) \\ \vdots \\ \varphi_w(y_1) \end{pmatrix}.$$

When an on-line interpolator is used to estimate the uncertain term, the interpolation error ς can be kept bounded, provided that a suitable interpolator structure is chosen (see, e.g., [38] and [42]).

Recently, neural networks have been widely used as universal approximators in the area of nonlinear mapping and control problems, and, among them, Radial Basis Functions Networks (RBFNs), are very interesting, because of their good performance despite of their simple structure.

Therefore, in this thesis, Gaussian RBFs have been adopted

$$\varphi_i(y_1) = \exp\left(-\frac{|y_1 - c_i|^2}{2\pi_i^2}\right), \quad i = 1, \ldots, w,$$

where c_i and π_i are the centroid and the width of the i_{th} RBF function, respectively.

The parameters vector is estimated on-line by using the following update law

$$\dot{\widehat{\boldsymbol{\eta}}} = \omega^{-1}\, \boldsymbol{\varphi}(y_1)\, \widetilde{y}_1, \tag{3.23}$$

where ω is a positive gain.

In the absence of interpolation error (i.e., $\varsigma = 0$), the convergence properties of both the state estimation error $\widetilde{\boldsymbol{x}}_E = \boldsymbol{x}_E - \widehat{\boldsymbol{x}}_E$ and the parameters estimation error, $\widetilde{\theta}_o = \theta - \widehat{\theta}_o$ and $\widetilde{\boldsymbol{\eta}} = \boldsymbol{\eta} - \widehat{\boldsymbol{\eta}}$, are stated by the following theorem.

Theorem 2. *Under the assumption of absence of interpolation error, there exists a set of observer gains such that the state estimation error $\widetilde{\boldsymbol{x}}_E$ is globally uniformly convergent to $\mathbf{0}$ as $t \to \infty$ and the parameters estimation error $\widetilde{\theta}_o$ and $\widetilde{\boldsymbol{\eta}}$ are bounded for every t.*

Proof. On the basis of equations (3.19), (3.20), (3.21) and (3.23), the dynamics of the estimation errors has the form

$$\begin{cases} \dot{\widetilde{\boldsymbol{x}}}_E &= \boldsymbol{A}_{E,o}(\theta)\, \widetilde{\boldsymbol{x}}_E + \boldsymbol{\psi}(\widehat{\boldsymbol{y}})\, \widetilde{\theta}_o + \widetilde{\boldsymbol{\xi}}(\boldsymbol{y}, \widetilde{\boldsymbol{\eta}}) \\ \dot{\widetilde{\theta}}_o &= -\lambda^{-1}\, \boldsymbol{\psi}^T(\widehat{\boldsymbol{y}})\, \widetilde{\boldsymbol{y}} \\ \dot{\widetilde{\boldsymbol{\eta}}} &= -\omega^{-1} \boldsymbol{\varphi}(y_1) \widetilde{y}_1 \\ \widetilde{\boldsymbol{y}} &= \widetilde{\boldsymbol{x}}_E\,, \end{cases} \tag{3.24}$$

where $\boldsymbol{A}_{E,o} = \boldsymbol{A}_E - \boldsymbol{L}_E$ and

$$\widetilde{\boldsymbol{\xi}}(\boldsymbol{y}, \widetilde{\boldsymbol{\eta}}) = \begin{bmatrix} \widetilde{q}(\boldsymbol{y}, \widetilde{\boldsymbol{\eta}}) \\ 0 \end{bmatrix} = \begin{bmatrix} \widetilde{\boldsymbol{\eta}}^T \boldsymbol{\varphi}(y_1) \\ 0 \end{bmatrix}.$$

Let consider the following positive definite candidate Lyapunov function

$$V_o(\widetilde{\boldsymbol{x}}, \widetilde{\theta}_o, \widetilde{\boldsymbol{\eta}}) = \frac{1}{2}\,\widetilde{\boldsymbol{x}}_E^T \widetilde{\boldsymbol{x}}_E + \frac{1}{2}\,\lambda\,\widetilde{\theta}_o^2 + \frac{1}{2}\,\omega\,\widetilde{\boldsymbol{\eta}}^T \widetilde{\boldsymbol{\eta}}\,, \tag{3.25}$$

The derivative of V_o along the trajectories of the error dynamics is given by

$$\begin{aligned}\dot{V}_o = &-(\alpha_r\theta + l_r)\widetilde{x}_{E_1}^2 - (\alpha_j\theta + l_j)\widetilde{x}_{E_2}^2 + (\alpha_r\theta + \alpha_j\theta)\widetilde{x}_{E_1}\widetilde{x}_{E_2} + \\ &\boldsymbol{\psi}(\widehat{\boldsymbol{y}})^T \widetilde{\boldsymbol{y}}\,\widetilde{\theta}_o - \lambda\widetilde{\theta}_o\,\dot{\widehat{\theta}}_o + \widetilde{\boldsymbol{\eta}}^T \boldsymbol{\varphi}(y_1)\widetilde{y}_1 - \omega\,\widetilde{\boldsymbol{\eta}}^T \dot{\widehat{\boldsymbol{\eta}}}\,,\end{aligned}$$

By considering the update laws (3.21) and (3.23), $\dot{V}_o$ can be bounded as follows

$$\begin{aligned}\dot{V}_o &\leq -(\alpha_r\theta + l_r)\widetilde{x}_{E_1}^2 - (\alpha_j\theta + l_j)\widetilde{x}_{E_2}^2 + (\alpha_r\theta + \alpha_j\theta)|\widetilde{x}_{E_1}||\widetilde{x}_{E_2}| \\ &= -\begin{bmatrix}|x_{E_1}| \\ |x_{E_2}|\end{bmatrix}^T \begin{bmatrix}\alpha_r\theta + l_r & -\dfrac{\alpha_r + \alpha_j}{2}\,\theta \\ -\dfrac{\alpha_r + \alpha_j}{2}\,\theta & \alpha_j\theta + l_j\end{bmatrix} \begin{bmatrix}|x_{E_1}| \\ |x_{E_2}|\end{bmatrix}.\end{aligned} \tag{3.26}$$

The matrix on the right hand-side of the above inequality is positive definite if the gains satisfy the following inequality

$$l_j > \frac{(\alpha_r + \alpha_j)^2\,\theta^2}{4\,(\alpha_r\theta + l_r)} - \alpha_j\theta\,, \tag{3.27}$$

Therefore, $\dot{V}_o$ can be upper bounded as follows

$$\dot{V}_o \leq -\zeta_o \|\boldsymbol{x}_E\|^2 \tag{3.28}$$

where ζ_o is the minimum eigenvalue of the matrix of inequality (3.26).

Hence, $\dot{V}_o$ is negative semi-definite: this guarantees boundedness of $\widetilde{\boldsymbol{x}}$, $\widetilde{\theta}_o$ and $\widetilde{\boldsymbol{\eta}}$. By invoking the Barbalat's Lemma [53], it can be recognized that $\dot{V}_o \to 0$, which implies global uniform convergence to $\mathbf{0}$ of $\widetilde{\boldsymbol{x}}$ as $t \to \infty$, while $\widetilde{\theta}_o$ is only guaranteed to be bounded (see Remark 1).

□

Remarks 1 and 2 can be easily extended to this observer.

3.3.2.2 A well-established model-free approach

Finally, the well-established approach proposed by [41] will be presented. Here, the heat released by reaction is considered as a further unknown parameter to be estimated, together with the heat transfer coefficient, via a suitably designed nonlinear observer [34].

The term $\widehat{q}$ and $\widehat{\theta}_o$ are obtained by means of the following observer

$$\begin{aligned}\begin{bmatrix}\dot{\widehat{T}}_r\\ \dot{\widehat{T}}_j\\ \dot{\widehat{q}}\\ \dot{\widehat{\theta}}_o\end{bmatrix} &= \begin{bmatrix}0 & 0 & 1 & -\alpha_r(T_r-T_j)\\ 0 & 0 & 0 & \alpha_j(T_r-T_j)\\ 0 & 0 & 0 & 0\\ 0 & 0 & 0 & 0\end{bmatrix}\begin{bmatrix}\widehat{T}_r\\ \widehat{T}_j\\ \widehat{q}\\ \widehat{\theta}_o\end{bmatrix} + \begin{bmatrix}0\\ \beta_j(T_{\text{in}}-T_j)\\ 0\\ 0\end{bmatrix}\\ &+ \begin{bmatrix}2\lambda_q & 0\\ 0 & 2\lambda_\theta\\ \lambda_q^2 & \frac{\alpha_r}{\alpha_j}\lambda_\theta^2\\ 0 & \frac{1}{\alpha_j(T_r-T_j)}\lambda_\theta^2\end{bmatrix}\begin{bmatrix}T_r-\widehat{T}_r\\ T_j-\widehat{T}_j\end{bmatrix},\end{aligned} \tag{3.29}$$

In the above observer, λ_q and λ_θ are suitable positive gains.

When $(T_r - T_j) \to 0$, the observer may suffer of singularities, due to the term $\dfrac{1}{\alpha_j(T_r-T_j)}$. In order to cope with the singularities, $(T_r - T_j)$ could be replaced by a constant value ϵ when $|T_r - T_j| \leq \epsilon$.

A stability analysis of the observer (3.29), can be found in [34, 41].

3.4 Model-based controller

The controller scheme developed in this thesis is based on the Generic Model Control (GMC). It is a well-established nonlinear model-based control approach [4, 24, 59], which has been recently extended via adaptive techniques [22, 41]. The key idea of the GMC is that of globally linearizing the reactor dynamics by acting on the jacket temperature T_j, which is, in turn, controlled by a standard linear (e.g., PID) controller. Since T_j does not play the role of the input manipulated variable, the only way to impose an assigned behavior to the jacket temperature is that of computing a suitable set-point $T_{j,d}$ to be passed by a control loop closed around T_j. Usually, the mathematical relationship between the jacket temperature and the set-point is assumed to be a known linear first-order differential equation, from which $T_{j,d}$ is computed.

Here, no assumptions on the closed-loop behavior of the jacket temperature have been done, and a two-loop control scheme is explicitly designed.

A first control loop (inner loop) is closed around the jacket temperature $y_2 = T_j$, so as to track a desired reference $y_{2,d} = T_{j,d}$ to be determined. Namely, the manipulated input

variable $u = T_{\text{in}}$ is computed as:

$$u = \frac{\dot{y}_{2,d} + g_j e_2 - \alpha_j (y_1 - y_2)\widehat{\theta}_c}{\beta_j} + y_2, \tag{3.30}$$

where $e_2 = y_{2,d} - y_2$ is the tracking error, g_j, is a positive gain and $\widehat{\theta}_c$ is an estimate of θ to be suitably computed.

Also, an outer control loop is closed around the reactor temperature so as to track the desired reactor temperature profile $y_{1,d} = T_{r,d}$. This can be done by computing the reference $y_{2,d}$ of the inner loop as a function of the reactor temperature tracking error $e_1 = y_{1,d} - y_1$ and of the estimate of the heat released by the reaction as follows

$$y_{2,d} = y_1 + \frac{\dot{y}_{1,d} + g_r e_1 - \widehat{q}}{\alpha_r \widehat{\theta}_c} = y_1 + \xi_{2,d}\,, \tag{3.31}$$

where $\widehat{q}$ is computed via one of the previously considered observers and g_r is a positive gain.

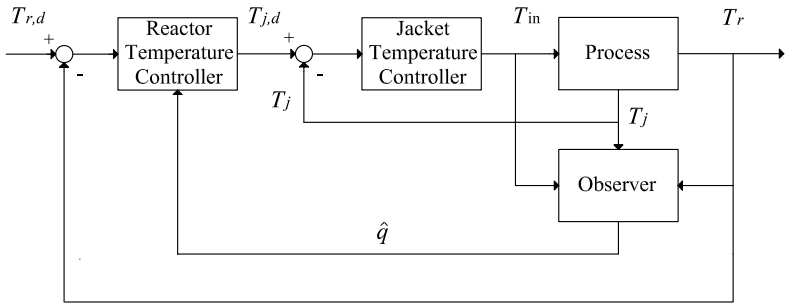

Figure 3.1: Block scheme of the control.

Let define $\boldsymbol{e}$ as the vector of the tracking errors

$$\boldsymbol{e} = \begin{bmatrix} e_1 \\ e_2 \end{bmatrix},$$

and $\boldsymbol{\psi}_c$ as the vector

$$\boldsymbol{\psi}_c(\boldsymbol{y}) = \begin{bmatrix} -\alpha_r \xi_{2,d} \\ -\alpha_j (y_1 - y_2) \end{bmatrix}.$$

Then, the update law for the estimate $\widehat{\theta}_c$ is given by

$$\dot{\widehat{\theta}}_c = \gamma^{-1}\, \boldsymbol{\psi}_c^T(\boldsymbol{y})\, \boldsymbol{e}, \tag{3.32}$$

where γ is a positive gain setting the update rate of the estimate.

3.5 Stability analysis of the controller-observer scheme

Let consider the controller with the observer (3.9). The convergence properties of the error variables for the overall controller-observer scheme, including the parameter estimation error $\widetilde{\theta}_c = \theta - \widehat{\theta}_c$, is stated by the following result.

Theorem 3. *If the rate constants are bounded as in (3.6),(3.7), then, there exists a set of observer gains such that the state estimation error $\widetilde{\boldsymbol{x}}$ and the tracking error $\boldsymbol{e}$ globally uniformly converge to $\mathbf{0}$ as $t \to \infty$, for any positive set of control gains. Moreover, the parameter estimation errors $\widetilde{\theta}_o$ and $\widetilde{\theta}_c$ are bounded for every t.*

Proof. The closed-loop dynamics can be derived by plugging equations (3.30) and (3.31) into (3.8) and taking into account that $y_2 = y_{2,d} - e_2$ and $\widetilde{\theta}_c = \theta - \widehat{\theta}_c$ (and thus, $\theta = \widehat{\theta}_c + \widetilde{\theta}_c$)

$$\dot{\boldsymbol{e}} = \boldsymbol{A}_c\, \boldsymbol{e} + \boldsymbol{\psi}_c(\boldsymbol{y})\, \widetilde{\theta}_c - \boldsymbol{A}_{co}(\boldsymbol{y})\, \widetilde{\boldsymbol{x}}\,, \tag{3.33}$$

where

$$\boldsymbol{A}_c = \begin{bmatrix} -g_r & \alpha_r \theta \\ 0 & -g_j \end{bmatrix}\,, \quad \boldsymbol{A}_{co} = \begin{bmatrix} \boldsymbol{A}_{M,E} & \boldsymbol{O}_{\mathbf{2}\times\mathbf{2}} \end{bmatrix}\,.$$

Consider the following positive definite scalar function

$$V(\widetilde{\boldsymbol{x}}, \boldsymbol{e}, \widetilde{\theta}_o, \widetilde{\theta}_c) = V_o(\widetilde{\boldsymbol{x}}, \widetilde{\theta}_o) + \delta\, V_c(\boldsymbol{e}, \widetilde{\theta}_c)\,,$$

where V_o is the same function defined in (3.13), V_c is given by

$$V_c(\boldsymbol{e}, \widetilde{\theta}_c) = \frac{1}{2}\, \boldsymbol{e}^T\, \boldsymbol{e} + \frac{1}{2}\, \gamma\, \widetilde{\theta}_c^2\,, \tag{3.34}$$

and $\delta > 0$ is a positive constant to be determined.

The derivative of V_c along the closed-loop the trajectories of the system (3.12),(3.33) is given by

$$\dot{V}_c = \boldsymbol{e}^T\, \boldsymbol{A}_c\, \boldsymbol{e} - \boldsymbol{e}^T\, \boldsymbol{A}_{co}\, \widetilde{\boldsymbol{x}} + \boldsymbol{\psi}_c^T\, \boldsymbol{e}\, \widetilde{\theta}_c - \gamma\, \dot{\widehat{\theta}}_c \widetilde{\theta}_c\,.$$

By taking into account the update law (3.32), $\dot{V}_c$ becomes

$$\dot{V}_c = \boldsymbol{e}^T\, \boldsymbol{A}_c\, \boldsymbol{e} - \boldsymbol{e}^T\, \boldsymbol{A}_{co}\, \widetilde{\boldsymbol{x}}\,.$$

The derivative $\dot{V}_c$ can be upper bounded as follows

$$\dot{V}_c \leq -\zeta_c \|\boldsymbol{e}\|^2 + \zeta_{c,o} \|\widetilde{\boldsymbol{x}}\| \|\boldsymbol{e}\|\,,$$

where $\zeta_c = \min\{g_r, g_j\}$ and (the constants $\overline{a}_i$ are defined in (3.14))

$$\zeta_{c,o} = \max_{i=1,\dots,p} \{\overline{a}_i\} \ .$$

Hence, $\dot{V}$ can be upper bounded as follows

$$\begin{aligned} \dot{V} &= \dot{V}_o + \delta \dot{V}_c \\ &\leq -\zeta_o \|\widetilde{\boldsymbol{x}}\|^2 - \delta\zeta_c \|\boldsymbol{e}\|^2 + \delta\zeta_{c,o} \|\widetilde{\boldsymbol{x}}\| \|\boldsymbol{e}\| \\ &= -\begin{bmatrix} \|\widetilde{\boldsymbol{x}}\| \\ \|\boldsymbol{e}\| \end{bmatrix}^T \begin{bmatrix} \zeta_o & -\delta\zeta_{c,o}/2 \\ -\delta\zeta_{c,o}/2 & \delta\zeta_c \end{bmatrix} \begin{bmatrix} \|\widetilde{\boldsymbol{x}}\| \\ \|\boldsymbol{e}\| \end{bmatrix} . \end{aligned}$$

The function $\dot{V}$ is guaranteed to be negative semi-definite if the arbitrary positive constant δ is chosen so as to satisfy the inequality

$$\delta < \frac{4\zeta_o\zeta_c}{\zeta_{c,o}^2} .$$

This guarantees boundedness of all error signals. By invoking the Barbalat's Lemma [53], it can be recognized that $\dot{V} \to 0$, which implies global convergence to $\mathbf{0}$ of both $\widetilde{\boldsymbol{x}}$ and $\boldsymbol{e}$, while the parameters estimation errors $\widetilde{\theta}_o$ and $\widetilde{\theta}_c$ are only guaranteed to be bounded. □

Remark 3. Remarks 1 and 2 on the exponential stability of the estimation error dynamics can be extended to the overall controller-observer scheme as well. Hence, robustness with respect to effects due to modeling uncertainties (e.g., due to inaccurate knowledge of the reaction kinetics) and/or disturbances is guaranteed.

Remark 4. Although the stability analysis considers the dynamics of the overall system (i.e., the dynamics of both the observer and the controller), tuning of the observer gains ($\boldsymbol{L}$ and λ) and of the controller gains (g_r, g_j and γ) can be achieved separately, since the stability conditions do not put mutual constraints on the two set of gains.

Remark 5. As can be noted from (3.32), the estimate $\widehat{\theta}_c$ used in the control law is different from the estimate $\widehat{\theta}_o$ computed by the observer. This is necessary, since the convergence of the latter to θ is not guaranteed unless the persistency of excitation condition is fulfilled. Hence, a different update law is adopted to ensure convergence of the controller tracking errors. However, it can be easily recognized that a unique update law could be adopted, ensuring convergence of both estimation and tracking errors. In this case,

however, stability conditions will put mutual constraints on the observer and controller parameters, and thus independent tuning of the two structures does not guarantee convergence of the estimation/tracking errors.

Remark 6. The stability analysis has been developed for the controller in conjunction with the observer (3.9). It can be easily verified that, if the observer (3.20) is considered instead of observer (3.9), the stability of the overall scheme can be proven using similar arguments.

3.6 Addition of an integral action

A slightly different version of the control laws (3.30) and (3.31), has been proposed in [17,83]. In particular, an integral term has been added to the control laws

$$u = \frac{\dot{y}_{2,d}+g_{\mathrm{p,j}}e_2+g_{\mathrm{i,j}}\int_0^t e_2(\tau)d\tau-\alpha_j(y_1-y_2)\widehat{\theta}_c}{\beta_j}+y_2\,, \tag{3.35}$$

$$y_{2,d} = y_1+\frac{\dot{y}_{1,d}+g_{\mathrm{p,r}}e_1+g_{\mathrm{i,r}}\int_0^t e_1(\tau)d\tau-\widehat{q}}{\alpha_r\widehat{\theta}_c}=y_1+\overline{\xi}_{2,d} \tag{3.36}$$

where $g_{\mathrm{p},*}$ and $g_{\mathrm{i},*}$ $(*=r,j)$ are positive gains, θ_c is an estimate of the parameter θ obtained via the update law

$$\dot{\widehat{\theta}}_c=\gamma^{-1}\boldsymbol{\chi}_c^T(\boldsymbol{y})\,\boldsymbol{P}_c\boldsymbol{\varepsilon}, \tag{3.37}$$

γ is a positive gain and the vectors $\boldsymbol{\varepsilon}$ and $\boldsymbol{\chi}_c$ are defined as

$$\boldsymbol{\varepsilon}=\begin{bmatrix}\int_0^t e_1(\tau)d\tau\\ e_1\\ \int_0^t e_2(\tau)d\tau\\ e_2\end{bmatrix},\quad \boldsymbol{\chi}_c(\boldsymbol{y})=\begin{bmatrix}0\\ -\alpha_r\,\overline{\xi}_{2,d}\\ 0\\ -\alpha_j\,(y_1-y_2)\end{bmatrix}.$$

The matrix $\boldsymbol{P}_c$ in (3.37) is symmetric and positive definite

$$\boldsymbol{P}_c=\begin{bmatrix}\boldsymbol{P}_r & \boldsymbol{O}\\ \boldsymbol{O} & \boldsymbol{P}_j\end{bmatrix},$$

and each matrix $\boldsymbol{P}_*$ $(*=r,j)$ is the symmetric and positive definite solution of the Lyapunov equations

$$\boldsymbol{A}_*^T\boldsymbol{P}_*+\boldsymbol{P}_*\boldsymbol{A}_*=-\boldsymbol{N}_*\,, \tag{3.38}$$

where

$$\boldsymbol{A}_* = \begin{bmatrix} 0 & 1 \\ -g_{\mathrm{i},*} & -g_{\mathrm{p},*} \end{bmatrix},$$

$\boldsymbol{N}_*$ is a symmetric positive definite matrix satisfying

$$\lambda_m(\boldsymbol{N}_j) > \frac{||\boldsymbol{P}_r||^2 \, ||\boldsymbol{A}_{rj}||^2}{\lambda_m(\boldsymbol{N}_r)}, \tag{3.39}$$

$$\boldsymbol{A}_{rj} = \begin{bmatrix} 0 & 0 \\ 0 & \alpha_r \theta \end{bmatrix}.$$

and $\lambda_m(\cdot)$ denotes the minimum eigenvalue of a matrix. Noticeably, since each $\boldsymbol{A}_*$ is Hurwitz (for any choice of the control gains), the solution of the above Lyapunov equations exist for any positive definite matrix $\boldsymbol{N}_*$. This implies that solutions satisfying condition (3.39) always exist.

The convergence of this controller combined with the observer (3.9) has been proven via a Lyapunov like argument in [83].

The presence of the integral in the control laws, could guarantee higher robustness of the control scheme. On the other hand, the tuning becomes much more difficult with respect to the tuning of the controller introduced in Section 3.4. In fact, the tuning of the controller requires the calibration of five different gains, $g_{\mathrm{p},*}$, $g_{\mathrm{i},*}$ $(* = r, j)$ and γ, and the choice of $\boldsymbol{P}_c$ satisfying (3.39).

Moreover, with good tuning, not difficult to obtain with a trial-and-error procedure, the controller in Section 3.4 achieves performance very close to the ones obtained using (3.35) and (3.36).

3.7 Concluding remarks

The attractive and/or novel features of the proposed controller-observer approach can be briefly reviewed:

- The approach is developed for a fairly wide class of processes, i.e., the class of irreversible non-chain reactions characterized by first-order kinetics. Although this is not the most general case, it encompasses several real reactive processes.

- A rigorous analysis of the main properties of the overall scheme (i.e., convergence and robustness) has been provided. In detail: convergence of state estimation and tracking errors is always guaranteed under mild assumptions. Moreover, when the

(stronger) persistency excitation condition is fulfilled, exponential convergence of all error signals is ensured. This, in turn, implies robustness of the proposed scheme in the face of unmodeled effects.

- The use of an accurate and reliable state observer, which is necessary for the proposed controller, can be advantageous for other purposes as well, (e.g., process monitoring and fault diagnosis).
- Since the design and the tuning of the observer can be achieved independently from the adopted controller, the latter can be adopted in conjunction with different observers, e.g., the observers (3.20) and (3.29).

The proposed observer (3.9) needs a good knowledge of the reaction kinetics: this may be regarded as a limitation for its practical application, where a certain degree of mismatch between the modeled and the real reaction mechanism is always present. Nevertheless, in the presence of bounded and/or vanishing uncertainties the property of exponential convergence ensures a certain degree of robustness of the controller-observer scheme. In other words, if the mismatch between the model and the real kinetics is bounded (vanishing), bounded (asymptotically convergent) estimation/tracking errors are expected. Of course, modeling errors must be kept as small as possible, via suitable modeling and identification techniques of the reaction dynamics (see Chapter 2).

When an accurate model of the reaction kinetics cannot be adopted the approach based on the estimation of the heat released via an universal interpolator (3.20) could be adopted. This observer may be adopted also in presence of a totally unknown kinetics.

3.8 Application to the phenol-formaldehyde reaction

The model-based controller-observer scheme requires to solve on-line the system of differential equations of the observer. The phenol-formaldehyde reaction model is characterized by fifteen differential equations and it could be unsuitable for on-line computations. To overcome this problem, a number of reduced-order models have been identified in Chapter 2.

The stability analysis of the controller-observer scheme is based on the assumption that the reactions are characterized by a first order kinetics. For this reason, one of the model characterized by first-order kinetics must be chosen to represent the reaction dynamics.

As will be shown in Chapter 5, the identified model that computes the best estimate of the heat released is the *Model* β with second-order kinetics and molar enthalpy changes variable with the temperature. Among the model with first-order kinetics, the best results have been obtained via the *Model* α with the molar enthalpy changes variable with the temperature.

The adoption of a simplified model of the reaction for the observer means unmodeled dynamics will affect the controller-observer scheme. However, in presence of unmodeled dynamics, due to the exponential convergence, the controller-observer scheme ensures a certain degree of robustness and good results both in term of temperature tracking error and control input.

The mass balances (3.1) become

$$\begin{cases} \dot{C}_{E_1} &= -k_1(T_r)C_{E_1} \\ \dot{C}_M &= k_1(T_r)C_{E_1} - k_2(T_r)C_M \\ \dot{C}_{E_7} &= k_2(T_r)C_M - k_3(T_r)C_{E_7} \end{cases} \tag{3.40}$$

while the heat released computed by the model is given by

$$\begin{aligned} Q &= [(-\Delta H_1(T_r))k_1(T_r)C_{E_1} + (-\Delta H_2(T_r))k_2(T_r)C_M \\ &\quad +(-\Delta H_3(T_r))k_3(T_r)C_{E_7}]\, V_r. \end{aligned} \tag{3.41}$$

The state vector can be defined as

$$\boldsymbol{x} = \begin{bmatrix} x_1 \\ x_2 \\ x_3 \\ x_4 \\ x_5 \end{bmatrix} = \begin{bmatrix} C_{E_1} \\ C_M \\ C_{E_7} \\ T_r \\ T_j \end{bmatrix},$$

and the matrix $\boldsymbol{A}(\boldsymbol{y})$ in equation (3.8) has the form

$$\boldsymbol{A}(\boldsymbol{y}) = \begin{bmatrix} -k_1(T_r) & 0 & 0 & 0 & 0 \\ k_1(T_r) & -k_2(T_r) & 0 & 0 & 0 \\ 0 & k_2(T_r) & -k_3(T_r) & 0 & 0 \\ a_1(y_1) & a_2(y_1) & a_3(y_1) & 0 & 0 \\ 0 & 0 & 0 & 0 & 0 \end{bmatrix},$$

$$a_1(y_1, T_r) = \frac{(-\Delta H_1(T_r))k_1(T_r)}{\rho_r c_{pr}}, \quad a_2(y_1, T_r) = \frac{(-\Delta H_2(T_r))k_2(T_r)}{\rho_r c_{pr}},$$

$$a_3(y_1, T_r) = \frac{(-\Delta H_3(T_r))k_3(T_r)}{\rho_r c_{pr}} .$$

Simulations results, aimed at testing the effectiveness of the proposed approaches, as well as at providing a comparative case study, are reported in the Chapter 5.

Chapter 4

Fault diagnosis

4.1 Introduction

Fault diagnosis in complex process plants is of utmost importance for human and plant safety. In particular, in the chemical industry, faults can occur due to sensors failures, equipment failures or changes in process parameters. Usually, faults in chemical processes can have serious consequences in term of human mortality, environmental impact and economic loss. Among the chemical processes, exothermic reactions in batch reactors are the most dangerous processes. In the United Kingdom between 1962 and 1987 there were 134 accidents in chemical plants due to *run-away* in batch reactors [7], and, among them, 64 are due to polymerization reactions and 13 to phenol-formaldehyde reaction.

Fault diagnosis (FD) consists of three main tasks:

(i) *fault detection*, i.e., the indication of the occurrence of a fault;

(ii) *fault isolation*, i.e., the determination of the type and/or location of the fault;

(iii) *fault identification*, i.e., the determination of the magnitude of the fault.

After a fault has been detected, in some applications a controller reconfiguration for the self-correction of the fault is required (*fault accommodation*). A control system with this kind of fault-tolerance capability is defined as fault-tolerant control system. Fault tolerant control has great importance in situations where the controlled system can have potentially damaging effects on the environment if faults in its components take place, for instance in hazardous chemical plants or nuclear plants.

The relative importance of three tasks are obviously depending by the application, however the detection is an absolute must for any practical system. Fault identification,

on the other hand, even if helpful, may not be essential if no reconfiguration action is required.

In the last decades, the fault diagnosis has interested several researchers and has grown as important research topic.

A traditional approach to fault diagnosis, in particular in dangerous contexts, is the so-called *physical redundancy*, i.e., the duplication of sensors, actuators, computers and softwares to measure and/or control a variable. Typically, a voting scheme is applied to the redundant system to detect and isolate a fault. The physical redundant methods are very reliable, but they need extra equipment and extra maintenance costs. Examples of redundancy methods can be found in [29].

Due to the high costs of physical redundancy, in the last years, researchers focused their attention on techniques that not require extra equipment. These techniques can be roughly classified into two general categories: model-free data-driven approaches and model-based approaches.

Among the model-free approaches, statistical techniques ([31, 52, 56, 66, 67, 99, 105]) and knowledge-based expert systems ([47, 70, 71, 75, 86–88, 101, 106]) have been widely applied for chemical plants.

The model-based methods can be divided into quantitative methods and qualitative methods. The researchers interest is focused mainly on quantitative methods, namely approaches based on observers, parameters estimation and parity equations. These approaches are based on the concept of analytical or functional redundancy, i.e., they use a mathematical model of the process to obtain the estimates of a set of variables characterizing the behavior of the monitored system. The inconsistencies between estimated and measured variables provide a set of residuals, sensitive to the occurrence of faults. Later, the residuals are evaluated aiming at localizing the fault. Although there is a close relationship among the quantitative model-based techniques, observer-based approaches have become very important and diffused, especially within the automatic control community. Reviews of several model-based techniques for FD can be found in [20, 37, 76] and, as for the observer-based methods, in [39, 77, 93].

The Figure 4.1 illustrates the physical and analytical redundancy.

The literature on FDI for chemical plants do not present a significant number of applications of observers: in [26] an unknown input observer is adopted for a CSTR, in [48] and in [19] an extended Kalmann filter (EKF) is used, but in these works the FDI is performed in open loop, while most chemical processes operate in closed-loop and the con-

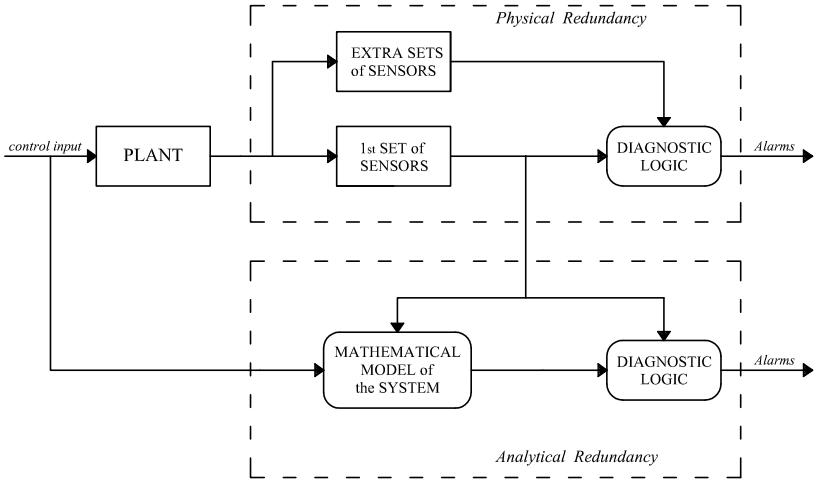

Figure 4.1: Physical versus Analytical redundancy.

trol action may affect the fault diagnosis system performance. A few papers deal with observer-based FDI in the presence of conventional regulators: in [62] and [21] EKFs are used for a distillation column and a CSTR, respectively, in [95] a generalized Luenberger observer is presented. As regards the use of observers for FDI in the presence of advanced control techniques, such as model predictive control or feedback linearizing control, only in [93] may be found an unknown input observer adopted in conjunction with model predictive control.

Interestingly enough, in [28] an approach based on physical redundancy is adopted for fault detection purposes, while an analytical redundancy method is adopted to perform fault identification. A similar approach is presented in this thesis: under the assumption of parallel physical redundancy of both reactor and cooling jacket sensors, a bank of two diagnostic observers has been designed to generate a set of residuals achieving fault detection and isolation for sensor and actuator faults.

4.2 Basic Principles of model-based fault diagnosis

Model-based fault diagnosis consists on detection, isolation and identification of faults in components of a system from the comparison of the system measurements with *a priori* information given by the mathematical model of the system. The differences between the real measurements, y_i, and their estimates, $\widehat{y}_i$, provided, for instance, by an observer, are

referred as residuals

$$r_i = y_i - \widehat{y}_i, \qquad i = 1, \cdots, m, \tag{4.1}$$

where m is the number of available measurements.

A model-based fault diagnosis system comprises two different stages: the residuals generation and the decision making.

The residuals must be designed to be equal to zero under fault-free conditions and nonzero under the occurrence of a fault. Since in practice residuals are never zero, due to model uncertainties and parameters variations, usually, suitable thresholds, ϱ_i, are adopted to avoid false alarms. The algorithm used to generate residuals is called residual generator.

After the generation, residuals must be evaluated in order to detect and isolate a fault. A decision process may consist of a simple threshold test on the instantaneous values or it may consist of methods of statistical decision theory.

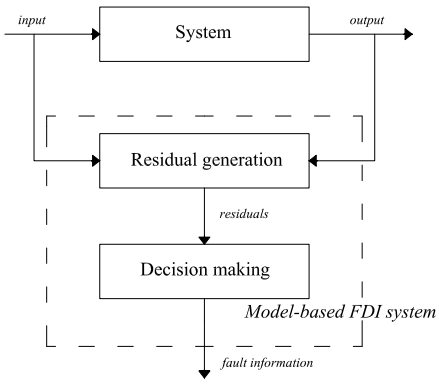

Figure 4.2: Model-based fault diagnosis.

Usually, the fault diagnosis is carried out during system operation, because the system input and output information are only available when the system is in operation. The information used for FDI are the measured output from sensor ad the input to the actuators. In practice, the system model required in model-based fault diagnosis is the open-loop system, hence, it is not necessary to consider the controller in the design of a fault diagnosis scheme [20]. Figure 4.3 shows the relationship between the fault diagnosis with the control loop.

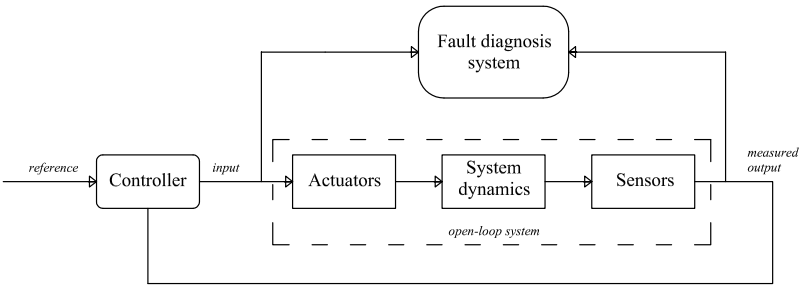

Figure 4.3: Fault diagnosis and control loop.

4.2.1 Fault isolation

Whilst a single residual may be sufficient to detect faults, a vector of residuals is usually required for fault isolation. For isolation purposes, residuals should be generated in such a way that each of them is affected only by a specific subset of faults and any fault affects only a specific subset of residuals (*structured residuals*) [20, 40]. This concept can be expressed in a mathematical form introducing a boolean fault code vector $\boldsymbol{\epsilon}$ and a boolean structure matrix $\boldsymbol{\Lambda}$ [20, 79].

Let consider q different kinds of faults $f_j(t)$ and the $(q \times 1)$ fault vector, $\boldsymbol{f}(t)$

$$\boldsymbol{f}(t) = \begin{bmatrix} f_1(t) \\ \vdots \\ f_q(t) \end{bmatrix}, \tag{4.2}$$

for each fault $f_i(t)$ a boolean fault code vector can be defined as

$$\boldsymbol{\epsilon}^{f_i}(t) = \begin{bmatrix} \epsilon_1^{f_i}(t) \\ \vdots \\ \epsilon_m^{f_i}(t) \end{bmatrix}, \qquad \epsilon_j^{f_i}(t) = \begin{cases} 1 & \text{if} \quad |r_j(t)| \geq \varrho_j \\ 0 & \text{if} \quad |r_j(t)| < \varrho_j \end{cases}. \tag{4.3}$$

Then, the $(m \times q)$ structure matrix $\boldsymbol{\Lambda}$ is defined as

$$\boldsymbol{\Lambda} = \begin{bmatrix} \boldsymbol{\epsilon}^{f_1} & \cdots & \boldsymbol{\epsilon}^{f_q} \end{bmatrix}. \tag{4.4}$$

Defining

$$\boldsymbol{\upsilon} = \boldsymbol{\Lambda} \boldsymbol{f},$$

the following conclusion can be obtained:

- if $\upsilon_i = 0$ the residual r_i is not affected by any fault;

- if $v_i = f_i(t)$ the residual r_i is affected only by the fault $f_i(t)$;
- if $v_i = f_i(t) + f_j(t)$ the residual r_i is affected by the faults $f_i(t)$ and $f_j(t)$ and not affected by the other faults;
- and so on.

A fault $f_i(t)$ is called undetectable if the vector $\boldsymbol{\epsilon}^{f_i}$ is the null vector: this fault cannot be detected using the residuals set defined in (4.1).

Two faults $f_i(t)$ and $f_j(t)$ are distinguishable if the vectors $\boldsymbol{\epsilon}^{f_i}$ and $\boldsymbol{\epsilon}^{f_j}$ are different.

4.2.2 Performance evaluation of a fault diagnosis system

Essentially, a FD system must avoid two kinds of errors: (i) false alarms and (ii) missed alarms. A false alarm occurs when a fault is declared although no fault occurred; typically they can be due to model uncertainties and their occurrence may be reduced with a suitable choice of the thresholds. To this aim, several adaptive thresholds have been introduced, see, e.g., [108]. On the other hand, a missed alarm occurs when, under faulty condition, the FD system does not detect anything; it may be due, for instance, to the adoption of too wide thresholds.

Of course, false alarm and missed alarm avoidance are conflicting requirements: the selection of the thresholds must be done as a compromise between them.

4.3 Fault classification

In the chemical process faults can be classified in process faults, sensor faults and actuator faults.

A process fault occurs when there is an unexpected variation on a process parameters, e.g., abrupt variation of the heat transfer coefficient due to foulness on reactor walls or side reaction due to impurity in the raw material.

In this thesis only sensor and actuator faults have been considered. As above discussed, in FDI the open-loop system is adopted. For purposes of modeling, an open-loop system can be separated into three parts: actuators, system dynamics and sensor (see Figure 4.4).

Referring to the Figure 4.4, $\boldsymbol{u}$ is the known control command, $\boldsymbol{u}_a$ is the actuator response, $\boldsymbol{y}$ is the output of the system and $\boldsymbol{y}_m$ is the known measured output, given by the sensors.

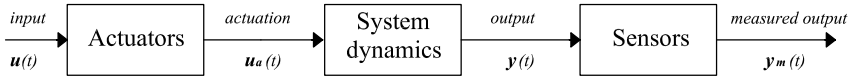

Figure 4.4: Open-loop system.

When, for the sake of simplicity, sensors and actuators dynamics and disturbs are neglected, fault-free condition is characterized by the following relations

$$\boldsymbol{y}_m = \boldsymbol{y}\,, \qquad \boldsymbol{u}_a = \boldsymbol{u}\,.$$

A sensor fault can be described mathematically as (see Figure 4.5)

$$\boldsymbol{y}_m(t) = \boldsymbol{y}(t) + \boldsymbol{f}_s(t)\,, \tag{4.5}$$

where $\boldsymbol{f}_s(t)$ is the sensor fault vector. By choosing the vector $\boldsymbol{f}_s$ correctly it is possible describe all sensor fault situations. For instance, an abrupt switch to zero of the measured signal is described by $\boldsymbol{f}_s(t) = -\boldsymbol{y}(t)$, in such a way that $\boldsymbol{y}_m = \boldsymbol{0}$; for an abrupt constant bias added to the measured signal the vector $\boldsymbol{f}_s(t) = \delta\boldsymbol{y}$ is added to the output and the measured signal become $\boldsymbol{y}_m(t) = \boldsymbol{y}(t) + \delta\boldsymbol{y}$.

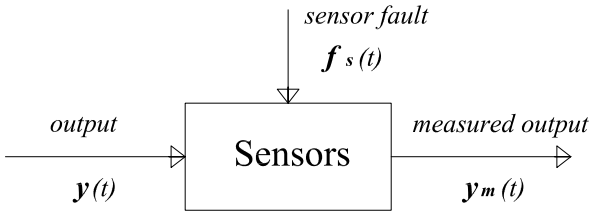

Figure 4.5: Sensor fault.

In a similar way, the actuator action in the presence of an actuator fault becomes (see Figure 4.6)

$$\boldsymbol{u}_a(t) = \boldsymbol{u}(t) + \boldsymbol{f}_a(t)\,, \tag{4.6}$$

where $\boldsymbol{f}_a$ is the actuator fault vector. Similar to sensor faults, different actuator faults situations can be represented by a proper fault vector. For instance an abrupt constant

bias on the actuator action can be represented via the vector $\boldsymbol{f}_a(t) = \delta\boldsymbol{u}$, such as the actuator action becomes $\boldsymbol{u}_a = \boldsymbol{u} + \delta\boldsymbol{u}$; if the actuator action is frozen at its current value at a certain time instant, the fault vector becomes $\boldsymbol{f}_a(t) = -\boldsymbol{u}(t)$ and $\boldsymbol{u}_a = \boldsymbol{0}$.

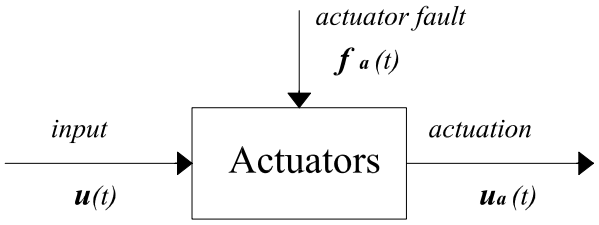

Figure 4.6: Actuator fault.

4.4 Proposed FDI scheme

Because of the high level of risk involving highly exothermic chemical processes, sensors for temperature monitoring are often duplicated in batch reactors. Hence, it is assumed that a duplex sensor architecture is adopted for the plant. Namely, two temperature sensors (hereafter labeled as $S_{r,1}$ and $S_{r,2}$) providing measurements of T_r, and two providing measurements of T_j (hereafter labeled as $S_{j,1}$ and $S_{j,2}$) are available. In order to achieve fault isolation, a bank of two observers has been adopted [2]; namely:

- the first observer, labeled as SM1, uses the measurements provided by $S_{r,1}$ and $S_{j,1}$ (i.e., $\boldsymbol{y}_{SM1} = (y_{r,1} \;\; y_{j,1})^T$),

- the second observer, labeled as SM2, uses the measurements provided by $S_{r,2}$ and $S_{j,2}$ (i.e., $\boldsymbol{y}_{SM2} = (y_{r,2} \;\; y_{j,2})^T$).

As regards the observers architecture, both observer (3.9) and (3.20) may be adopted. In [80], this FDI scheme has been proposed in conjunction with a robust observer. The observers gain matrix $\boldsymbol{L}_E$ are designed via a $\mathcal{H}_\infty$ approach, so as to guarantee robustness even in the presence of external disturbances and modeling errors, such as the uncertainties on the parameter θ. The heat released by the reaction is estimated via the same on-line linear-in-the-parameters approximator (3.22), adapted via (3.23).

Different strategies have been designed for sensor faults and actuator faults. As regards sensor faults, both detection and isolation can be achieved and the control system can be reconfigured in such a way to end the batch process even in the presence of a faulty sensor, without significant loss of quality of the final product. As regards actuators faults only detection can be achieved.

4.4.1 Residuals generation

Four different residuals have been adopted for achieving detection and isolation.

The first couple of residuals may be defined, on the basis of the available measures, as

$$r_{S_r} = \frac{y_{r,1} - y_{r,2}}{\mu_1}, \qquad r_{S_j} = \frac{y_{j,1} - y_{j,2}}{\mu_2}, \tag{4.7}$$

where μ_1 and μ_2 are normalization factors to be properly determined.

The second couple of residuals can be obtained via the diagnostic observers as

$$\boldsymbol{r}_{\text{SM1}} = \frac{\widetilde{\boldsymbol{y}}_{\text{SM1}}}{\rho_1}, \quad \boldsymbol{r}_{\text{SM2}} = \frac{\widetilde{\boldsymbol{y}}_{\text{SM2}}}{\rho_2}, \tag{4.8}$$

where ρ_1 and ρ_2 are normalization factors to be properly determined and $\widetilde{\boldsymbol{y}}_{\text{SMi}}$ is the output estimate error of the observer SMi ($i = 1, 2$).

4.4.2 Sensor faults

The defined residuals are able to achieve both detection and isolation when a sensor fault occurs.

As detection residuals the quantities r_{S_r} and r_{S_j} can be adopted. Hence, if one of the S_r (S_j) is affected by a fault, the norm of r_{S_r} (r_{S_j}) is expected to exceed a certain threshold.

For isolation purposes of the sensor faults, the other couple of residuals, $\boldsymbol{r}_{\text{SM1}}$ and $\boldsymbol{r}_{\text{SM2}}$ may be used. If the norm of $\boldsymbol{r}_{\text{SM1}}$ ($\boldsymbol{r}_{\text{SM2}}$) exceeds a certain threshold, a fault is declared on $S_{r,1}$ or $S_{j,1}$ ($S_{r,2}$ or $S_{j,2}$), depending on which detection residual exceeds the threshold. In fact, the output of the SM1 observer is not affected by faults on $S_{r,2}$ and $S_{j,2}$, while the output of the SM2 observer is not affected by faults on $S_{r,1}$ and $S_{j,1}$.

The normalization factors ρ_i and μ_i ($i = 1, 2$) are chosen by evaluating the effect of disturbances and variations of the uncertain parameter on the residuals; they can be set, e.g., on the basis of experimental data collected in healthy conditions and in the presence of disturbances and variations of the uncertain parameter. By virtue of these

normalization factors the thresholds on the residuals have been fixed to 1 and the infinity norm [1] of vectors has been used to detect and isolate faults. In particular if $||\boldsymbol{r}_{\text{SM1}}||_\infty > 1$ ($||\boldsymbol{r}_{\text{SM2}}||_\infty > 1$) for a fixed time interval, a fault is declared on the first (second) sensor.

4.4.3 Actuators faults

If an actuator fault occurs, in the absence of sensor failures, the norms of residuals r_{S_r} and r_{S_j} remain below the thresholds but the observers dynamics are affected by the faulted input, therefore the norms of both residuals $\boldsymbol{r}_{\text{SM1}}$ and $\boldsymbol{r}_{\text{SM2}}$ exceed the thresholds.

Concluding, an actuator fault is declared if both $\|r_{S_r}\|$ and $\|r_{S_j}\|$ are below the thresholds and both $\|\boldsymbol{r}_{\text{SM1}}\|$ and $\|\boldsymbol{r}_{\text{SM2}}\|$ exceed the thresholds.

Of course, since in the proposed scheme actuator redundancy is not present, it is only possible detect the actuator faults, but after a fault occurs it is not possible to brought to completion the batch execution.

4.4.4 Decision Making System

The key point for faults detection and isolation is the design of a suitable *Decision Making System* (DMS), which, on the basis of the available measurements (physical sensors) and their estimates (virtual sensors), declares the occurrence of a fault, isolates the possible faulty sensor, and outputs an healthy signal.

Let define the fault code vector

$$\boldsymbol{\epsilon}(t) = \begin{bmatrix} \epsilon_{S_r} \\ \epsilon_{S_j} \\ \epsilon_{\text{SM1}} \\ \epsilon_{\text{SM2}} \end{bmatrix}, \qquad \epsilon_* = \begin{cases} 1 & \text{if} \quad \|\boldsymbol{r}_*(t)\|_\infty \geq 1 \\ 0 & \text{if} \quad \|\boldsymbol{r}_*(t)\|_\infty < 1 \end{cases}, \quad * = \{S_r, S_j, \text{ SM1}, \text{SM2}\}.$$

On the basis of the values that the vector $\boldsymbol{\epsilon}(t)$ assumes during the batch execution the DMS can declare and, eventually, isolate a fault. Under the assumption that simultaneous faults on different sensors and/or on the actuator do not occur, the possible values that the vector $\boldsymbol{\epsilon}(t)$ can assume during a batch are summarized in Table 4.1, together with the decision taken by the DMS for each situation.

Thanks to the sensor redundancy, the batch can be brought to completion even in presence of a sensor fault, provided that a suitable voting of the correct signal is performed. The logic of the *Voter/Monitor* (the sub-system of the DMS which votes the

[1] The infinity norm of a vector $\boldsymbol{v}$ is defined as $\|\boldsymbol{v}\|_\infty = \max_i(|v(i)|)$

ϵ_{S_r}	ϵ_{S_r}	ϵ_{SM1}	ϵ_{SM1}	DMS Decisions
0	0	0	0	No fault declared
1	0	1	0	Fault declared on sensor $S_{r,1}$
1	0	0	1	Fault declared on sensor $S_{r,2}$
1	0	0	0	Fault declared but not isolated
0	1	1	0	Fault declared on sensor $S_{j,1}$
0	1	0	1	Fault declared on sensor $S_{j,2}$
0	1	0	0	Fault declared but not isolated
0	0	1	1	Fault declared on the actuator

Table 4.1: Decisions of DMS on the basis of the residuals.

correct signal) is described in the following procedure and diagramatically depicted in Figure 4.7. As usual, the procedure is based on the assumption that simultaneous faults on different sensors do not occur.

Voter procedure

Step 1. Compute the detection residuals defined in (4.7), then:

(i) If the residuals do not exceed the fixed thresholds (no fault condition), vote the signal given by the average of the two redundant sensors, i.e., the so-called standard duplex measure.

(ii) If a threshold is exceeded (fault condition), check the isolation residuals defined in (4.8), so as to decide if the faulty signal can be isolated; in this case determine the healthy signal.

Step 2. If in the case (ii) faults isolation is not achieved (i.e., both $\boldsymbol{r}_{\text{SM1}}$ and $\boldsymbol{r}_{\text{SM2}}$ are below the respective thresholds), a missed isolation is declared. In this case, the weighted average of the signals provided by the physical and virtual sensors is voted. The weighted average is computed as the arithmetic mean of the measured variable and the output of the sole observer not signaling the occurrence of the fault. ■

It is of the utmost importance to guarantee that the worst-case performance of the proposed scheme, in terms of voted signal, is not worse than those of a standard duplex measure. Hence, a further elaboration of the residuals is performed. Namely, if the absolute value of the difference between the weighted average and each sensor signal is

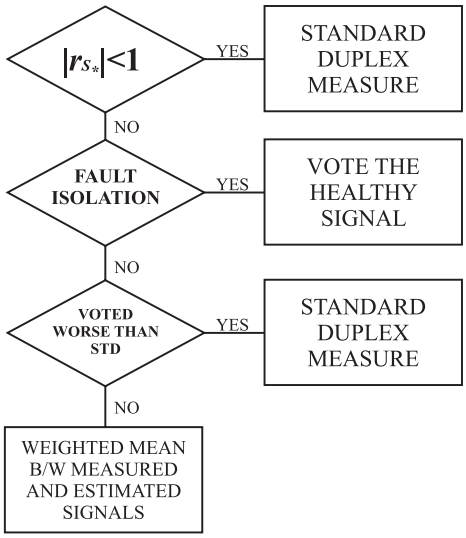

Figure 4.7: DMS Voter Logic.

larger than the difference between the standard duplex measure and the sensor signals, then the standard duplex measure is voted as *healthy* measure.

Of course, in the presence of an actuator faults, due the absence of actuator redundancy, the batch must be stopped.

The DMS logic is then completed as follows:

- A rate limiter on the voted signal is adopted, so as to avoid sudden changes of the signals due, for example, to abrupt faults.

- A step-by-step check verifies if one of the observers is brought to divergence. In this case the related outputs are inhibited and the quadruplex scheme changes into a triplex voter/monitor system.

- If the measurements variance exceeds a prespecified value, a fault is signaled. This check is introduced because high frequency (and zero mean) additive faults may be filtered by the observer dynamics, causing missed alarms.

- Variations of logical signals are taken into account only if they remain constant for a fixed time window.

Chapter 5

Case studies

5.1 Introduction

In order to prove the effectiveness of the identification, control and diagnosis approaches, proposed in this thesis, a detailed simulation model of a batch reactor has been developed. The identification techniques, described in Chapter 2, have been applied to the phenol-formaldehyde reaction, in order to obtain simplified models, suitable for model-based control design. These models have been validated on the basis of the root mean squared error, both for concentrations estimation and for heat estimation, obtained when they are forced to track an assigned temperature profile. To this aim, a number of test profiles have been selected.

Then, the first-order model that achieves the best performance in term of concentrations and heat estimates, has been adopted to design the model-based observer (3.9). The model-based observer-controller scheme performance have been compared with the ones obtained by using the model-free observer (3.20) and the observer proposed by [41].

Finally, some sensor and actuator faults have been simulated on the plant and the fault diagnosis technique described in Chapter 4 has been tested, using both the observer (3.9) and the observer (3.20).

5.2 Simulation model

The simulation model has been developed in the Matlab/Simulink© environment. The reaction phenol-formaldehyde has been simulated considering the system of differential equations given by the 13 mass balances written in Section 1.5.3. The heat released by the

Parameter	Value	Parameter	Value
V_r	6 [m^3]	V_j	1.729 [m^3]
U	0.7205 [kJ m^{-2} s^{-1} K^{-1}]	S	15.961 [m^2]
θ	11.5 [kJ s^{-1} K^{-1}]	R	0.0083 [kJ mol^{-1} K^{-1}]
ρ_r	$1.0 \cdot 10^3$ [kJ m^{-3} K^{-1}]	ρ_j	$1.0 \cdot 10^3$ [kJ m^{-3} K^{-1}]
c_{pr}	$1.712 \cdot 10^3$ [kJ m^{-3} K]	c_{pj}	$4.19 \cdot 10^3$ [kJ m^{-3} K]
$C_{E_1}(0)$	4200 [mol m^{-3}]	$C_{E_2}(0)$	8400 [mol m^{-3}]
$T_r(0)$	293.15 [K]	$T_j(0)$	293.16 [K]
$T_{j,min}$	285 [K]	$T_{j,max}$	370 [K]
F	0.1 [m^3 s^{-1}]		

Table 5.1: Simulation parameters.

reaction has been computed via equation (1.19).

Some assumptions on the experimental set-up have been done. A geometric model of the reactor and the cooling jacket has been built, characterized by the values in Table 5.1. The energy balances for the reactor and the jacket are given by the equations (1.8) and (1.10). For the values of the mass heat capacities, it has been considered that the cooling fluid is water and, for the reactant mixture, the value in [82] has been adopted.

In order to simulate a realistic industrial context, where several parameters are uncertain and/or bounded by physical limitations, the following assumptions on the actuator and the sensors have been done. The temperature of the water entering the jacket ranges from $T_{\text{in},m} = 285$ [K] to $T_{\text{in},M} = 370$ [K]; the water flow rate is fixed and equal to $F = 0.1$ [m^3 s^{-1}]; moreover a first-order linear dynamics (with a time constant of 2 [s]) between the commanded control input (computed by the controller) and the real temperature of the water entering the jacket has been introduced in the simulation model. Concerning the sensor equipment, only the reactor temperature and the jacket temperature are measured, while direct measurements of the concentrations and/or of the heat released by the reaction are not available in real-time. Also, gaussian white noise with zero mean and variance of $5 \cdot 10^{-3}$ is added to the temperature measurements.

Finally some initial conditions for the reactant concentrations and the temperatures of the vessel and the jacket are assumed, and these values are reported in Table 5.1.

5.3 Identification of the reaction kinetics

In order to obtain the set of experimental data, as described in Section 2.5.1, the phenol-formaldehyde reaction has been simulated at nine different constant temperatures ($\mathcal{T}$=$\{60°C, 65°C, 70°C, 75°C, 80°C, 85°C, 90°C, 95°C, 100°C\}$) and the batch time has been specified as $t_b = 15$ hours. A PID controller, based on the feedback of the reactor temperature, has been used to heat the reactor until the desired temperature and to keep it constant during the reaction. The PID parameters, tuned via trial-and-error procedure, are $K_P = 9 \cdot 10^{-4}$, $K_I = K_D = 10^{-7}$. The actuator and the temperature sensors are characterized by the features described in the previous Section. For each temperature, the values of the concentrations of the 13 compounds, at 71 different time instants, t_i, have been measured: the first instant is the initial time ($t_0 = 0$), then, in the first hour 12 samples have been collected with a 5 minutes step, in the second hour 6 samples have been collected with a 10 minutes step, and, in the following hours, 4 samples per hour have been collected with a 15 minutes step. Different steps for the first hours have been selected, because in these hours the reaction is much more faster than in the following, due to the higher concentrations of reactants. In practice, since the concentrations can be measured only off-line, it has been supposed that at each instant t_i a sample of reacting mixture has been drawn and analyzed. Finally, in order to simulate the measurement errors, gaussian white noise has been added to the concentration measurements (zero means and variance equal to 10^2).

As regards the heat released by the reaction, it has been supposed that, at the same nine constant temperatures, the reaction occurred in a calorimeter and the value of the heat released for a unit volume at the instants t_i, has been collected [91]. In order to simulate the measurement errors, gaussian white noise has been added to the heat values (zero means and variance equal to 10).

In this way a total number of 639 samples has been considered both for the concentration and for the heat estimation.

5.3.1 Estimation of kinetic parameters

The kinetics parameters to be estimated are the parameters φ_i and ψ_i ($i = 1, \ldots, p$, and $p = 3$ for *Model* α and $p = 4$ for *Model* β), defined in (2.45) and (2.46). The reference temperature for the parameters φ_i has been assumed equal to $T^* = 353.15$ [K].

The Levenberg-Marquardt algorithm (2.20) has been adopted with the following val-

ues for the algorithm parameters: the step size $\kappa = 0.10$, the initial damping factor $\lambda_0 = 1000$ and $\nu = 10$.

The identification procedure has been replicated for different initial values of the parameters. For the parameters φ_i initial values of -20 or -25 have been considered, while for the parameters ψ_i initial values of 8.5 or 9.5 have been chosen. Therefore, for the *Model* α, in which there are 6 parameters to be estimated, 64 different replication have been considered; for *Model* β, in which there are 8 parameters to be estimated, 256 replication with different initial conditions have been done.

The parameters that achieve the best fit of the data set, together with the initial conditions and the value of the objective function (2.43) for *Model* α and *Model* β, are reported in Tables 5.2 and 5.3, respectively, where φ_i^0 and ψ_i^0 are the initial estimates of φ_i and ψ_i.

Model	α first-order kinetics	α second-order kinetics
Objective Function	$1.178 \cdot 10^8$	$9.725 \cdot 10^6$
φ_1^0	-20	-25
ψ_1^0	9.5	9.5
φ_2^0	-20	-25
ψ_2^0	9.5	9.5
φ_3^0	-20	-20
ψ_3^0	9.5	9.5
φ_1	-9.499	-17.333
ψ_1	9.144	9.259
φ_2	-10.433	-18.160
ψ_2	8.854	9.145
φ_3	-10.094	-17.527
ψ_3	8.569	8.880

Table 5.2: Best fit kinetic parameters for *Model* α.

The best fit parameters may be expressed in terms of pre-exponential factors and activation energies; the resulting values are reported in Tables 5.4 and 5.5.

5.3.2 Estimation of the molar enthalpy changes

Once the kinetic parameters have been estimated, the expression of the heat released becomes linear in the unknown parameters ΔH_i. Therefore, it is possible to use equation

Model	β first-order kinetics	β second-order kinetics
Objective Function	$1.223 \cdot 10^8$	$9.864 \cdot 10^6$
φ_1^0	-20	-25
ψ_1^0	8.5	9.5
φ_2^0	-25	-20
ψ_2^0	9.5	8.5
φ_3^0	-25	-25
ψ_3^0	8.5	8.5
φ_4^0	-25	-25
ψ_4^0	9.5	9.5
φ_1	-9.518	-17.325
ψ_1	9.045	9.268
φ_2	-74.224	-20.809
ψ_2	10.309	9.052
φ_3	-10.403	-18.223
ψ_3	8.909	9.151
φ_4	-10.238	-17.706
ψ_4	8.732	9.009

Table 5.3: Best fit kinetic parameters for *Model* β.

(2.12) to compute the values of the molar enthalpy changes that minimize the objective function (2.48). Following the procedure described in Section 2.4.3.2, the molar enthalpy changes have been estimated first as constant values, then, in order to improve the heat estimation, as parameters dependent upon the temperature.

In Tables 5.6 and 5.7, are reported the values obtained for the molar enthalpy changes considered as constants.

It is worth noticing that for the *Model* β with first-order kinetics, the molar enthalpy change ΔH_2 is negligible.

When the molar enthalpy changes are considered as parameters dependent upon the temperature, a value for each temperature has been estimated and, then, an interpolating polynomial function has been considered. The values of the parameters for each temperature are reported in Tables 5.8-5.11. Since the values of the parameter ΔH_2 for the *Model* β with first-order kinetics is negligible, they are not reported in the Table 5.10. The

Model	α first-order kinetics	α second-order kinetics
$k_{0,1}$	$2.416 \cdot 10^7$ [s^{-1}]	$2.396 \cdot 10^5$ [$m^3 \cdot mol^{-1} \cdot s^{-1}$]
$E_{a,1}$	77.850 [kJ mol^{-1}]	87.312 [kJ mol^{-1}]
$k_{0,2}$	$1.203 \cdot 10^4$ [s^{-1}]	$4.319 \cdot 10^3$ [$m^3 \cdot mol^{-1} \cdot s^{-1}$]
$E_{a,2}$	58.253 [kJ mol^{-1}]	77.944 [kJ mol^{-1}]
$k_{0,3}$	$1.236 \cdot 10^2$ [s^{-1}]	$1.687 \cdot 10$ [$m^3 \cdot mol^{-1} \cdot s^{-1}$]
$E_{a,3}$	43.807 [kJ mol^{-1}]	59.793 [kJ mol^{-1}]

Table 5.4: Kinetic parameters for *Model* α: pre-exponential factors and activation energies.

Model	β first-order kinetics	β second-order kinetics
$k_{0,1}$	$1.950 \cdot 10^6$ [s^{-1}]	$3.188 \cdot 10^5$ [$m^3 \cdot mol^{-1} \cdot s^{-1}$]
$E_{a,1}$	70.512 [kJ mol^{-1}]	88.128 [kJ mol^{-1}]
$k_{0,2}$	$4.570 \cdot 10^4$ [s^{-1}]	$2.881 \cdot 10$ [$m^3 \cdot mol^{-1} \cdot s^{-1}$]
$E_{a,2}$	249.582 [kJ mol^{-1}]	71.008 [kJ mol^{-1}]
$k_{0,3}$	$3.804 \cdot 10^4$ [s^{-1}]	$4.732 \cdot 10^3$ [$m^3 \cdot mol^{-1} \cdot s^{-1}$]
$E_{a,3}$	61.546 [kJ mol^{-1}]	78.397 [kJ mol^{-1}]
$k_{0,4}$	$1.500 \cdot 10^3$ [s^{-1}]	$2.320 \cdot 10^2$ [$m^3 \cdot mol^{-1} \cdot s^{-1}$]
$E_{a,5}$	51.562 [kJ mol^{-1}]	68.019 [kJ mol^{-1}]

Table 5.5: Kinetic parameters for *Model* β: pre-exponential factors and activation energies.

interpolating polynomial functions are reported in the following; they are expressed in terms of the temperature normalized with respect to the mean value (μ) and the standard deviation (σ) of the set of temperatures $\mathcal{T}$

$$T_n = \frac{T - \mu}{\sigma}.$$

Cubic or 4_{th} degree polynomial function have been adopted. In particular, the 4_{th} degree polynomial function has been adopted when the cubic function achieves poor interpolating performance. Since the data set is referred only to the range of temperature between $60°C$ and $100°C$, the polynomial functions $f_i(T)$ are able to interpolate the true values of the molar enthalpy changes only in this range. To overcome this drawback, for all the models the following assumptions have been done ($i = 1, \cdots, p$)

$$\Delta H_i(T^*) = \begin{cases} \Delta H_i(60°C) & \text{if} \quad T^* \leq 60°C\,, \\ f_i(T^*) & \text{if} \quad 60°C < T^* < 100°C\,, \\ \Delta H_i(100°C) & \text{if} \quad T^* \geq 100°C \end{cases}$$

Model	α first-order kinetics	α second-order kinetics
ΔH_1	-40.646 [kJ mol^{-1}]	-26.178 [kJ mol^{-1}]
ΔH_2	-10.510 [kJ mol^{-1}]	-66.200 [kJ mol^{-1}]
ΔH_3	-21.372 [kJ mol^{-1}]	19.690 [kJ mol^{-1}]

Table 5.6: Molar enthalpy changes for *Model* α.

Model	β first-order kinetics	β second-order kinetics
ΔH_1	-44.395 [kJ mol^{-1}]	-19.876 [kJ mol^{-1}]
ΔH_2	$1.612 \cdot 10^{-14}$ [kJ mol^{-1}]	-1647.3 [kJ mol^{-1}]
ΔH_3	-2.087 [kJ mol^{-1}]	6.4777 [kJ mol^{-1}]
ΔH_4	-26.897 [kJ mol^{-1}]	-20.768 [kJ mol^{-1}]

Table 5.7: Molar enthalpy changes for *Model* β.

***Model* α first-order kinetics**

T	$60°C$	$65°C$	$70°C$	$75°C$	$80°C$	$85°C$	$90°C$	$95°C$	$100°C$
ΔH_1	-24.72	-26.50	-29.20	-31.97	-34.84	-37.28	-39.81	-41.84	-43.75
ΔH_2	-40.04	-40.14	-34.43	-26.24	-19.57	-15.11	-12.23	-9.92	-7.94
ΔH_3	37.78	36.60	23.36	6.81	-5.68	-13.63	-19.15	-23.39	-27.04

Table 5.8: Molar enthalpy changes variable with the temperature for *Model* α with first-order kinetics.

Model α first-order kinetics

The molar enthalpy changes are represented via the following polynomial functions

- $\Delta H_1(T) = p_{1,1}T_n^3 + p_{1,2}T_n^2 + p_{1,3}T_n + p_{1,4}$,
- $\Delta H_2(T) = p_{2,1}T_n^4 + p_{2,2}T_n^3 + p_{2,3}T_n^2 + p_{2,4}T_n + p_{2,5}$,
- $\Delta H_3(T) = p_{3,1}T_n^4 + p_{3,2}T_n^3 + p_{3,3}T_n^2 + p_{3,4}T_n + p_{3,5}$,

where

$$p_{1,1} = 0.460; \quad p_{1,2} = 0.248; \quad p_{1,3} = -7.513; \quad p_{1,4} = -34.656;$$
$$p_{2,1} = 2.762; \quad p_{2,2} = -2.612; \quad p_{2,3} = -7.885; \quad p_{2,4} = 16.642; \quad p_{2,5} = -19.700;$$
$$p_{3,1} = -5.528; \quad p_{3,2} = 4.305; \quad p_{3,3} = 16.889; \quad p_{3,4} = -31.635; \quad p_{3,5} = -5.542.$$

***Model* α second-order kinetics**

T	$60°C$	$65°C$	$70°C$	$75°C$	$80°C$	$85°C$	$90°C$	$95°C$	$100°C$
ΔH_1	-20.43	-21.52	-22.97	-24.17	-25.39	-25.95	-26.56	-26.54	-26.36
ΔH_2	-125.1	-94.16	-79.79	-70.58	-66.65	-66.16	-67.09	-67.03	-65.55
ΔH_3	1112.6	291.65	108.65	50.94	31.86	24.28	20.94	18.60	16.64

Table 5.9: Molar enthalpy changes variable with the temperature for *Model* α with second-order kinetics.

***Model* β first-order kinetics**

T	$60°C$	$65°C$	$70°C$	$75°C$	$80°C$	$85°C$	$90°C$	$95°C$	$100°C$
ΔH_1	-21.67	-24.19	-27.70	-31.46	-35.52	-39.28	-43.27	-46.83	-50.34
ΔH_3	-41.54	-41.32	-35.39	-26.24	-17.75	-10.84	-5.00	0.735	6.64
ΔH_4	41.46	39.75	25.02	6.72	-7.35	-16.69	-23.70	-29.75	-35.72

Table 5.10: Molar enthalpy changes variable with the temperature for *Model* β with first-order kinetics.

***Model* α second-order kinetics**

The molar enthalpy changes are represented via the following polynomial functions

- $\Delta H_1(T) = q_{2,1}T_n^3 + q_{2,2}T_n^2 + q_{2,3}T_n + q_{2,4}$,
- $\Delta H_2(T) = q_{2,1}T_n^3 + q_{2,2}T_n^2 + q_{2,3}T_n + q_{2,4}$,
- $\Delta H_3(T) = q_{3,1}T_n^4 + q_{3,2}T_n^3 + q_{3,3}T_n^2 + q_{3,4}T_n + q_{3,5}$,

where

$$
\begin{array}{llll}
q_{1,1} = 0.254; & q_{1,2} = 0.889; & q_{1,3} = -2.579; & q_{1,4} = -25.221; \\
q_{2,1} = 7.584; & q_{2,2} = -13.255; & q_{2,3} = 4.012; & q_{2,4} = -66.226; \\
q_{3,1} = 149.46; & q_{3,2} = -208.37; & q_{3,3} = -77.08; & q_{3,4} = 81.125; \qquad q_{3,5} = 45.736.
\end{array}
$$

***Model* β first-order kinetics**

The molar enthalpy changes are represented via the following polynomial functions

- $\Delta H_1(T) = s_{1,1}T_n^3 + s_{1,2}T_n^2 + s_{1,3}T_n + s_{1,4}$,

***Model* β second-order kinetics**

T	$60°C$	$65°C$	$70°C$	$75°C$	$80°C$	$85°C$	$90°C$	$95°C$	$100°C$
ΔH_1	-17.87	-17.82	-18.42	-18.59	-18.83	-18.79	-19.08	-19.23	-19.47
ΔH_2	-874.4	-998.3	-1145	-1285	-1447	-1600	-1789	-1957	-2135
ΔH_3	-7.14	-2.27	2.08	5.64	9.45	13.09	17.28	20.04	22.37
ΔH_4	45.40	3.94	-8.17	-13.01	-16.98	-21.08	-25.52	-28.59	-30.97

Table 5.11: Molar enthalpy changes variable with the temperature for *Model* β with second-order kinetics.

- $\Delta H_2(T) = 0$;
- $\Delta H_3(T) = s_{3,1}T_n^4 + s_{3,2}T_n^3 + s_{3,3}T_n^2 + s_{3,4}T_n + s_{3,5}$,
- $\Delta H_4(T) = s_{4,1}T_n^4 + s_{4,2}T_n^3 + s_{4,3}T_n^2 + s_{4,4}T_n + s_{4,5}$,

where

$$s_{1,1} = 0.515; \quad s_{1,2} = -0.265; \quad s_{1,3} = -10.924; \quad s_{1,4} = -35.349;$$
$$s_{3,1} = 2.539; \quad s_{3,2} = -2.655; \quad s_{3,3} = -5.176; \quad s_{3,4} = 22.210; \quad s_{3,5} = -17.917;$$
$$s_{4,1} = -6.002; \quad s_{4,2} = 4.323; \quad s_{4,3} = 17.504; \quad s_{4,4} = -35.926; \quad s_{4,5} = -7.196.$$

***Model* β second-order kinetics**

The molar enthalpy changes are represented via the following polynomial functions

- $\Delta H_1(T) = g_{1,1}T_n^3 + g_{1,2}T_n^2 + g_{1,3}T_n + g_{1,4}$,
- $\Delta H_2(T) = g_{2,1}T_n^3 + g_{2,2}T_n^2 + g_{2,3}T_n + g_{2,4}$,
- $\Delta H_3(T) = g_{3,1}T_n^3 + g_{3,2}T_n^2 + g_{3,3}T_n + g_{3,4}$,
- $\Delta H_4(T) = g_{4,1}T_n^4 + g_{4,2}T_n^3 + g_{4,3}T_n^2 + g_{4,4}T_n + g_{4,5}$,

where

$$g_{1,1} = -0.0378; \quad g_{1,2} = 0.0585; \quad g_{1,3} = -0.498; \quad g_{1,4} = -18.730;$$
$$g_{2,1} = 4.7489; \quad g_{2,2} = -28.150; \quad g_{2,3} = -442.06; \quad g_{2,4} = -1445.2;$$
$$g_{3,1} = -0.132; \quad g_{3,2} = -0.906; \quad g_{3,3} = 10.381; \quad g_{3,4} = 9.7556;$$
$$g_{4,1} = 7.8329; \quad g_{4,2} = -9.3896; \quad g_{4,3} = -5.6314; \quad g_{4,4} = -5.5769; \quad g_{5,4} = -16.504.$$

5.3.3 Model validation

Once all the parameters characterizing the identified models have been estimated, it is possible to compare the performance of each model, both in terms of concentrations estimates and of the heat released estimate.

To this aim, the complete and identified models are forced to track some temperature profiles, using the PID controller described in Section 5.3, and the comparison between the models have been performed via the root mean squared errors (see equations (2.53) and (2.54)). In particular, 4 temperature profiles, similar to the ones adopted in industrial context, have been tested. Figures 5.1-5.16 show the concentrations and heat estimates for each identified model and each test profile; the root mean squared errors obtained for each profile are reported in Table 5.12. In Table the symbols $RMSE_C$, $RMSE_Q^c$ and $RSME_Q^v$ indicate the root mean squared errors for the concentrations, the heat released computed considering the molar enthalpy changes as constants and the heat released computed considering the molar enthalpy changes variable with the temperature, respectively. The errors values are obtained considering 1000 samples for each profile.

From the analysis of the results some remarks can be done:

- The best identified model, both in terms of concentration estimation and heat estimation accuracy is the *Model* β with second-order kinetics.
- The second-order models have good performance in terms of concentration estimation accuracy.
- Despite its good performance in terms of concentration estimation, the *Model* α with second-order kinetics performs badly in terms of in heat estimation accuracy.
- The first-order models show comparable results: *Model* β achieves better accuracy of the concentrations estimates, while *Model* α achieves better accuracy of the heat estimate.
- Except the *Model* α with second-order kinetics, the models with molar enthalpy changes variable with the temperature achieve better estimation of the heat released.

Temperature profile no.1

Model	$RMSE_C$	$RMSE_Q^c$	$RSME_Q^v$
α first-order kinetics	310.0	0.580	0.217
α second-order kinetics	98.39	0.710	1.404
β first-order kinetics	284.1	0.768	0.243
β second-order kinetics	82.80	0.678	0.035

Temperature profile no.2

Model	$RMSE_C$	$RMSE_Q^c$	$RSME_Q^v$
α first-order kinetics	552.8	1.141	0.655
α second-order kinetics	163.4	2.136	2.527
β first-order kinetics	530.9	1.465	0.830
β second-order kinetics	163.8	0.806	0.245

Temperature profile no.3

Model	$RMSE_C$	$RMSE_Q^c$	$RSME_Q^v$
α first-order kinetics	527.6	1.899	1.431
α second-order kinetics	172.2	2.569	3.115
β first-order kinetics	491.9	2.124	1.793
β second-order kinetics	160.7	1.556	1.167

Temperature profile no.4

Model	$RMSE_C$	$RMSE_Q^c$	$RSME_Q^v$
α first-order kinetics	492.5	0.552	0.368
α second-order kinetics	113.8	1.301	2.543
β first-order kinetics	443.6	0.679	0.401
β second-order kinetics	109.0	0.374	0.106

Average $RMSE$

Model	$RMSE_C$	$RMSE_Q^c$	$RSME_Q^v$
α first-order kinetics	470.7	1.043	0.668
α second-order kinetics	136.9	1.679	2.397
β first-order kinetics	437.6	1.259	0.817
β second-order kinetics	129.2	0.854	0.388

Table 5.12: $RMSE$ on the test temperature profiles.

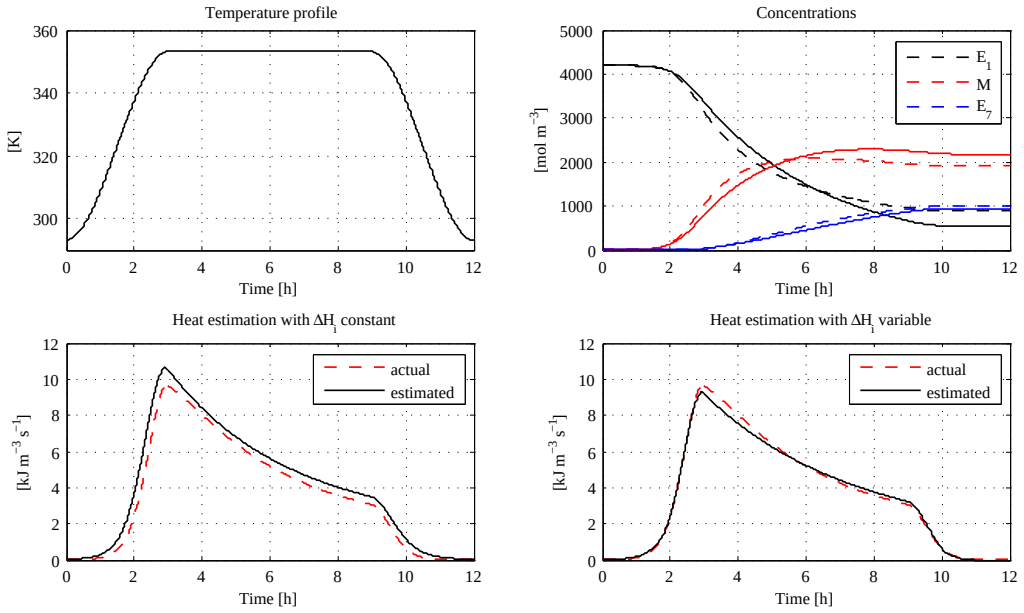

Figure 5.1: *Model* α first-order kinetics: temperature profile no.1.

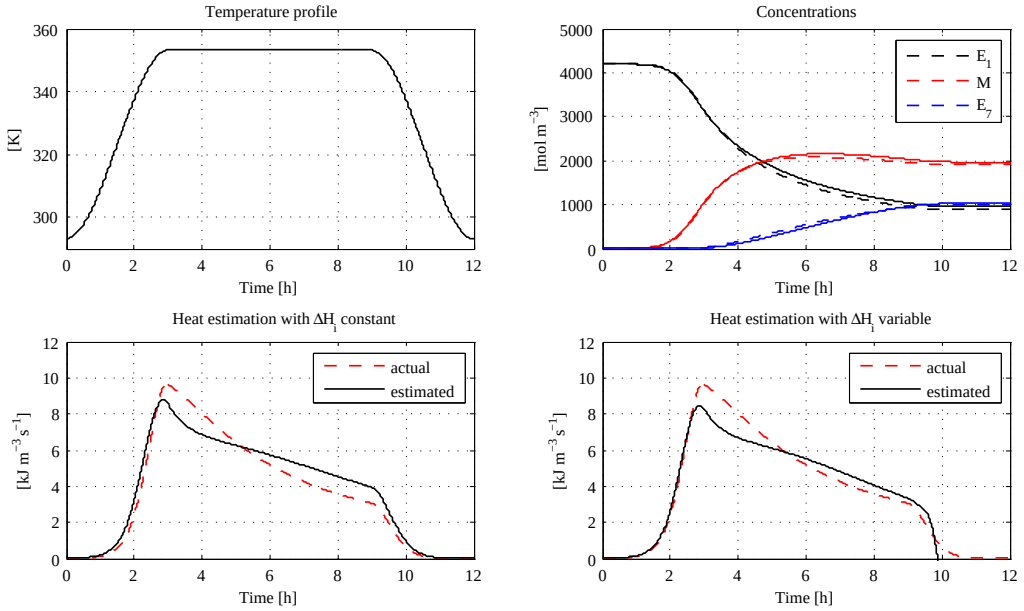

Figure 5.2: *Model* α second-order kinetics: temperature profile no.1.

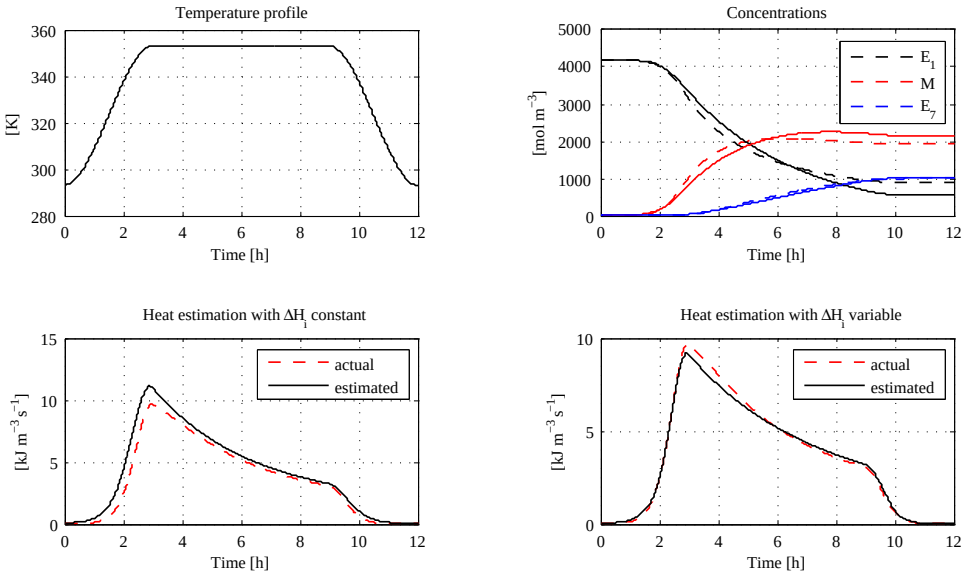

Figure 5.3: *Model β* first-order kinetics: temperature profile no.1.

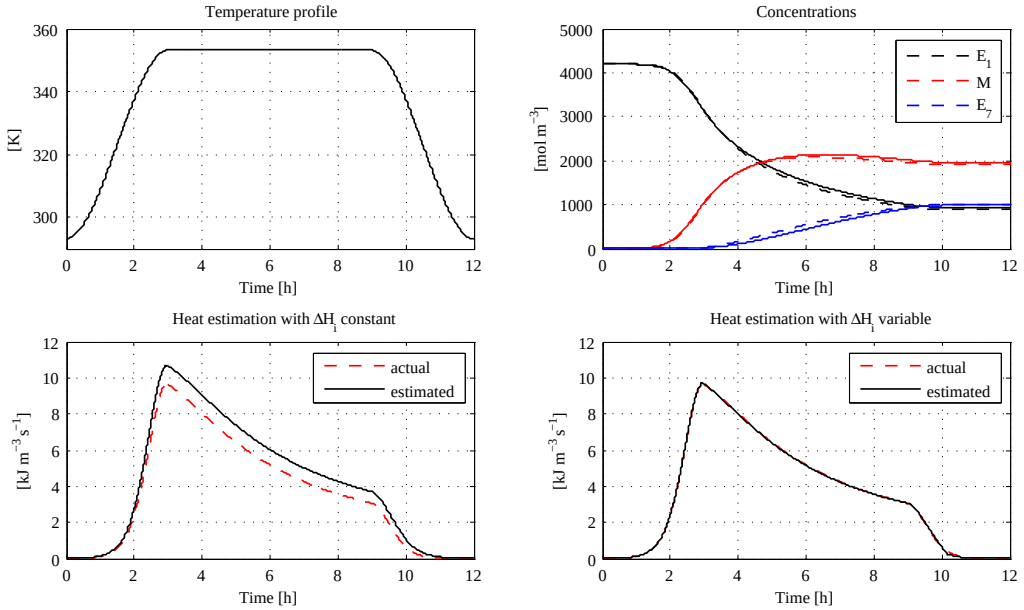

Figure 5.4: *Model β* second-order kinetics: temperature profile no.1.

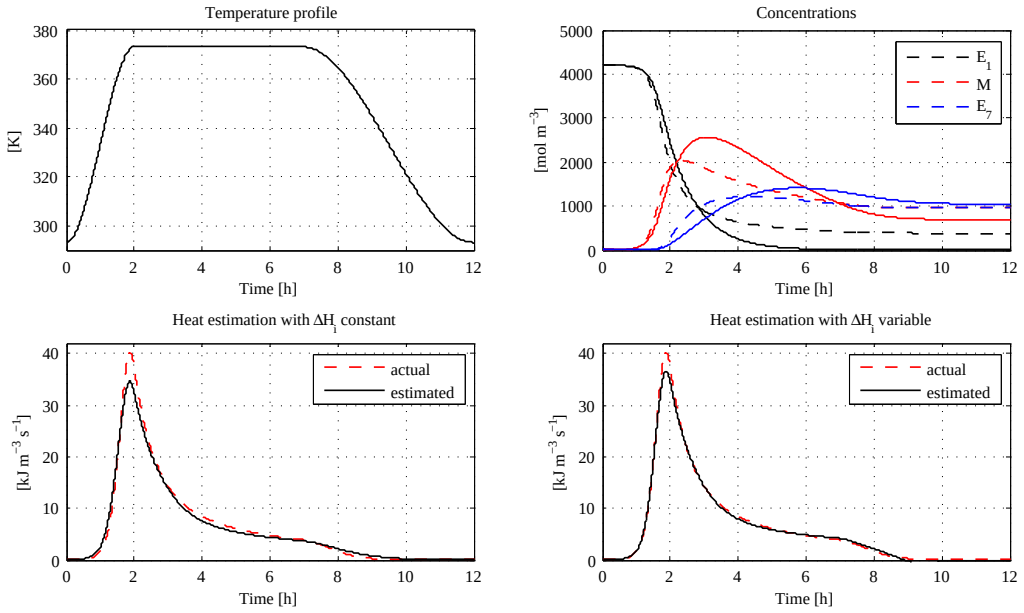

Figure 5.5: *Model* α first-order kinetics: temperature profile no.2.

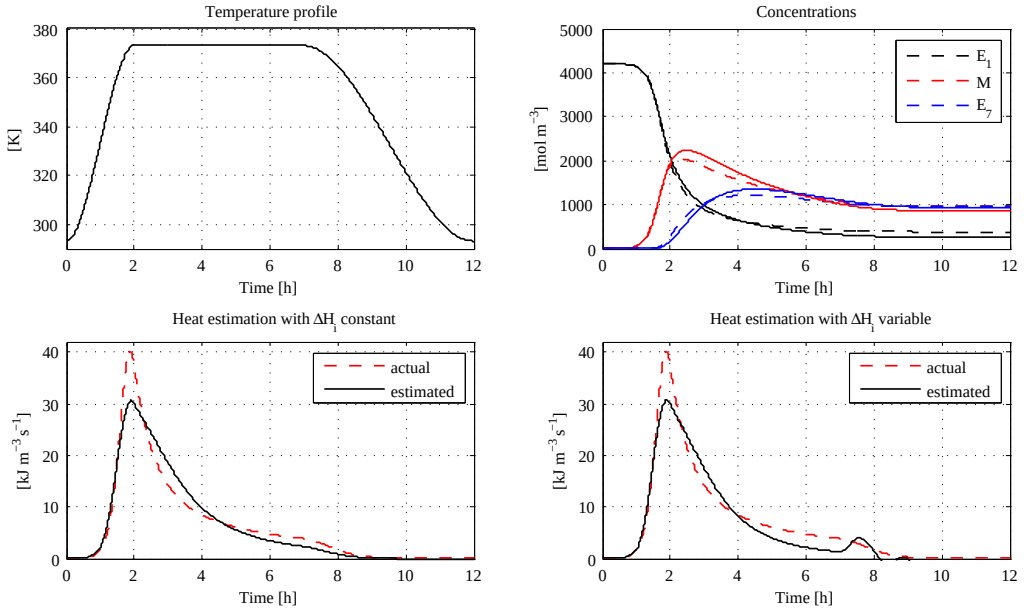

Figure 5.6: *Model* α second-order kinetics: temperature profile no.2.

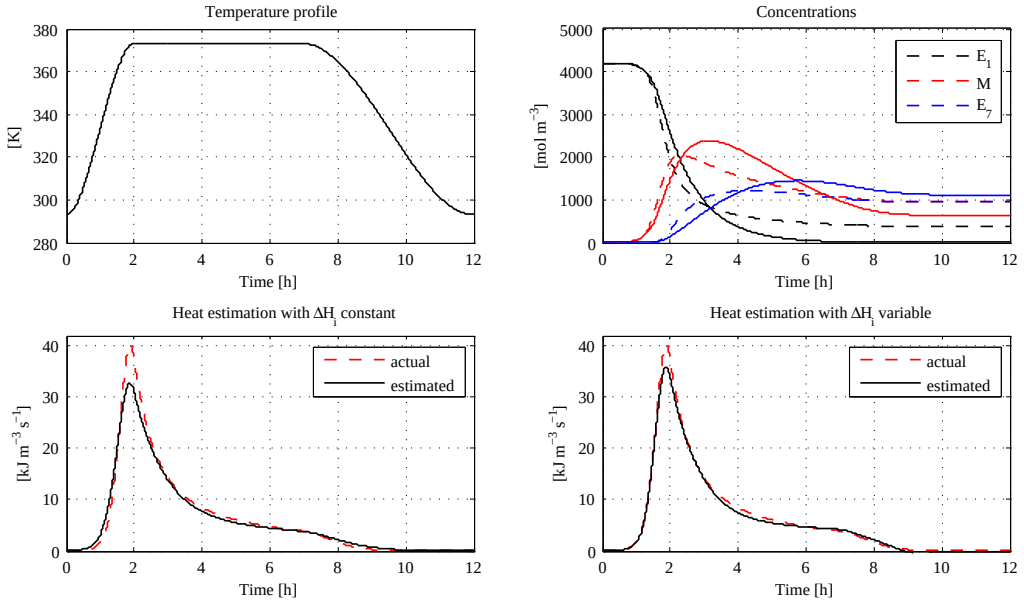

Figure 5.7: *Model β* first-order kinetics: temperature profile no.2.

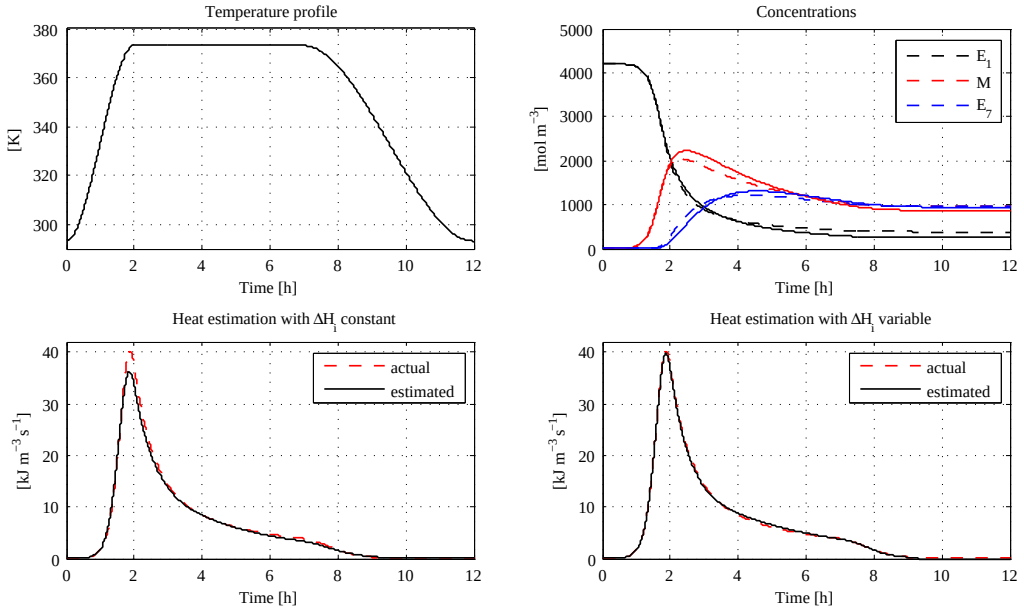

Figure 5.8: *Model β* second-order kinetics: temperature profile no.2.

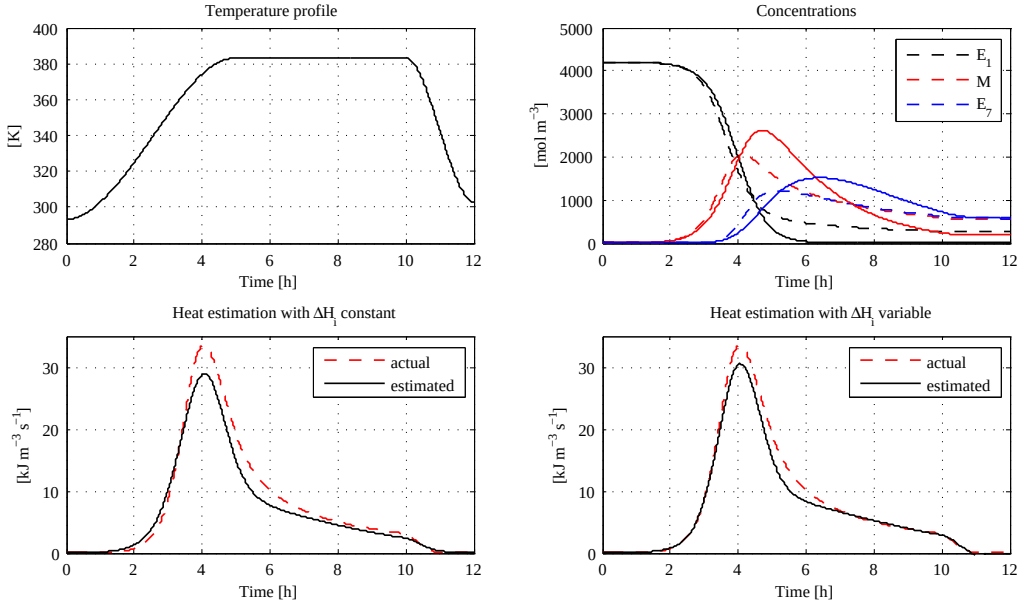

Figure 5.9: *Model* α first-order kinetics: temperature profile no.3.

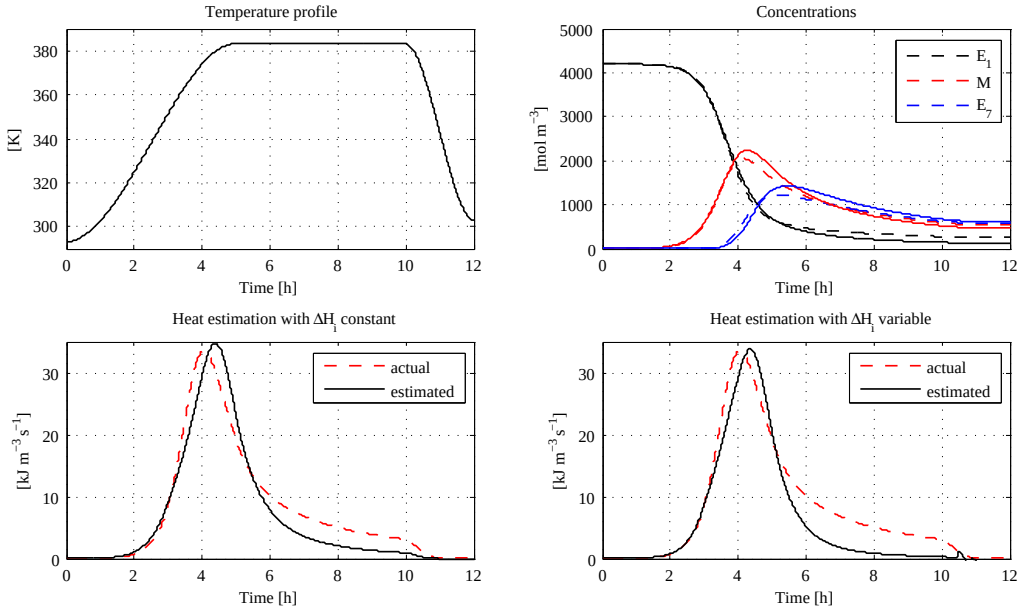

Figure 5.10: *Model* α second-order kinetics: temperature profile no.3.

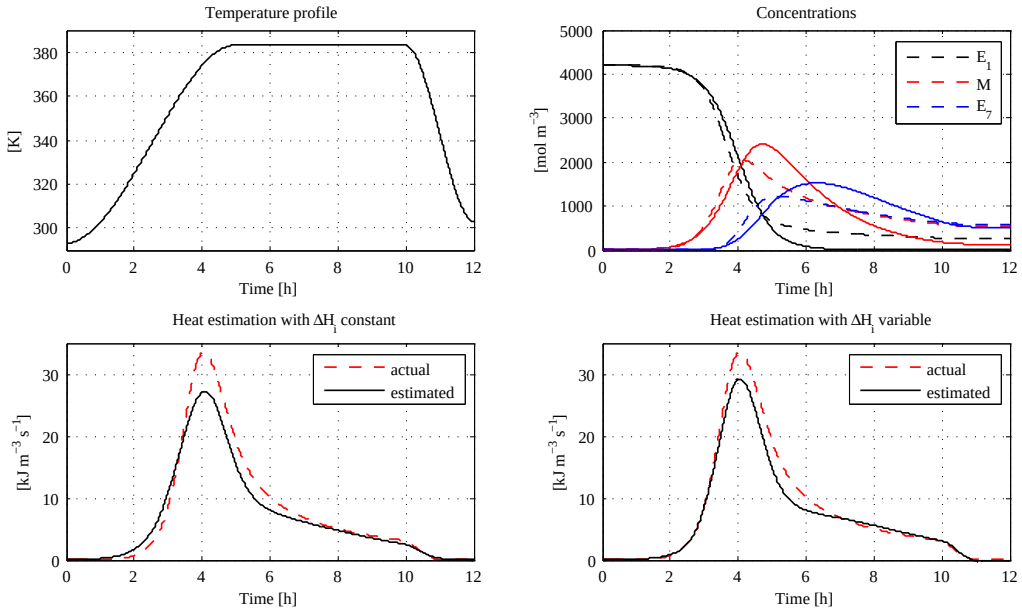

Figure 5.11: *Model* β first-order kinetics: temperature profile no.3.

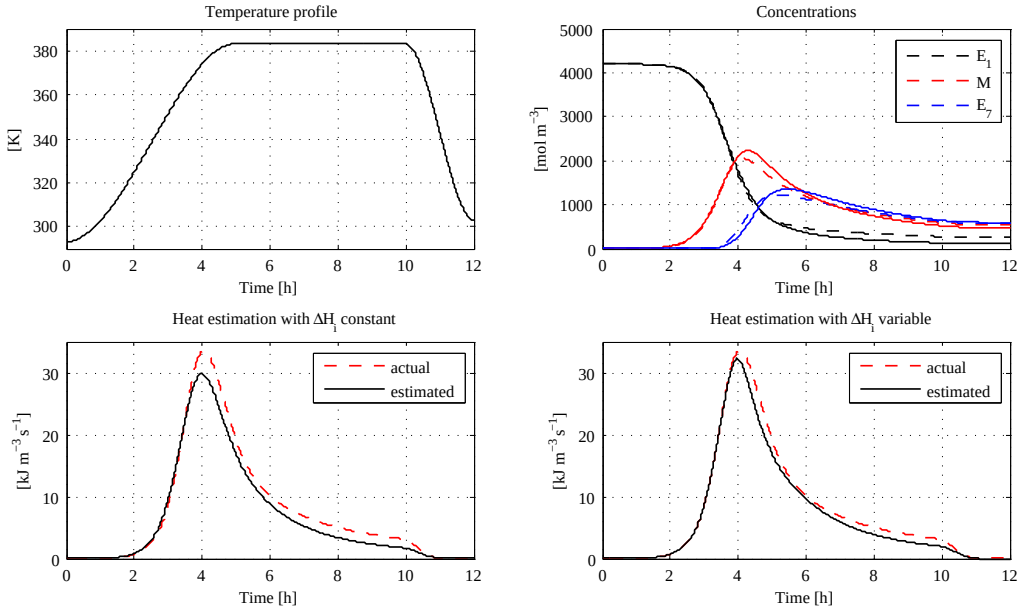

Figure 5.12: *Model* β second-order kinetics: temperature profile no.3.

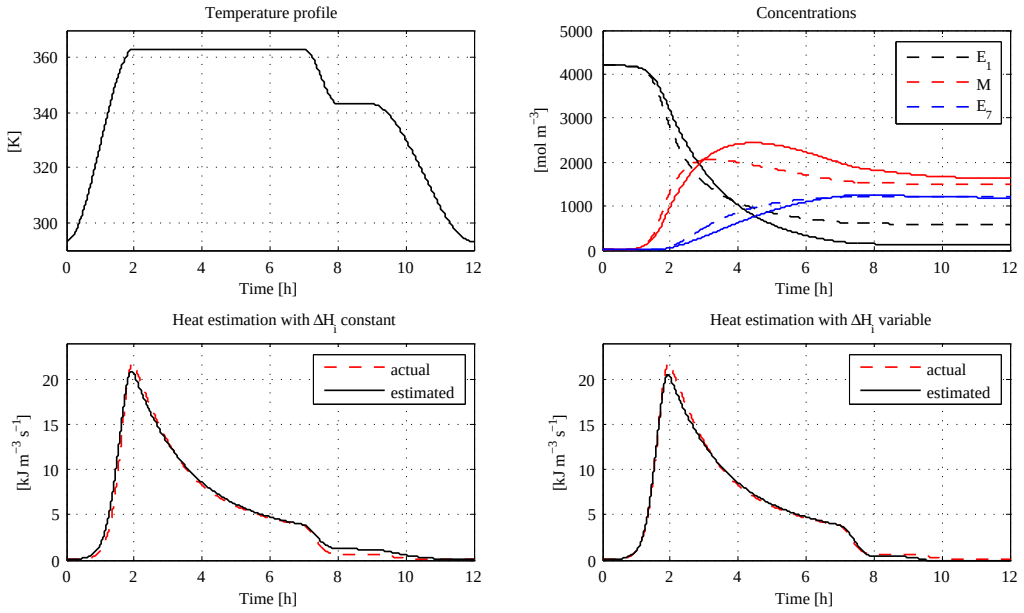

Figure 5.13: *Model* α first-order kinetics: temperature profile no.4.

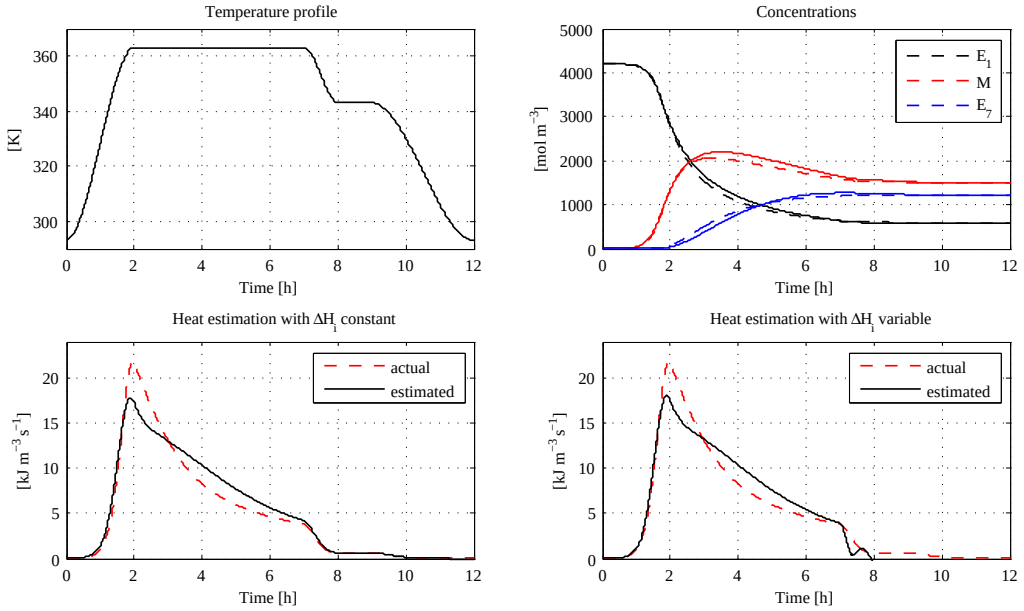

Figure 5.14: *Model* α second-order kinetics: temperature profile no.4.

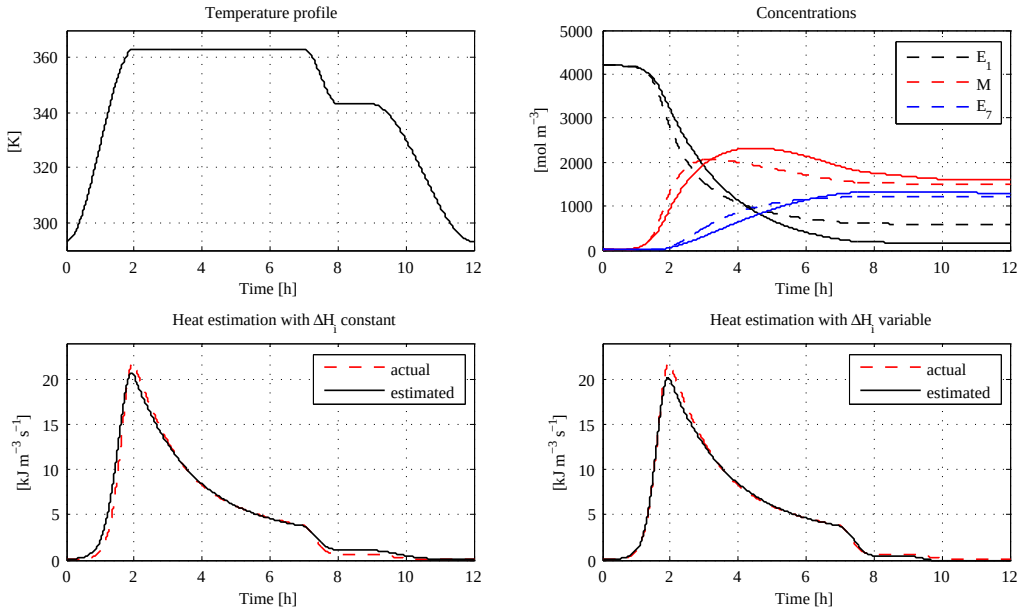

Figure 5.15: *Model β* first-order kinetics: temperature profile no.4.

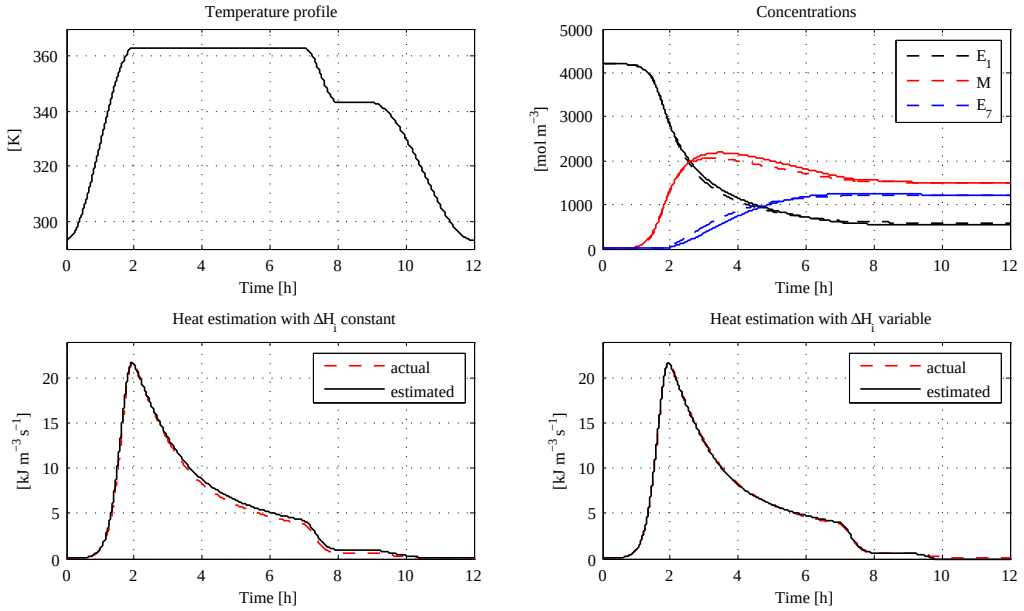

Figure 5.16: *Model β* second-order kinetics: temperature profile no.4.

5.4 Control

Two comparative case studies have been developed to test the effectiveness of the control scheme proposed in Chapter 3 on a realistic simulation model.

In the first case study, the control schemes have been tested in ideal conditions, i.e., in the absence of measure disturbances and actuator dynamics.

In the second case study, the same control schemes have been tested in the presence of actuator dynamics and measurement disturbances, such as described in Section 5.2.

In each case study four different schemes have been tested:

- The model-free approach proposed in [41] and described in Section 3.3.2.2. Namely, the two-loop scheme (3.30), (3.31) is adopted, in which $\widehat{q}$ and $\widehat{\theta}$ are obtained by means of observer (3.29). In order to cope with the singularities occurring when $(T_r - T_j) \to 0$, this term has been replaced by the constant value 0.1 when $|T_r - T_j| \leq 0.1$.

- The model-free approach proposed in Section 3.3.2.1. Namely, the two-loop scheme (3.30), (3.31) is adopted, in which $\widehat{q}$ is obtained by means of observer (3.20), using 15 Radial Basis Functions. The centroids are chosen evenly distributed in the interval [293 K, 368 K], considered as the range of temperatures of the reaction. The width π, equal for all the RBF functions, has been set as 10^2.

- The model-based controller-observer scheme (eqs. (3.9), (3.30) and (3.31)), without updating the parameters estimate, i.e., the available nominal estimates are used. The dynamics of the phenol-formaldehyde reaction has been estimated via the *Model* α, with first-order kinetics and molar enthalpy changes depending upon the temperature.

- The adaptive model-based controller-observer scheme (eqs. (3.9), (3.30) and (3.31)), with update of the parameters estimates via (3.10) and (3.32). The dynamics of the phenol-formaldehyde reaction has been estimated via the *Model* α, with first-order kinetics and molar enthalpy changes depending upon the temperature.

In order to perform a fair comparison between the model-free and the model-based approaches, the four schemes have been tuned so as to achieve the same control effort (i.e., so as to obtain the same time histories of u, as far as possible). All the schemes have been tuned via a trial-and-error procedure.

The assumptions on the set-up, on the initial conditions and on the reactor geometry have been assumes such as described in Section 5.2 and are reported in Table 5.1.

The desired temperature profile $T_{r,d}(t)$, reported in Figure 5.17, develops in three phases:

- Heating. In this phase the desired reactor temperature is raised from its initial value, 293 [K], to 368 [K] in 6000 [s] via a third-order polynomial with null initial and final derivatives.
- Isothermal phase. In this phase a constant set-point temperature (368 [K]) is commanded for 7500 [s].
- Cooling. In this phase the desired temperature is driven to 298 [K] in 4000 [s]; the profile is a third-order polynomial with null initial and final derivatives. The final temperature is then kept constant for 500 [s].

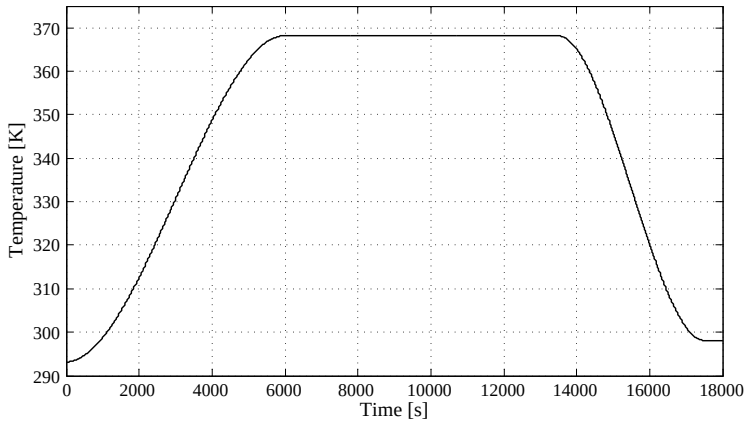

Figure 5.17: Desired reactor temperature profile.

An initial estimation error on the concentrations, which amounts to the 5% of their true values, has been assumed. Moreover, a wrong nominal estimate of θ has been considered, which is assumed to be equal to 1.6 times its true value (i.e., a 60% error).

The parameters of the controller-observer schemes are summarized in Table 5.13. It is worth noticing that the parameters of the controller (g_r, g_j) are the same for all the control schemes.

Results: Case Study 1

The results of the simulations are reported in Figures 5.18–5.21. It can be recognized that all the tested control laws achieve satisfactory temperature tracking performance

Parameter	Value	Parameter	Value
l_1	10	g_r	$5 \cdot 10^{-1}$
l_2	$5 \cdot 10^{2}$	g_j	$5 \cdot 10^{-1}$
l_3	$1 \cdot 10^{-1}$	γ	$6 \cdot 10^{-1}$
l_r	1	ω	$3 \cdot 10^{-2}$
l_j	1	l_q	$2 \cdot 10^{-2}$
λ	$1.5 \cdot 10^{-1}$	l_θ	$6.5 \cdot 10^{-3}$

Table 5.13: Controller-observer parameters.

(Figure 5.18) and are characterized by very similar peak values of the control input (Figure 5.19). Noticeably, the model-based adaptive scheme achieves tracking performance comparable with respect to the model-free schemes, also in the presence of wide model uncertanties; as expected, the adaptive model-based approaches outperform the non-adaptive model-based scheme, since the latter does not take into account the parametric uncertainties at all.

It can be argued that the differences between the compared schemes are mainly due to the different estimation accuracy of the heat released by the reaction (Figure 5.20) and of the parameter θ (Figure 5.21). All the adaptive (model-based and model-free) approaches achieve very good performance. Since the parameter estimate converge to the true value of θ, it is possible to argue that the persistency of excitation condition is fulfilled.

Results: Case Study 2

The results in Figures 5.22–5.25 show that good performance are still achieved, even in the presence of measurement noise and actuator dynamics, although all the variables (especially the control input, as can be seen in Figure 5.23) are affected by noise and oscillations. In particular the model-free observer based on RBFs is the most sensitive to measurement noise. It can be concluded that the exponential stability property confers to the adaptive model-based scheme a satisfactory degree of robustness.

The estimates of θ (Figure 5.25) are still fairly accurate. Also, the effect of the singularity in the model-free observer is clearly visible in the last part of the batch, where T_r and T_j tends to be equal at the steady-state. In this conditions the parameter estimate diverges from the real value.

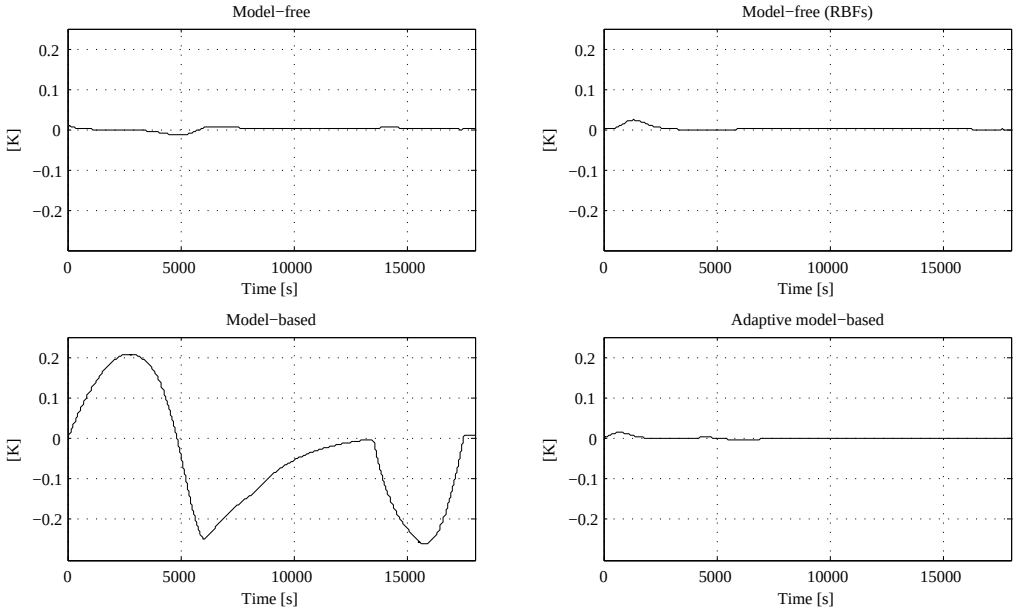

Figure 5.18: Case study 1: reactor temperature tracking errors.

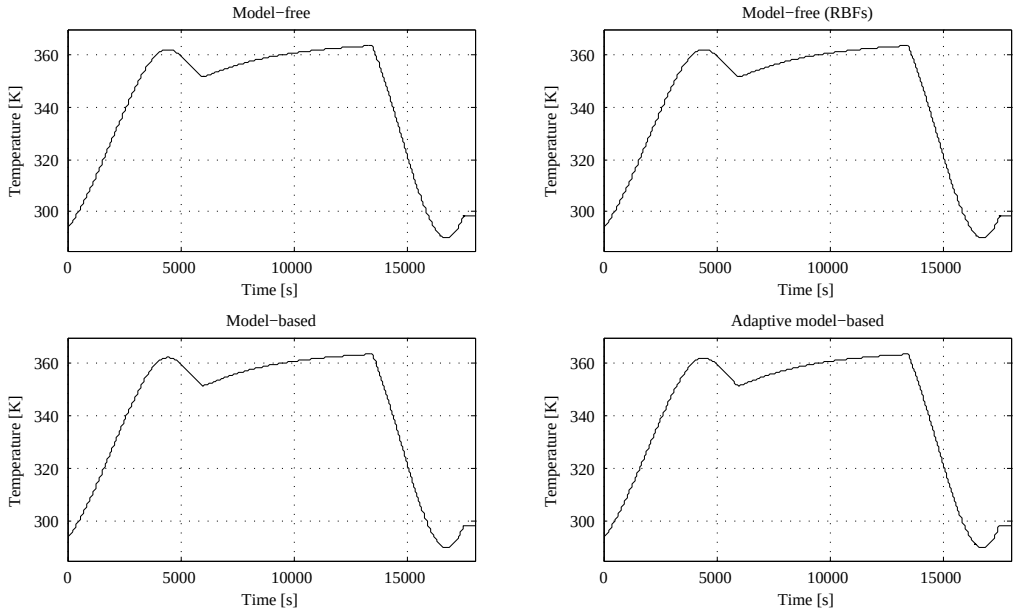

Figure 5.19: Case study 1: commanded temperature of the fluid entering the jacket.

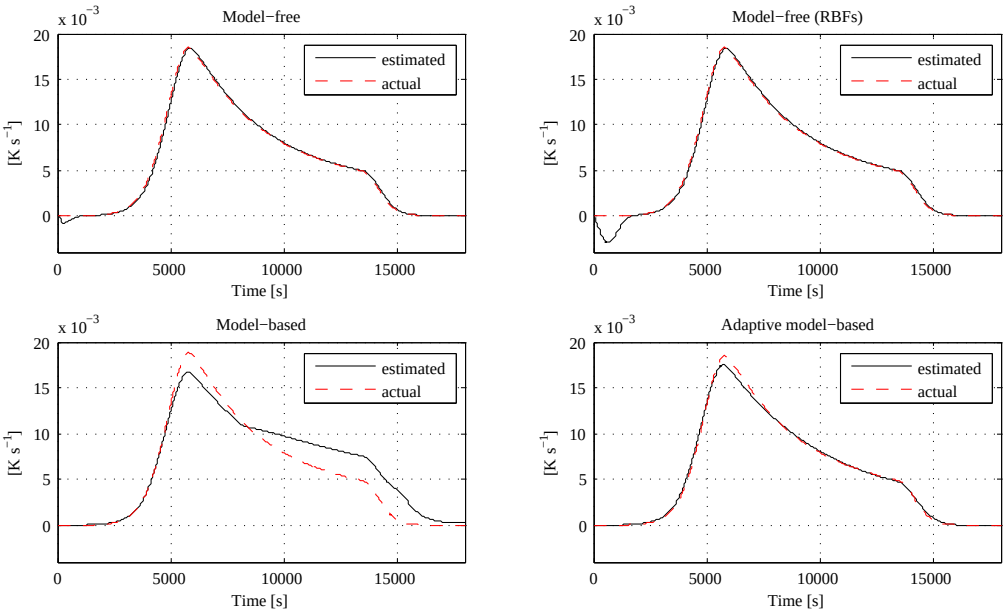

Figure 5.20: Case study 1: estimates of the heat released by the reaction.

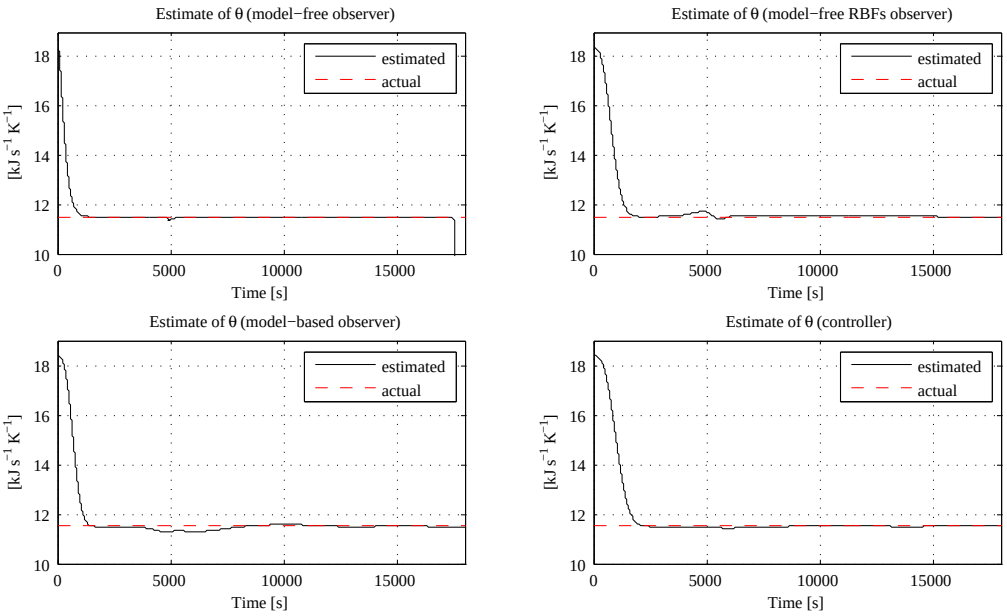

Figure 5.21: Case study 1: estimates of θ.

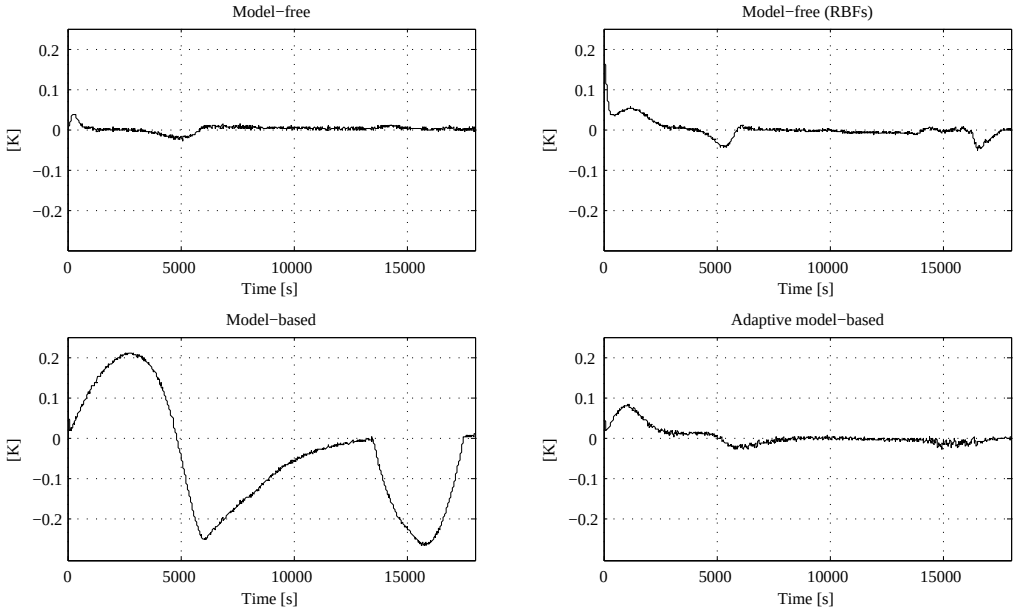

Figure 5.22: Case study 2: reactor temperature tracking errors.

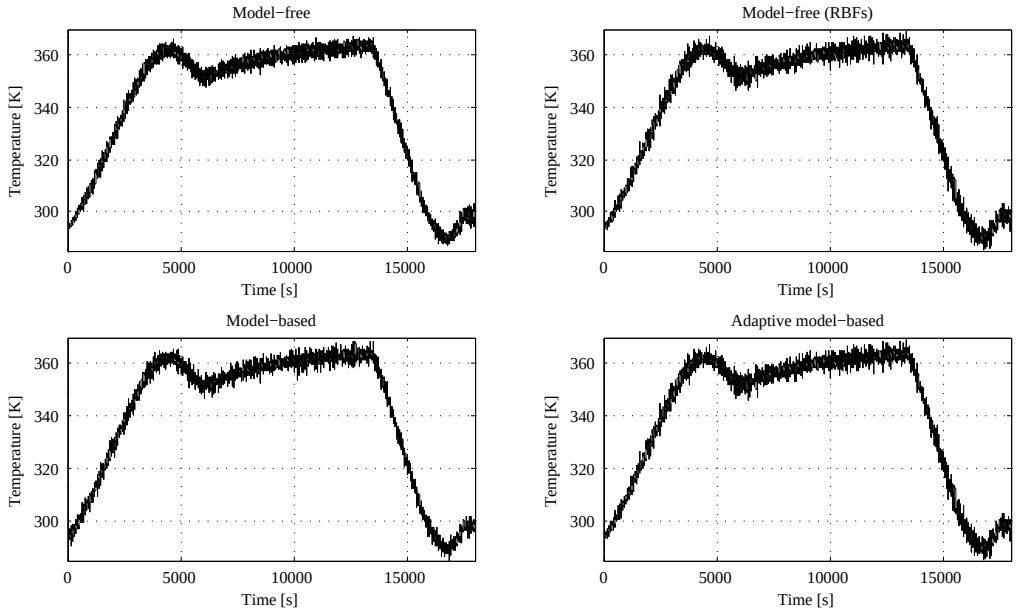

Figure 5.23: Case study 2: commanded temperature of the fluid entering the jacket.

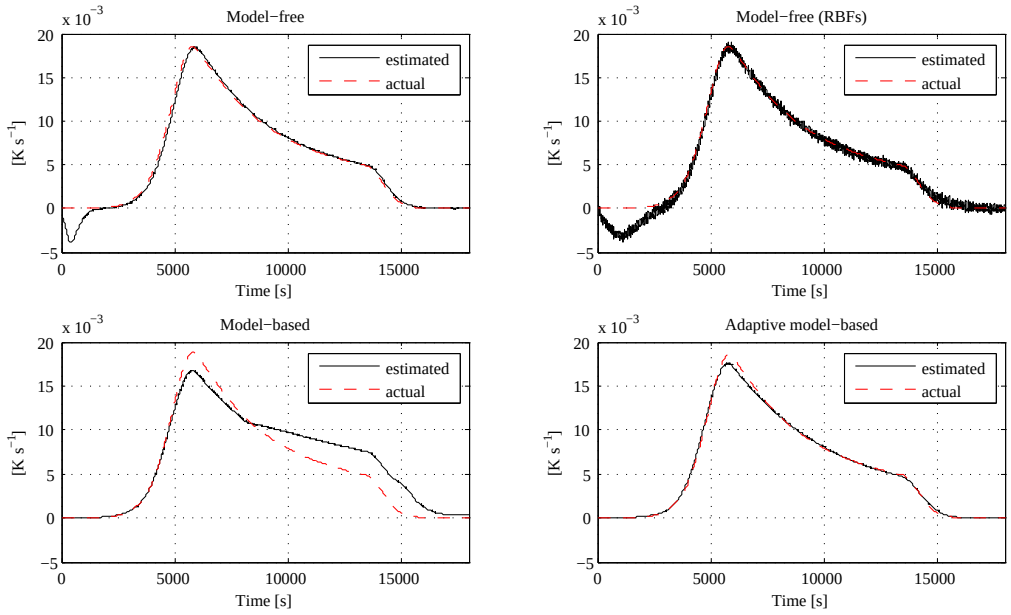

Figure 5.24: Case study 2: estimates of the heat released by the reaction.

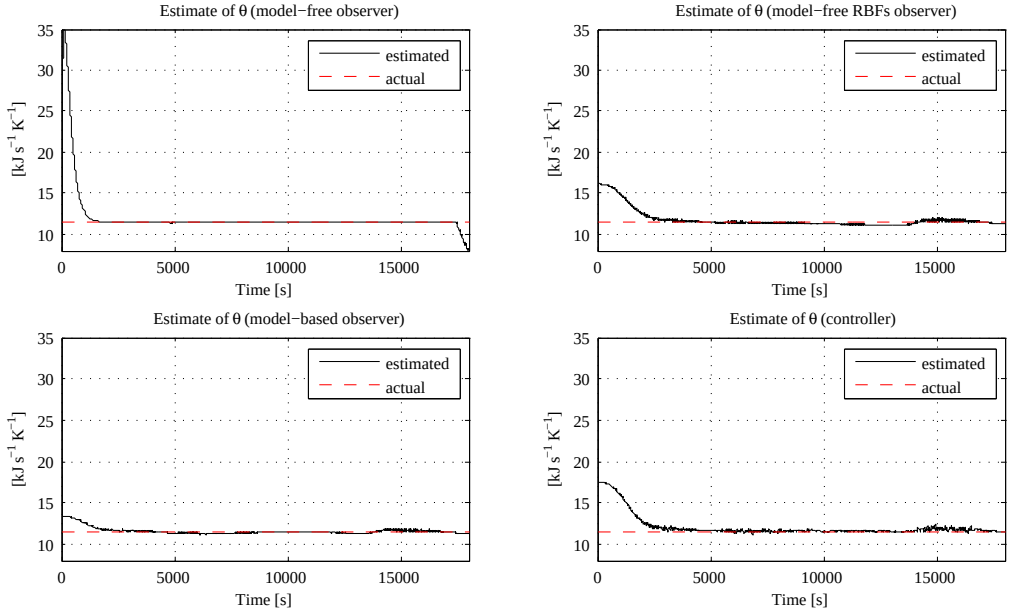

Figure 5.25: Case study 2: estimates of θ.

5.5 Fault diagnosis

The effectiveness of the proposed FDI scheme has been tested on the simulation model of the reactor, with the adaptive controller (3.30), (3.31) with update of the parameters estimates via (3.32). The estimation of the heat released and the residual generation can be performed both by the model-based observer (3.9) and by the model-free observer (3.20). In the following, for the sake of brevity, only the results obtained using the model-based observer have been reported, since the same results have been obtained, using the model-free observer.

The relevant parameters of the reactor and jacket models and of the controller-observer scheme are the same used in the previous Section and are summarized in Tables 5.1 and 5.13.

In the simulations, the following classes of faults on the temperature sensors have been considered:

- *Abrupt switches to zero* of the measured signal.
- *Slow drifts*, i.e., a linearly increasing signal is added to the measured data.
- *Abrupt constant biases*, i.e., a step disturbance is added to the measured data.
- *Abrupt freezing* of the measured signal, i.e., the measured signal is frozen at its current value at a certain time instant.
- *Increasing noise*, i.e., a gaussian noise with increasing variance is added to the measured data.

As regards the actuator faults, two kind of faults have been considered:

- *Abrupt constant biases*, i.e., a value δu is added to the value of the input computed via the control law (3.30).
- *Abrupt freezing* of the input, i.e., the input is frozen at its current value at a certain time instant.

The normalization factors ρ_i, μ_i ($i = 1, 2$) have been chosen equal to 0.2 on the basis of the values of the output estimation errors of the observers in healthy condition, that are always below this threshold (see Figure 5.26).

The obtained results show that the proposed diagnostic scheme has been able to detect and isolate all the simulated sensor faults. In detail, Figures 5.27-5.36 show the voted

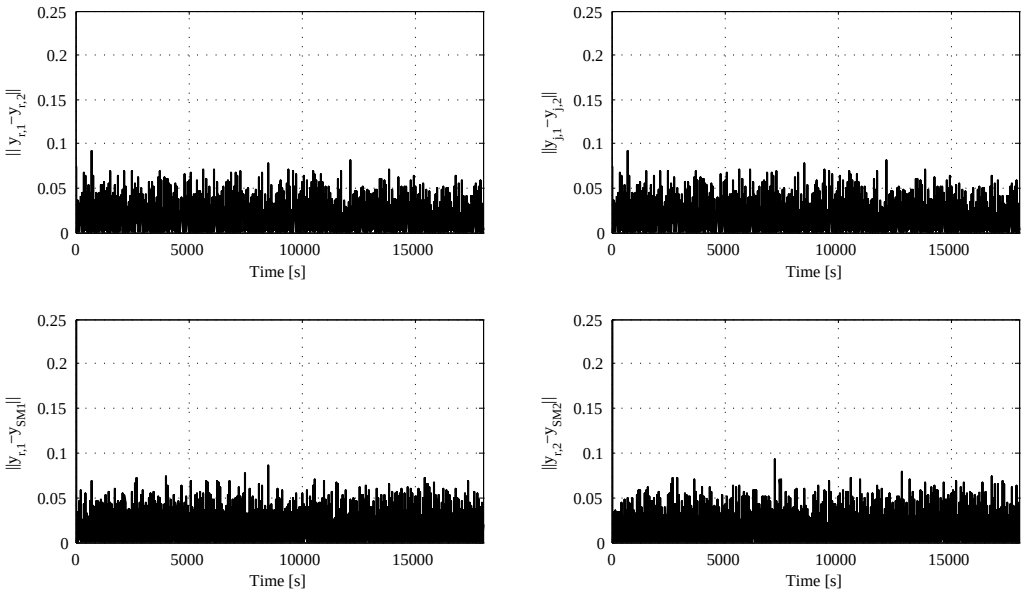

Figure 5.26: Output errors of the observers in healthy conditions.

measures, as well as the norm of both the detection and the isolation residuals, in the presence of different sensor faults.

Figures 5.27 and 5.28 are referred to an *abrupt constant bias* with an amplitude of 10 [K], occurring at time $t^* = 10000$ [s], on the sensor $S_{j,1}$.

Figures 5.29 and 5.30 show the voted measure and the residuals when the measure of sensor $S_{r,2}$ *switches to zero* at time $t^* = 8000$ [s].

Figures 5.31 and 5.32 are referred to a *slow drift* of about 0.01 [K·s^{-1}], starting at time $t^* = 1000$ [s], on the sensor $S_{j,1}$.

Figures 5.33 and 5.34 show the results obtained for an *increasing noise* on the sensor $S_{r,1}$. Namely a white noise with zero mean and increasing variance has been added to the sensor output starting at time 12000 [s].

Figures 5.35 and 5.36 show the results obtained when the measured signal of sensor $S_{j,1}$ has been frozen at its value at time $t^* = 3000$ [s].

It can be easily recognized that all the faults have been correctly detected and identified. During a wide simulation campaign it results that when an abrupt freezing on reactor temperature sensors ($S_{r,1}$ or $S_{r,2}$) occurs during the isothermal phase, the fault can be detected but not isolate. Finally, the measure voted by the DMS results to be always better than the standard duplex measure.

As regards the actuators faults, Figures 5.37-5.40 show the faulted input, as well as the norm of the residuals. It can be recognized that the detection of actuator faults has been obtained.

In particular Figures 5.37 and 5.38 are referred on an *abrupt constant bias* of 20 [K] at time $t^* = 10000$ [s].

Figures 5.39 and 5.40 are obtained when input has been frozen at its value at time $t^* = 14000$ [s]. When this kind of fault occurs in the heating phase, it may cause a run-away of the reactor, with potentially fatal consequences.

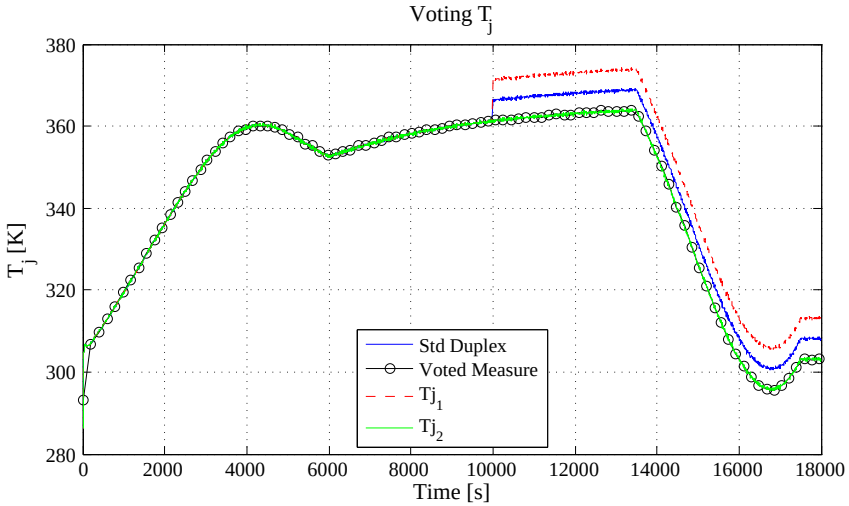

Figure 5.27: Voting measure of T_j (abrupt bias at sensor $S_{j,1}$).

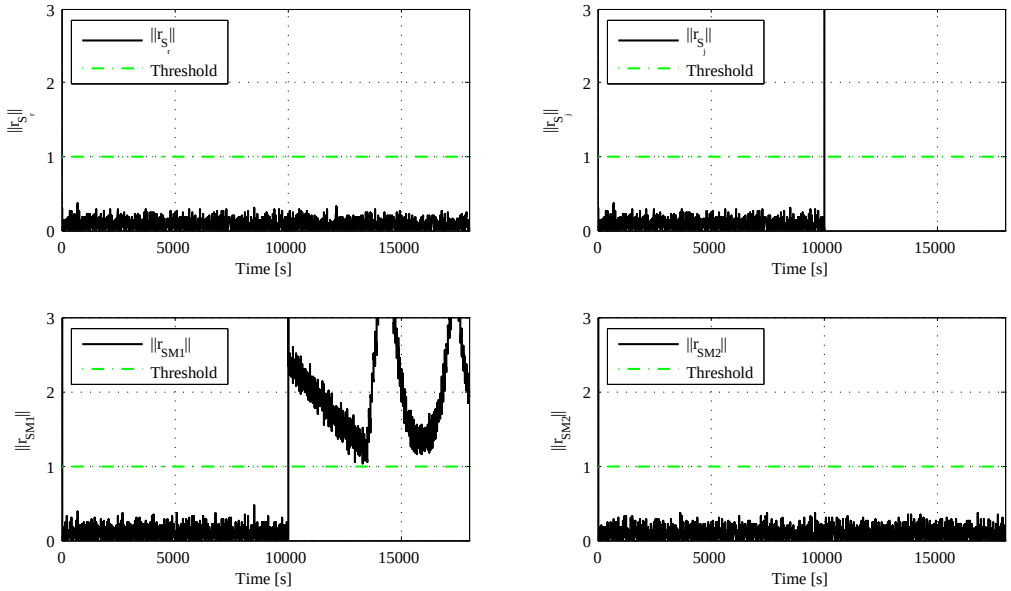

Figure 5.28: Detection and isolation residuals (abrupt bias at sensor $S_{j,1}$).

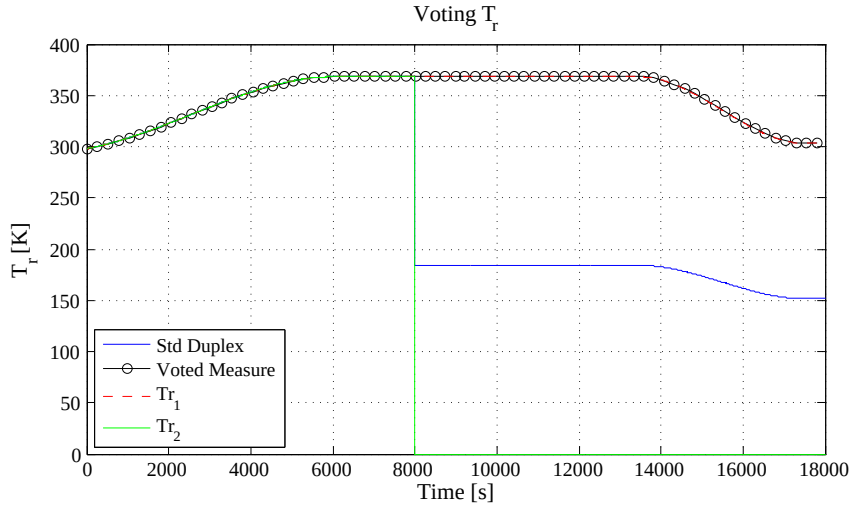

Figure 5.29: Voting measure of T_r (abrupt switch to zero at sensor $S_{r,2}$).

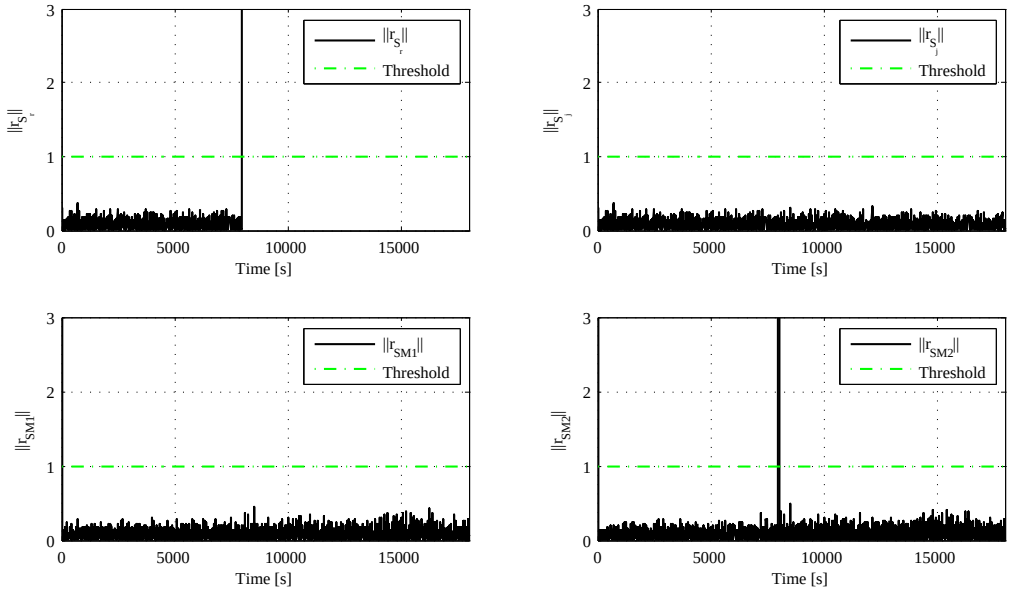

Figure 5.30: Detection and isolation residuals (abrupt switch to zero at sensor $S_{r,2}$).

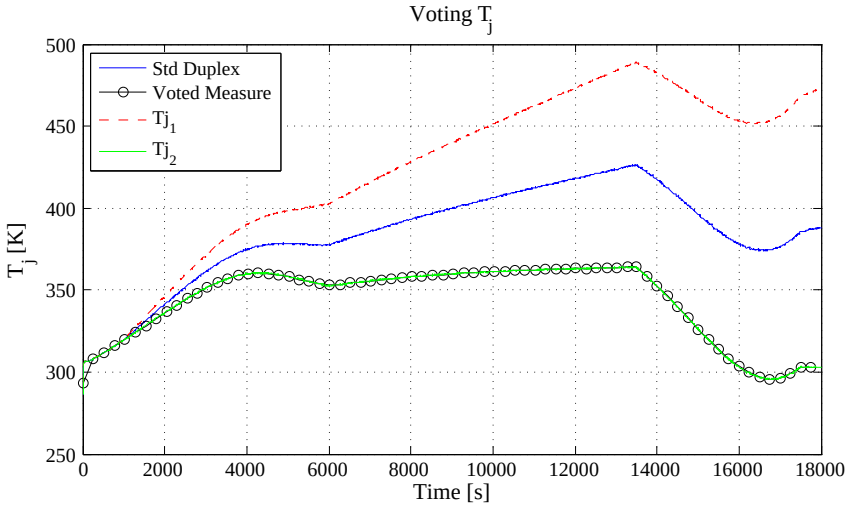

Figure 5.31: Voting measure of T_j (slow drift at sensor $S_{j,1}$).

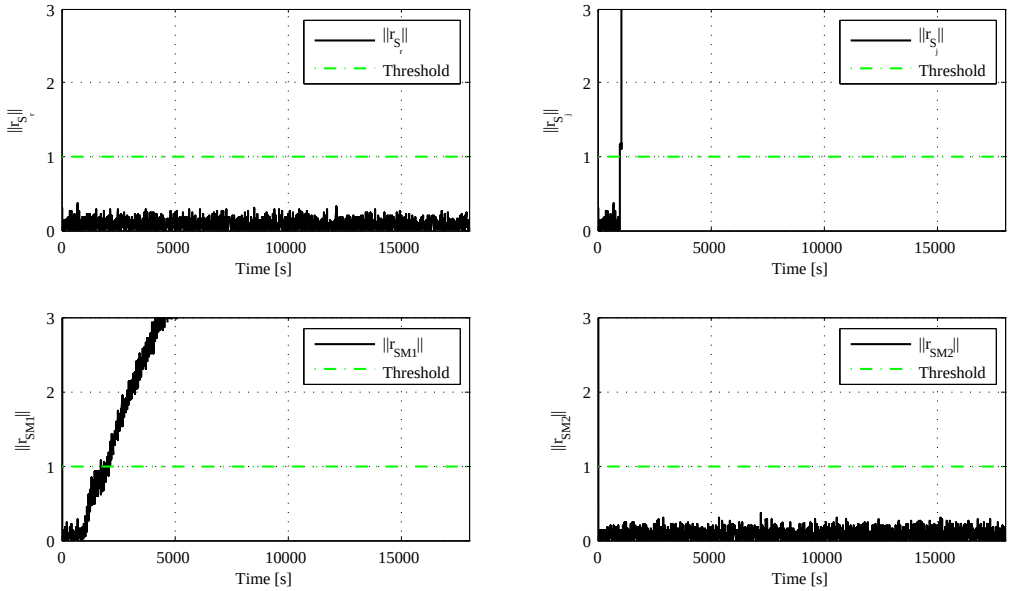

Figure 5.32: Detection and isolation residuals (slow drift at sensor $S_{j,1}$).

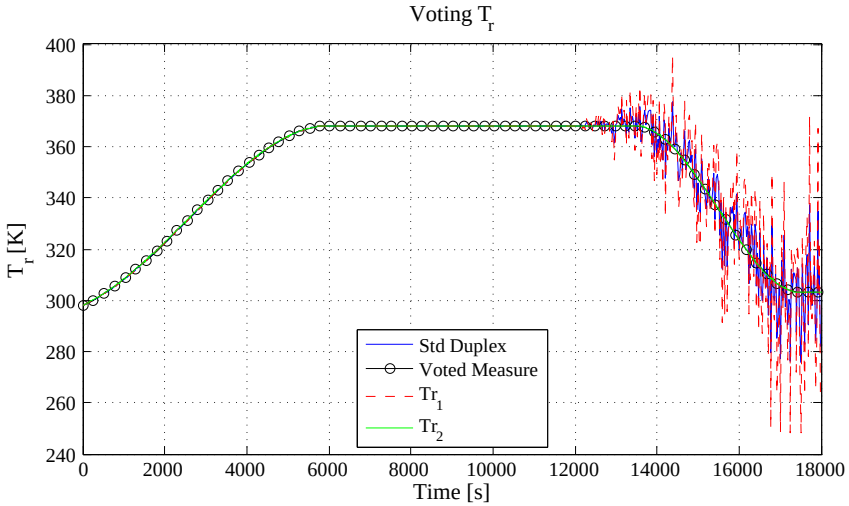

Figure 5.33: Voting measure of T_r (increasing noise at sensor $S_{r,1}$).

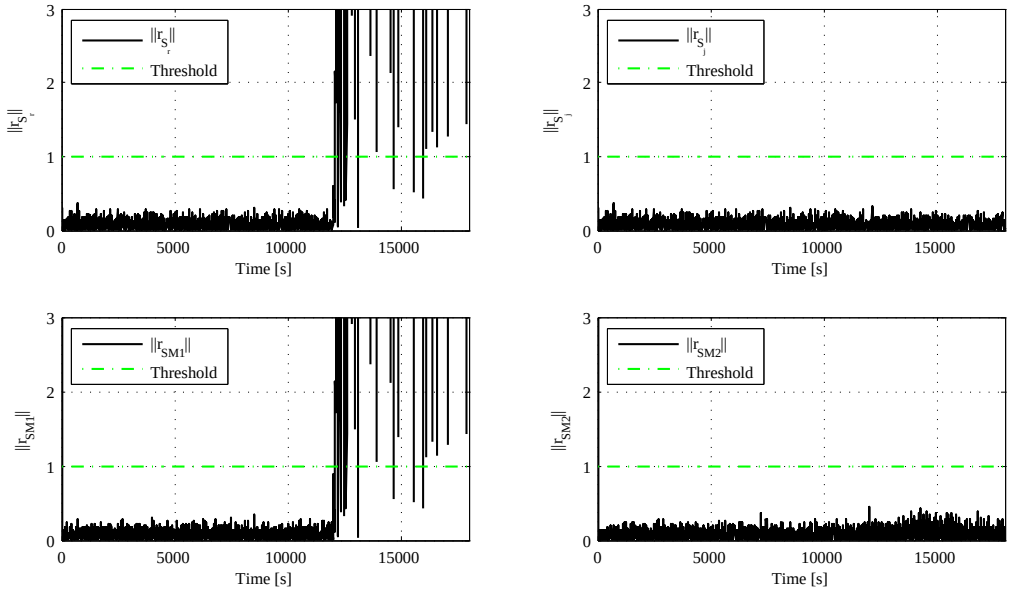

Figure 5.34: Detection and isolation residuals (increasing noise at sensor $S_{r,1}$).

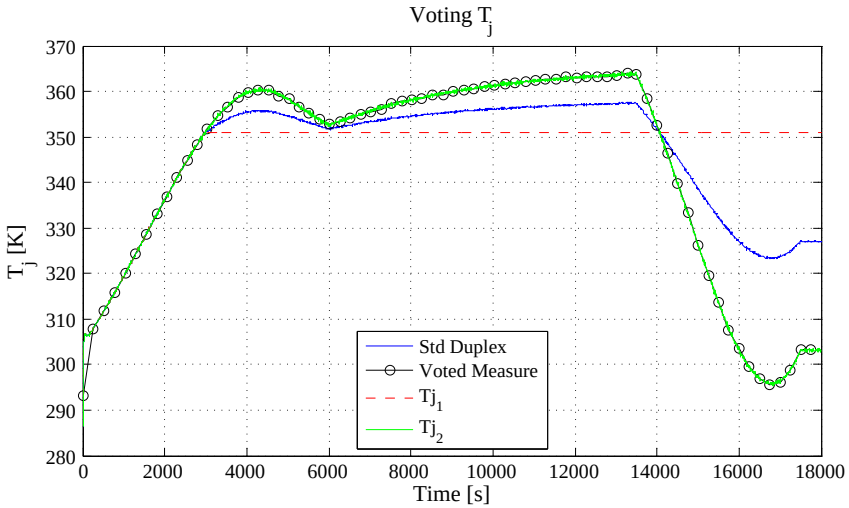

Figure 5.35: Voting measure of T_j (abrupt freezing of the measured signal on sensor $S_{j,1}$).

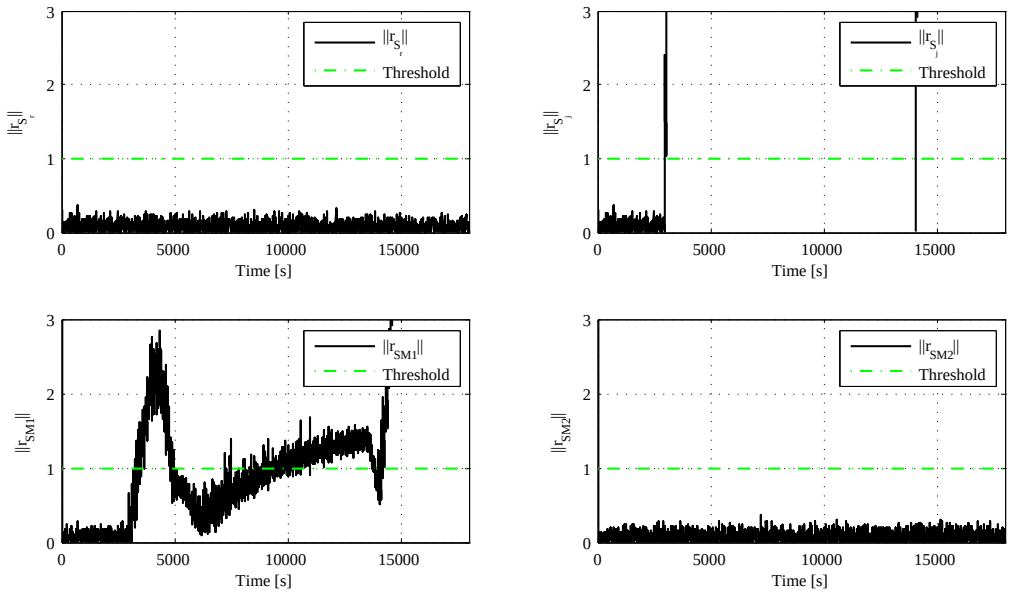

Figure 5.36: Detection and isolation residuals (abrupt freezing of the measured signal on sensor $S_{j,1}$).

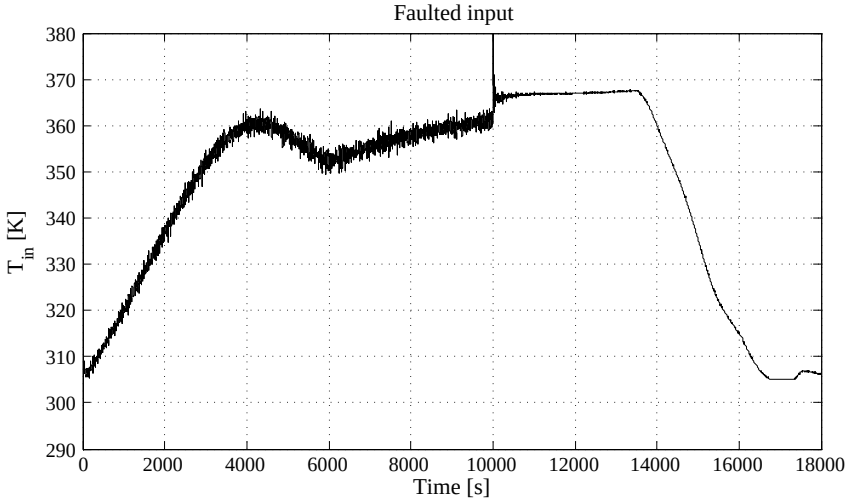

Figure 5.37: Actuator fault: faulted input (abrupt constant bias).

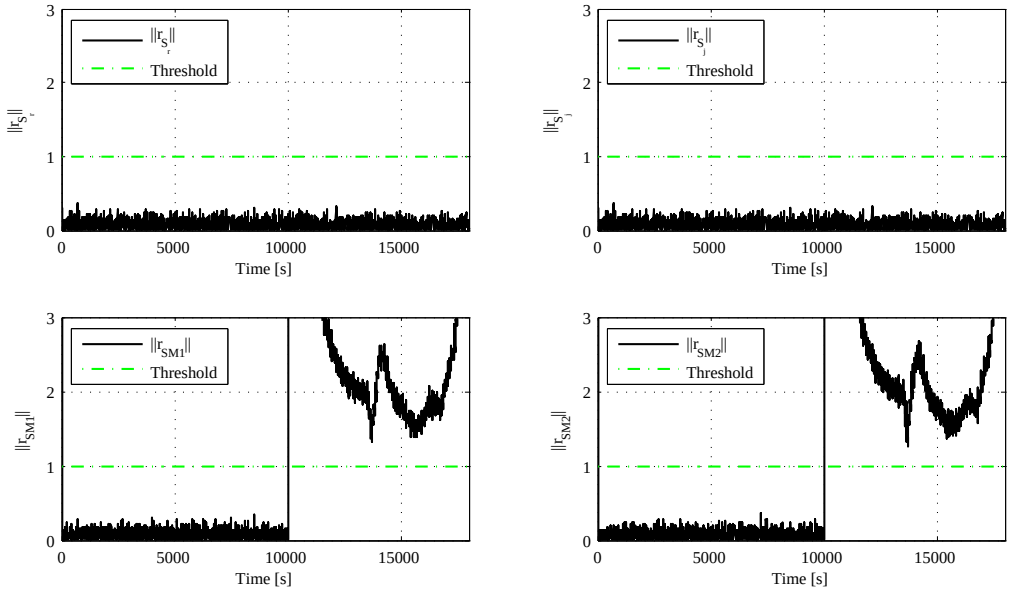

Figure 5.38: Actuator fault: residuals (abrupt constant bias).

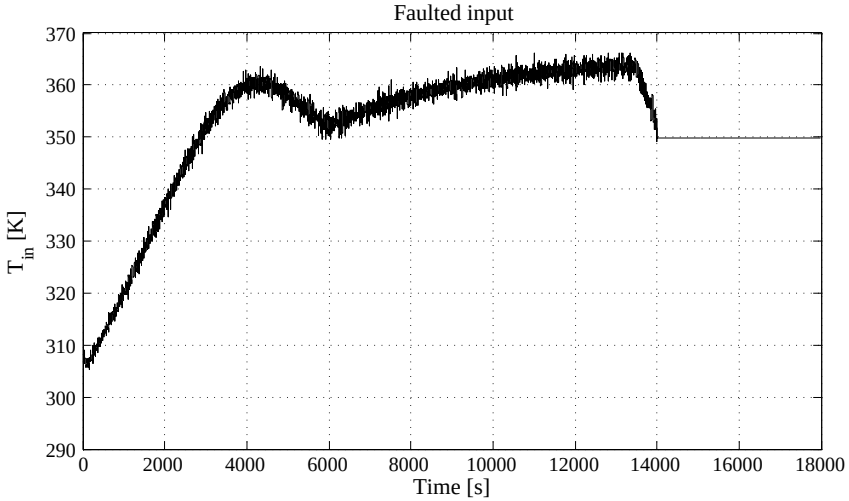

Figure 5.39: Actuator fault: faulted input (abrupt freezing).

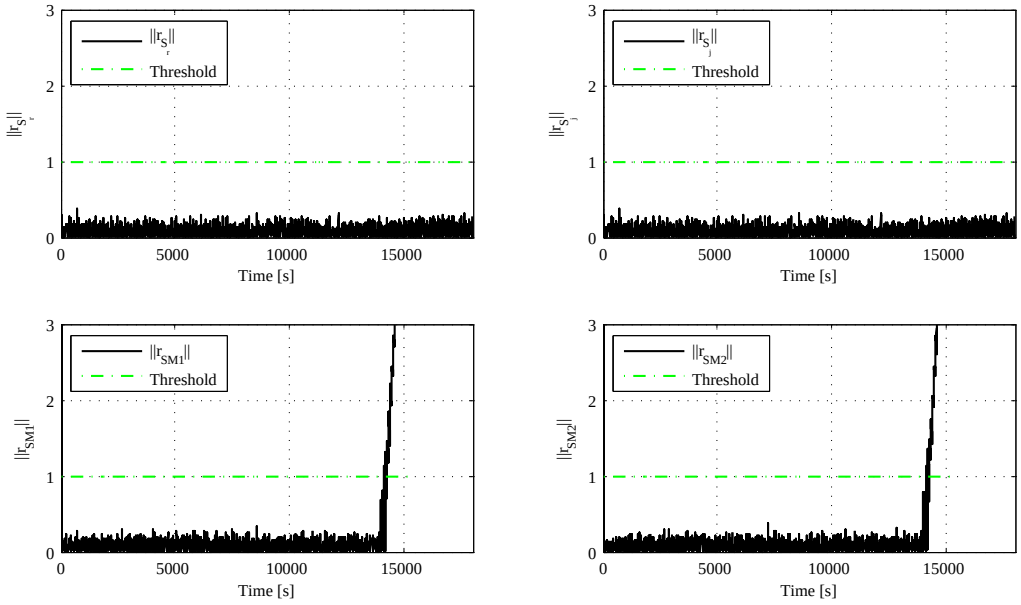

Figure 5.40: Actuator fault: residuals (abrupt freezing).

Conclusions and future work

This thesis deals with some fundamental problems regarding batch reactors. Batch reactors represent an engineering challenge because of their strong nonlinearities, the unsteady operating conditions and the lack of complete state and parameters measurements.

Theoretical aspects of modeling, control and fault diagnosis of batch reactors have been tackled.

First, the full model of the reactor, involving a system of 15 differential equations, has been developed. Then, well-known techniques for nonlinear implicit systems have been applied to identify a number of reduced-order models, able to represent the heat released by the reaction and the concentrations of the most relevant species. In simulation an experimental procedure, for data generation and model validation, has been reproduced.

A novel model-based controller-observer scheme for temperature control has been designed. The scheme is based on the adoption of a nonlinear model-based observer and a nonlinear temperature controller. The observer is in charge of estimating the heat released by the reaction. The controller is based on the closure of an inner loop on the jacket temperature and an outer loop on the reactor temperature. The performance, in terms of tracking accuracy and robustness to unmodeled dynamics, of the overall scheme has been tested through a realistic simulation set-up and compared with the performance of well-established techniques.

Finally, a fault detection and isolation technique, based on the physical redundancy of the temperature sensors and a bank of two diagnostic observers, has been developed for actuator and sensor faults. The performance in terms of detection and isolation capability and of effectiveness of the voting procedure has been proven via computer simulations.

The major contributions of this thesis can be summarized as follows:

- The controller-observer scheme is developed for a fairly wide class of process, i.e., the class of irreversible non-chain reactions characterized by first-order kinetics.

- A rigorous analysis of the main properties of the overall scheme (i.e., convergence and robustness) has been provided. In detail: convergence of state estimation and tracking errors is always guaranteed under mild assumptions. Moreover, when the (stronger) persistency excitation condition is fulfilled, exponential convergence of all error signals is ensured. This, in turn, implies robustness of the proposed scheme in the face of unmodeled effects.

- Since the design and the tuning of the controller can be achieved independently from the adopted observer, the controller can be adopted in conjunction with other observers and *vice versa*.

- The same observer adopted for control purpose, may be used also for achieve fault detection and isolation.

Future work will be devoted to extension of the proposed approaches to more complex reaction schemes, e.g., reactions characterized by second-order kinetics. Also, the integration of the proposed model-based observer with an universal approximator for the estimation of the model uncertainties is currently subject of investigation.

Concerning fault diagnosis, the proposed approach could be improved in the following directions:

- implementation of a fault identification system;

- extension of the technique to more general process faults , such as abrupt variation of the heat transfer coefficient due to foulness on reactor walls or side reaction due to impurity in the raw material;

- development of fault-tolerant control strategies.

Bibliography

[1] M. Agarwal, "Combining neural and conventional paradigms for modeling, predicition and control," *International Journal of Systems Science*, vol. 28, pp. 65–81, 1997.

[2] F. Amato, C. Cosentino, M. Mattei, and G. Paviglianiti, "An hibryd direct/functional redundancy scheme for the FDI on a small commercial aircraft," *IFAC Sympo. SAFEPROCESS'03*, 2003.

[3] K. J. Aström and B. Wittenmark, *Adaptive control (2nd Edition)*. Addison-Wesley, 1995.

[4] N. Aziz, M. A. Hussain, and I. M. Mujtaba, "Performance of different types of controllers in tracking optimal temperature profiles in batch reactors," *Computers and Chemical Engineering*, vol. 24, pp. 1069–1075, 2000.

[5] J. B. Balchen, B. Lie, and I. Solberg, "Internal decoupling in nonlinear process control," *Model. Ident. Control*, vol. 9, pp. 137–148, 1988.

[6] Y. A. Bard, *Nonlinear parameter estimation*. New York: Accademic Press, 1974.

[7] J. A. Barton and P. F. Nolan, "Hazards x: process safety in fine and speciality chemical plants," *I Chem E Symposium Series*, vol. 115, pp. 3–18, 1998.

[8] R. D. Bartusiak, C. Georgakis, and M. J. Reilly, "Nonlinear feedforward/feedback control structures designed by reference synthesis," *Chemical Engineering Science*, vol. 44, pp. 1837–1851, 1989.

[9] B. W. Bequette, "Nonlinear control of chemical processes: a review," *Industrial & Engineering Chemistry Research*, vol. 30, no. 7, pp. 1391–1413, 1991.

[10] N. V. Bhat and T. J. McAvoy, "Use of neural nets for dynamic modelling and control of chemical process systems," *Computer and Chemical Engineering*, vol. 14, pp. 583–599, 1990.

[11] L. T. Biegler and J. J. Damiano, "Nonlinear parameter estimation: a case study comparison," *AIChE Journal*, vol. 32, no. 1, pp. 29–45, 1986.

[12] P. Bilardello, X. Joulia, J. M. Le Lann, H. Delmas, and B. Koehret, "A general strategy for parameter estimation in differential-algebraic systems," *Computer and Chemical Engineering*, vol. 17, no. 5/6, pp. 517–525, 1993.

[13] D. Bonvin, "Optimal operation of batch reactors - a personal view," *Journal of Process Control*, vol. 8, no. 5/6, pp. 355–368, 1998.

[14] D. Bonvin, P. de Valliére, and D. W. T. Rippin, "Application of estimation techniques to batch reactors. i. modelling termal effects," *Computers and Chemical Engineering*, vol. 13, pp. 1–9, 1989.

[15] M. W. Brown, P. L. Lee, G. R. Sullivan, and W. Zhou, "A constrained nonlinear multivariable control algorithm," *Transactions IChemE*, vol. 68, pp. 464–476, 1990.

[16] F. Caccavale, M. Iamarino, F. Pierri, G. Satriano, and V. Tufano, "Effect of non-ideal mixing on control of cooled batch reactors," in *Proc. of 5th Mathmod*, Wien, 2006.

[17] F. Caccavale, M. Iamarino, F. Pierri, and V. Tufano, "A model-based control scheme for chemical batch reactors," in *Proc. of International Symposium on Intelligent Control & 13th Mediterranean Conference on Control and Automation*, pp. 914–919, Limassol, Cyprus, 2005.

[18] F. Caccavale and L. Villani, "An adaptive observer for fault diagnosis in nonlinear discrete-time systems," in *Proceedings of the 2004 American Control Conference*, pp. 2463–2468, Boston, MA, 2004.

[19] C. T. Chang and J. W. Chen, "Implementation issues concerning the ekf-based fault diagnosis techniques," *Chemical Engineering Science*, vol. 50, no. 18, pp. 2861–2882, 1995.

[20] J. Chen and R. J. Patton, *Robust model-based fault diagnosis for dynamic systems*. Dordrecht: Kluver Academic Publishers, 1999.

[21] Y. Chetouani, N. Mouhab, J. M. Cosmao, and L. Estel, "Application of extended kalman filtering to chemical reactor fault detection," *Chemical Engineering Communications*, vol. 189, no. 9, pp. 1222–1241, 2002.

[22] T. Clark-Pringle and J. MacGregor, "Nonlinear adaptive temperature of multi-product semi-batch polimerization reactors," *Computers in Chemical Engineering*, vol. 21, pp. 1395–1405, 1997.

[23] S. Claudel, C. Fonteix, J. P. Leclerc, and H. G. Lintz, "Application of the possibility theory to the compartment modelling of fow pattern in industrial processes," *Chemical Engineering Science*, vol. 58, pp. 4005–4016, 2003.

[24] B. J. Cott and S. Macchietto, "Temperature control of exothermic batch reactors using generic model control (gmc)," *Industrial Engineering Chemical Research*, vol. 28, pp. 1177–1184, 1989.

[25] Y. Q. Cui, R. G. J. M. Van der Lans, H. J. Noorman, and K. C. A. Luyben, "Compartment mixing model for stirred reactors with multiple impellers," *Trans IChemE*, vol. 74, pp. 261–271, 1996.

[26] S. K. Dash, R. Rengaswamy, and V. Venkatasubramanian, "Fault diagnosis in a nonlinear cstr using observers," in *Proceedings of the 2001 Annual AIChE Meeting*, p. Paper 282i, Reno, NV, 2001.

[27] J. A. Dean, *The Analytical Chemistry Handbook*. New York: McGraw Hill, 1995.

[28] J. Deckert, M. N. Desai, J. J. Deyst, and A. S. Willsky, "F-8 dfbw sensor failure identification using analytical redundancy," *IEEE Transactions on Automatic Control*, pp. 795–805, 1977.

[29] R. Dorr, F. Kratz, J. Ragot, F. Loisy, and J. L. Germain, "Detection, isolation, and identification of sensor faults in nuclear power plants," *IEEE Transactions on Control Systems Technology*, vol. 5, no. 1, pp. 42–52, 1997.

[30] A. Doyle, F. Aoyama, and V. Venkatasubramanian, "Control-affine fuzzy neural network approach for nonlinear process control," *Journal of Process Control*, 1995.

[31] R. Dunia and S. Joe Qin, "Joint diagnosis of process and sensor faults using pricipal component analysis," *Control Engineering Practice*, vol. 6, pp. 457–469, 1998.

[32] K. C. Eapen and L. M. Yeddenapalli, "Kinetics and mechanism of the alkali-catalyzed addition of formaldehyde to phenol and substituted phenols," *Die Makromolekulare Chemie*, vol. 119, no. 2766, pp. 4–16, 1968.

[33] J. W. Eaton and J. B. Rawlings, "Feedback control chemical processes using on-line optimization techniques," *Chemical Engineering Communication*, vol. 14, no. 4/5, pp. 469–497, 1990.

[34] M. Farza, K. Busawon, and H. Hammouri, "Simple nonlinear observers for on-line estimation of kinetic rates in bioreactors," *Automatica*, vol. 34, pp. 301–318, 1998.

[35] C. Filippi, J. L. Greffe, J. Bordet, J. Villermaux, J. L. Barnay, B. Ponte, and C. Georgakis, "Tendency modeling of semi-batch reactors for optimization and control," *Chemical Engineering Science*, vol. 41, pp. 913–920, 1986.

[36] D. J. Francis and L. M. Yeddenapalli, "Kinetics and mechanism of the alkali-catalysed condensations of di- and tri- methylol phenols by themselves and with phenols," *Die Makromolekulare Chemie*, vol. 125, no. 3070, pp. 119–125, 1969.

[37] P. M. Frank, "Analytical and qualitative model-based fault diagnosis – a survey and some new results," *European Journal of Control*, vol. 2, pp. 6–28, 1996.

[38] K. Funahashi, "On the approximate realization of continuous mappings by neural networks," *Neural Networks*, vol. 2, pp. 183–192, 1989.

[39] E. A. Garcia and P. M. Frank, "Deterministic nonlinear observer-based approaches to fault diagnosis: a survey," *Control Engineering Practice*, vol. 5, no. 5, pp. 663–670, 1997.

[40] J. J. Gertler, *Fault detection and diagnosis in engineering systems*. Marcel Dekker Inc., 1998.

[41] B. Guo, A. Jiang, X. Hua, and A. Jutan, "Nonlinear adaptive control for multivariable chemical processes," *Chemical Engineering Science*, vol. 56, pp. 6781–6791, 2001.

[42] S. Haykin, *Neural Networks: A Comprehensive Foundation*. Upper Saddle River, NJ: Prentice Hall, 1998.

[43] M. A. Henson and D. E. Seborg, "An internal model control strategy for nonlinear systems," *AIChE Journal*, vol. 37, pp. 1065–1081, 1991.

[44] ——, "Adaptive nonlinear control of ph neutralization process," *IEEE Transactions on Control Systems Technology*, vol. 2, pp. 169–179, 1994.

[45] ——, *Nonlinear process control*. Upper Saddle River, New Jersey: Prentice Hall, 1997.

[46] W. Hesse, "Phenolic resins," in *Ullmann's Encyclopedia of Industrial Chemistry-6th Edition*. John Whiley & Sons, 2001.

[47] J. C. Hoskins and D. M. Himmelblau, "Artificial neural networks models of knowledge rapresentation in chemical engeineering," *Computers and Chemical Engineering*, vol. 12, pp. 881–890, 1988.

[48] Y. Huang, G. V. Reklaitis, and V. Venkatasubramanian, "A heuristic extended kalmann filter based estimator for fault identification in a fluid catalytic carcking unit," *Industrial & Engineering Chemistry Research*, vol. 42, pp. 3361–3371, 2003.

[49] S. B. Jorgensen and K. M. Hangros, "Grey-box modeling for control: qualitative models as unifying framework," *International Journal of Adaptive Control and Signal Processing*, vol. 28, pp. 65–81, 1995.

[50] P. Kaborè, S. Othman, T. F. McKenna, and H. Hammouri, "Observer-based fault diagnosis for a class of nonlinear systems – application to a free radical copolymerization reaction," *International Journal of Control*, vol. 73, pp. 787–803, 2000.

[51] D. I. Kamenski and S. D. Dimitrov, "Parameter estimation in differential equations by application of rational functions," *Computers and Chemical Engineering*, vol. 17, no. 7, pp. 643–651, 1993.

[52] P. Kesavan and J. H. Lee, "A set based approach to detection of faults in multivariable systems," *Computers and Chemical Engineering*, vol. 25, pp. 925–940, 2001.

[53] H. K. Khalil, *Nonlinear Systems (2nd ed.)*. Upper Saddle River, NJ: Prentice Hall, 1996.

[54] C. Kravaris and C. B. Chung, "Nonlinear state feedback synthesis by global input-output linearization," *AIChE Journal*, vol. 33, pp. 592–603, 1987.

[55] C. Kravaris and J. Kantor, "Geometric methods for nonlinear process control," *Industrial Engineering Chemistry Research, part I and II*, vol. 29, pp. 2295–2323, 1990.

[56] J. Kresta, J. F. MacGregor, and T. E. Marlin, "Multivariable statistical monitoring of process operating performance," *Canadian Journal of Chemical Engineering*, vol. 69, pp. 35–47, 1991.

[57] K. S. Lee and J. H. Lee, "Model predictive control for non linear batch processes with asymptotically perfect tracking," *Computers and Chemical Engineering*, vol. 21, pp. 873–879, 1997.

[58] P. L. Lee and R. B. Newell, "Generic model control-a case study," *Canadian Journal of Chemical Engineering*, vol. 67, pp. 478–483, 1989.

[59] P. L. Lee and G. R. Sullivan, "Generic model control," *Computer and Chemical Engineering*, vol. 12, pp. 573–580, 1988.

[60] P. L. Lee and W. Zhou, "A new multivariable deadtime control algorithm," *Chemical Engineering Communications*, vol. 91, no. 1, pp. 49–63, 1990.

[61] K. Levenberg, "A method for the solution of certain problems il least squares," *Quart. Appl. Math.*, vol. 2, pp. 164–168, 1944.

[62] R. Li and J. H. Olson, "Fault detection and diagnosis in a closed-loop nonlinear distillation process: application of extended kalman filter," *Industrial Engineering Chemical Research*, vol. 30, no. 5, pp. 898–908, 1991.

[63] L. Ljung, *System identification. Theory fot the user*. Upper Saddle River, New Jersey: Prentice Hall, 1999.

[64] L. Ljung, J. Sjoberg, and H. Hjalmarsson, "On neural networks model structures in system identification," in *Identification, Adaptation, Learning*, S. Bittanti and G. Picci, Eds. Springer-Verlag, 1996, pp. 366–393.

[65] D. L. Ma and R. D. Braatz, "Robust identification and control of batch processes," *Computers and Chemical Engineering*, vol. 27, pp. 1175–1184, 2003.

[66] J. F. MacGregor, J. Christiana, K. Costas, and M. Koutoudi, "Process monitoring and diagnosis by multiblock pls methods," *AIChE Journal*, vol. 40, no. 5, pp. 826–838, 1994.

[67] R. S. H. Mah and A. C. Tamhane, "Detection of gross errors in process data," *AIChE Journal*, vol. 28, p. 828, 1982.

[68] L. B. Manfredi, C. C. Riccardi, O. de la Osa, and A. Vazquez, "Modelling of resol resin polymerization with variuous formaldehyde/phenol molar ratios," *Polymer International*, vol. 50, pp. 796–802, 2001.

[69] D. Marquardt, "An algorithm for least squares estimation of nonlinear parameters," *SIAM J. Appl. Math.*, vol. 11, pp. 431–441, 1963.

[70] N. Mehranbod, M. Soroush, and C. Panjapornpon, "A method of sensor fault detection and identification," *Journal of Process Control*, vol. 15, pp. 321–339, 2005.

[71] N. Mehranbod, M. Soroush, M. Piovoso, and B. Ogunnaike, "A probabilistic model for sensor fault detection and identification," *AIChE Journal*, vol. 49, no. 7, p. 1787, 2003.

[72] Z. K. Nagy and R. D. Braatz, "Robust nonlinear model predictive control of batch processes," *AIChE Journal*, vol. 49, pp. 1776–1786, 2003.

[73] A. W. Nienow, "On impeller circulation and mixing effectiveness in the turbulent flow regime," *Chemical Engineering Science*, vol. 52, pp. 2557–2565, 1997.

[74] P. K. Pal, A. Kumar, and A. Gupta, "Modeling of resole type phenol formaldehyde polymerization," *Polymer*, vol. 22, pp. 1699–1704, 1981.

[75] K. Patan and T. Parisini, "Identification of neural dynamic models for fault detection and isolation: the case of a real sugar evaporation process," *Journal of Process Control*, vol. 15, pp. 67–79, 2005.

[76] R. J. Patton, P. M. Frank, and R. N. Clark, *Issues in Fault Diagnosis for Dynamic Systems*. London, UK: Springer-Verlag, 2000.

[77] R. J. Patton, F. J. Uppal, and C. J. Lopez-Toribio, "Soft computing approaches to fault diagnosis for dynamic systems: a survey," in *Preprints of the 4th IFAC Symposium on Fault Detection Supervision and Safety for Technical Processes*, pp. 298–311, Budapest, H, 2001.

[78] A. A. Patwardhan, J. B. Rawlings, and T. Edgar, "Nonlinear model predictive control," *Chemical Engineering Communications*, vol. 87, pp. 1–23, 1990.

[79] G. Paviglianiti, "Model-based $\mathcal{H}_\infty$ and adaptive techniques for sensor and actuators fault detection and isolation for small commercial aircraft," Ph.D. dissertation, Università degli Studi Mediterranea, Reggio Calabria, 2005.

[80] G. Paviglianiti and F. Pierri, "Sensor fault detection and isolation for chemical batch reactors," in *Proc. of the IEEE International Conference on Control Application*, Munich, Germany, 2006.

[81] R. K. Pearson, "Nonlinear input/output modeling," in *Proc. of the IFAC ADCHEM '94*, pp. 1–15, Kyoto, Japan, 1994.

[82] I. Pektas, "High-temperature degradation of reinforced phenolic insulator." *Journal of Applied Polymer Science*, vol. 67, pp. 1877–1883, 1998.

[83] F. Pierri, F. Caccavale, M. Iamarino, and V. Tufano, "A controller-observer scheme for adaptive control of chemical batch reactors," in *Proc. of the 2006 American Control Conference*, pp. 5524–5529, Minneapolis, MM, 2006.

[84] M. M. Polycarpou and A. J. Helmicki, "Automated fault detection and accomodation: a learning systems approach," *IEEE Transactions on Systems, Man, and Cybernetics*, vol. 25, pp. 1447–1458, 1995.

[85] C. C. Riccardi, G. Astarloa Aierbe, J. M. Echeverria, and I. Mondragon, "Modelling of phenolic resin polymerisation," *Polymer*, vol. 43, pp. 1631–1639, 2002.

[86] C. Rojas-Guzman and M. A. Kramer, "Comparison of belief networks and rule-based expert systems for fault diagnosis of chemical processes," *Engineering Application of Artificial Intelligence*, vol. 6, p. 191, 1993.

[87] D. Ruiz, J. Canton, J. M. Nougues, A. E. na, and L. Puigjaner, "On-line fault diagnosis system support for reactive scheduling in multipurpose batch chemical plants," *Computers and Chemical Engineering*, vol. 25, pp. 829–837, 2001.

[88] D. Ruiz, J. M. Nougues, and L. Puigjaner, "Fault diagnosis support system for complex chemical plants," *Computers and Chemical Engineering*, vol. 25, pp. 151–160, 2001.

[89] S. A. Russel, P. Kesavan, J. H. Lee, and B. A. Ogunnaike, "Recursive data-based prediction and control of product quality for batch and semi-batch processes applied to a nylon 6,6 autoclave," in *Proc. of the AIChE Annual Meeting*, Los Angeles, CA, 1997.

[90] V. Sampath, S. Palanki, J. C. Cockburn, and J. P. Corriou, "Robust controller design for temperature tracking problems in jacketed batch reactors," *Journal of Process Control*, vol. 12, pp. 27–38, 2002.

[91] H. Schuler and C. U. Schmidt, "Calorimetric state estimators for chemical reactor diagnosis and control: reviews of methods and application," *Chemical Engineering Science*, vol. 47, no. 4, pp. 899–915, 1992.

[92] P. D. Signal and P. L. Lee, "Generic model adaptive control," *Chemical Engineering Communications*, vol. 115, no. 1, pp. 35–52, 1992.

[93] O. A. Z. Sotomayor and D. Odloak, "Observer-based fault diagnosis in chemical plants," *Chemical Engineering Journal*, vol. 112, pp. 93–108, 2005.

[94] W. J. H. Stortelder, "Parameter estimation in chemical engineering; a case study for resin production," Dutch National Research Institute for Mathematics and Computer Science, Department of Numerical Mathematics, Amsterdam, The Netherlands, Tech. Rep. NM-R9610, 1996.

[95] R. Tarantino, F. Szigeti, and E. Colina-Morles, "Generalized Luenberger observer-based fault detection filter design: An industrial application," *Control Engineering Practice*, vol. 8, pp. 665–671, 2000.

[96] V. Tufano, "Identificazione dei parametri cinetici di reti complesse," *Quaderni dell' Ingegnere Chimico Italiano*, no. 1, pp. 7–12, 1991.

[97] D. Tyner, M. Soroush, and M. C. Grady, "Adaptive temperature control of multiproduct jacketed reactors," *Industrial Engineering Chemical Research*, vol. 38, pp. 4337–4344, 1999.

[98] J. M. T. Vasconcelos, S. S. Alves, and J. M. Barata, "Mixing in gas-liquid contactors agitated by multiple turbines," *Chemical Engineering Science*, vol. 50, pp. 2343–2354, 1995.

[99] H. Vedam and V. Venkatasubramanian, "Pca-sdg based process monitoring and fault diagnosis," *Control Engineering Practice*, vol. 7, pp. 903–917, 1999.

[100] V. Venkatasubramanian, R. Rengaswamy, K. Yin, and S. N. Kavuri, "A review of process fault detection and diagnosis part i: quantitative model-based methods," *Computers and Chemical Engineering*, vol. 27, pp. 293–311, 2003.

[101] V. Venkatasubramanian, R. Vaidyanathan, and Y. Yamamoto, "Process fault detection and diagnosis using neural networks-i steady state process," *Computers and Chemical Engineering*, vol. 14, pp. 699–712, 1990.

[102] D. Wang, D. H. Zhou, Y. H. Jin, and S. J. Qin, "Adaptive generic model control for a class of nonlinear time-varying processes with input delay," *Journal of Process Control*, vol. 14, pp. 517–531, 2004.

[103] ——, "A strong tracking predictor for nonlinear processes with input time delay," *Computers and Chemical Engineering*, vol. 28, pp. 2523–2540, 2004.

[104] X. Q. Xie, D. H. Zhou, and Y. H. Jin, "Strong tracking filter based adaptive generic model control," *Journal of Process Control*, vol. 9, pp. 337–350, 1999.

[105] S. Yoon and J. F. MacGregor, "Fault diagnosis with multivariate statistical models part i: using steady state fault signature," *Journal of Process Control*, vol. 11, pp. 387–400, 2001.

[106] D. L. Yu, J. B. Gomm, and D. Williams, "Sensor fault diagnosis in a chemical process via rbf neural networks," *Control Engineering Practice*, vol. 7, pp. 49–55, 1999.

[107] J. Zhang and R. Smith, "Design and optimisation of batch and semi-batch reactors," *Chemical Engineering Science*, vol. 59, pp. 459–478, 2004.

[108] X. Zhang, M. M. Polycarpou, and T. Parisini, "A robust detection and isolation scheme for abrupt and incipient faults in nonlinear systems," *IEEE Transactions on Automatic Control*, vol. 47, pp. 576–593, 2002.

[109] W. Zhou and P. L. Lee, "Robust stability analysis of generic model control," *Chemical Engineering Communications*, vol. 117, no. 1, pp. 41–72, 1992.